UC RIVERSIDE
School of Public Policy

Working Paper Series
(DECEMBER) (2025) – WP#25-01

TABLE OF CONTENTS

Optimal groundwater management to mitigate water table decline and land subsidence impacts on groundwater-dependent ecosystems

Nelson Ndakolute Ndahangwapo[a], Djiby Racine Thiam[b], Ariel Dinar[c]
[a,b]*School of Economics, University of Cape Town, South Africa.*
[c]*School of Public Policy, University of California, Riverside, USA.*

SUMMARY:

Rising surface water scarcity has intensified groundwater extraction, which drives land subsidence (LS) and, in turn, damages groundwater-dependent ecosystems (GDEs). However, the LS-GDEs relationship remains largely underexplored in the economic literature. In this paper, we develop a dynamic economic optimization model that explicitly incorporates LS within a GDEs (LS-GDEs) framework and evaluate alternative policy instruments aimed at curbing overexploitation to mitigate the negative effects of groundwater depletion. These instruments include quota systems, taxes on land sinking and on aquifer storage loss, as well as packaging and sequencing of taxes and quotas. Using data from a major aquifer in South Africa, we calibrate the model and assess the private and social welfare implications. Our results show that taxes on land sinking and aquifer storage loss significantly influence extraction behaviour and raise water table levels, thereby enhancing social welfare. Among the policies, quotas yield the lowest private net benefits to farmers (0.1395 million USD), while the baseline scenario generates the highest. The LS–GDEs and no policy intervention scenario delivers the second-highest private net benefits. Packaging and sequencing of policy interventions provides private net benefits equal to those under the tax policy. Overall, these findings highlight the importance of designing policies that account for LS-driven impacts to safeguard GDEs' health.

Optimal groundwater management to mitigate water table decline and land subsidence impacts on Groundwater-Dependent Ecosystems

Nelson Ndakolute Ndahangwapo [a], Djiby Racine Thiam [b], Ariel Dinar [c]

[a,b] *School of Economics, University of Cape Town, South Africa.*

[c] *School of Public Policy, University of California, Riverside, USA.*

Abstract

Rising surface water scarcity has intensified groundwater extraction, which drives land subsidence (LS) and, in turn, damages groundwater-dependent ecosystems (GDEs). However, the LS-GDEs relationship remains largely underexplored in the economic literature. In this paper, we develop a dynamic economic optimization model that explicitly incorporates LS within a GDEs (LS-GDEs) framework and evaluate alternative policy instruments aimed at curbing overexploitation to mitigate the negative effects of groundwater depletion. These instruments include quota systems, taxes on land sinking and on aquifer storage loss, as well as packaging and sequencing of taxes and quotas. Using data from a major aquifer in South Africa, we calibrate the model and assess the private and social welfare implications. Our results show that taxes on land sinking and aquifer storage loss significantly influence extraction behaviour and raise water table levels, thereby enhancing social welfare. Among the policies, quotas yield the lowest private net benefits to farmers (0.1395 million USD), while the baseline scenario generates the highest. The LS–GDEs and no policy intervention scenario delivers the second-highest private net benefits. Packaging and sequencing of policy interventions provides private net benefits equal to those under the tax policy. Overall, these findings highlight the importance of designing policies that account for LS-driven impacts to safeguard GDEs' health.

Keywords: Land subsidence; Groundwater dependend ecosystems; Groundwater over-extraction; Aquifer system storage capacity; Taxes; Quotas; Packaging and sequencing; Social benefits; Dendron aquifer; South Africa.

JEL codes: Q25, Q51, Q57, Q58, O13, C61

1. Introduction

Groundwater-dependent ecosystems (GDEs) are ecological systems that rely on groundwater for some or all of their water needs (Rohde et al., 2020). These include springs, wetlands, rivers and streams, lakes, riparian forests, caves, and lagoons (Klove et al., 2011a). The well-being of human societies is intrinsically linked to the health of these ecosystems. For example, GDEs provide essential ecosystem services, including flood mitigation, water purification, erosion control, groundwater recharge, and natural irrigation (Klove et al., 2011b). Eamus et al. (2006) categorize GDEs into three types: (1) fully groundwater-dependent ecosystems (e.g., karsts, aquifers, and cave ecosystems), (2) those dependent on the surface expression of groundwater (e.g., base-flow rivers, streams, wetlands, and springs), and (3) ecosystems reliant on subsurface groundwater within rooting depths (e.g., woodlands and riparian forests). A large share of the global economic value of ecosystem services, estimated at 125 to145 trillion US dollars annually as of 2014, is derived from groundwater-related ecosystems (Costanza et al., 2014). In addition, the global mean values (international dollars/ha/year) of ecosystem services for water-related ecosystems were estimated at 2,398 for coastal systems, 6,791 for mangroves, 612 for inland wetlands, and 364 for rivers and lakes, etc. (Brander et al., 2024). Yet, excessive groundwater extraction has led to severe environmental and economic losses, with damages estimated at 4.3 to 20.2 trillion US dollars per year (Costanza et al., 2014). One critical consequence of excessive groundwater abstraction is the lowering of the water table, which threatens GDEs (Eamus et al., 2006). When the water table declines beyond the reach of plant roots, terrestrial ecosystems lose access to groundwater, leading to habitat degradation (Rohde et al., 2020).

Groundwater depletion also reduces streamflow in rivers and springs, negatively affecting aquatic biodiversity and water availability (Rohde et al., 2020). Beyond the negative effects on ecosystem services, continuous groundwater overextraction leads to land subsidence (LS). LS refers to the process where the ground surface sinks due to the compaction of subsurface materials, often caused by the removal of groundwater among others. In addition, LS progresses in two phases: (1) elastic compaction, which is reversible, and (2) inelastic compaction, which is irreversible (Esteban et al. 2024; Ndahangwapo et al., 2024). The transition to the inelastic phase signifies permanent damage, reducing groundwater availability and degrading GDEs. LS reduces aquifer storage capacity, exacerbating groundwater depletion impacts and leading to ecosystem stress. Ecosystem stress arises not only from reduced water availability for consumption, but also from LS–related impacts such as deteriorating water quality, altered hydraulic flows, and other associated impacts (Dinar et al., 2021). The magnitude and severity of the LS damages depend on a combination of physical and environmental factors: (i) depth to the water table, (ii) groundwater pressure, (iii) groundwater flux, and (iv) groundwater quality (Clifton & Evans, 2001).[1]

Economic research on groundwater regulation has largely focused on depth externalities while overlooking GDE health and LS (Gisser & Sanchez, 1980; Brill & Burness, 1994; Guilfoos et al., 2013; de Frutos Cachorro et al., 2014; Tomini, 2014; Allen & Gisser, 1984; Brown & Deacon, 1972). Studies on LS and aquifer storage loss (Dinar et al., 2020; Esteban et al., 2024; Ndahangwapo et al., 2024) have not accounted for GDEs. Meanwhile, studies on GDE damages from groundwater depletion (Esteban & Albiac, 2011; Roumasset & Wada, 2013; Esteban & Dinar, 2016; Esteban et al., 2021) have not considered the impact of LS on GDE health. This disparity in the literature leads to underestimates of the impact of overexploitation of groundwater and bias in the value of the suggested policy interventions. This paper bridges these gaps by analyzing the interdependence between LS, aquifer storage loss, and GDE health. We offer the first economic study that explicitly links land subsidence with GDE health and explores the extent to which changes in groundwater use may affect their dynamics.

To quantify these relationships, we develop a GDE health status function that links GDE health with both the level of water table height and land subsidence. Several papers have defined ecosystem health as a function of the depth to the water table (Esteban et al., 2021; Esteban and Dinar, 2016; Eamus et al., 2006; Gutrich et al., 2016). Alternatively, GDEs' health can be expressed as a function of the water table height (Esteban et al., 2021). There are two distinct effects in our analysis. First, groundwater extraction affects aquifer reserve which affects in turn the state of the ecosystem health. When the aquifer is full, the ecosystem remains in its

[1] Groundwater pressure refers to the force per unit area exerted by water within a confined aquifer, often related to the height of the water column above a reference point. Groundwater flux refers to the rate at which groundwater flows through a unit area of porous medium, usually expressed as volume per time per area.

pristine state, but once the water table drops to the aquifer bottom, the ecosystem collapses. Reduction of the water table height beyond a certain threshold (denoted H_u) triggers the deterioration of the health status of the GDEs. From H_u, the state of the GDEs enters the unhealthy phase. Second, when the water table height surpasses another threshold, (denoted H_c) this creates LS from elastic compaction alone (severe unhealthy phase). During the severe unhealthy phase, the ecosystem suffers loss of biodiversity, collapse of vegetation cover, permanent aquifer damage, and breakdown of groundwater–surface water linkages. To simplify the analysis, we assume that threshold H_u is reached first, followed by a second threshold H_c, then, a third threshold H_T can be reached. The third threshold marks the beginning of irreversible land subsidence (inelastic compaction). This means, land subsidence is reached within the interval of the unhealthy state of the ecosystem health. The damage inflicted on the ecosystem health caused by land subsidence can therefore be seen as a cumulative effect.

We model GDE health over four states: a healthy phase, an unhealthy phase, a severe unhealthy phase, and a critical unhealthy phase. We follow Scheffer and Carpenter (2003) and Crepin et al (2012) in distinguishing between the healthy and unhealthy phases and the extent to which ecosystem changes are triggered by external conditions. The healthy phase corresponds to the state where GDEs are fully functional, and all ecological and hydrological processes are functioning in a stable, undisturbed, and ecologically ideal state, supporting long-term sustainability without intervention. Ecological processes are the natural interactions and functions that sustain ecosystems and the organisms within them. Phase 2, the unhealthy phase, reflects a state where some ecological processes are not efficient or disrupted. During the severe unhealthy phase, GDEs experience major or severe functional impairment, with key or essential ecological processes significantly compromised. Phase 4, the critical unhealthy phase, represents a state in which essential ecological processes have largely ceased or critically impaired, indicating that the GDE is on the verge of complete failure.

The ecosystem state in our study is represented by a function ($GDEsHS(H, LS(H))$) that links the health of the ecosystem ($GDEsHS$) with both the level of water in the aquifer (H) and the level of cumulative land subsidence ($LS(H)$). The function represents how a decrease in the water table level affects the functioning of depending aquatic ecosystems. Cumulative land subsidence represents the net amount of LS that has occurred since surpassing the critical threshold H_c up to and including the current time. The health of the GDEs decreases as the water table height decreases and cumulative LS increases. The GDEs' health status (GDEsHS, ranging from 0 to 1) functional represents the condition or level of health of the GDEs. A value equal to 1 implies that the health of the GDEs is in its pristine state. A reduction in the value of the health function beyond a certain threshold (denoted δ) triggers the deterioration of the health status of the GDEs. From δ, the state of the GDEs enters the unhealthy phase. Second, when the value of the health function falls below another threshold, (denoted ρ) the health status enters the severe unhealthy phase. The last health threshold, γ, marks the beginning of the critical unhealthy phase. A higher level or status of ecosystem health provides a higher level or amount of ecosystem services compared to a lower level of ecosystem health. The stated ecosystem function is described in Figure 1.

Our model incorporates several policy intervention mechanisms, such as taxes and quotas that are widely used to correct groundwater overextraction externalities (Brown & Deacon, 1972; Ndahangwapo et al., 2024; Dinar et al., 2020). A Pigouvian tax charged per unit of land sinking at every time step or quotas to limit water extraction are compared. The paper evaluates the effectiveness of these regulatory tools and their packaging and sequencing ability to mitigate LS-induced damages to GDEs. We compare three policy scenarios: (1) taxes, (2) quotas, setting extraction limits to prevent excessive groundwater withdrawal and preserve GDEs health, and (3) combined approach, a hybrid of quotas and taxes, considering their optimal sequencing for policy effectiveness. Such analysis provides insights into which policy mechanisms can best align private extraction incentives with social welfare objectives.

The remainder of the paper is structured as follows: Section 2 presents a review of the relevant literature. Section 3 introduces the dynamic optimization model for groundwater management, outlining the effects of LS and policy interventions. Section 4 details the empirical approach, while Section 5 discusses the study area and data. Section 6 discusses the results and policy implications. Section 7 concludes with recommendations for sustainable groundwater management.

2. Literature review

Various institutional arrangements and policy instruments, such as taxes and quotas, have been proposed to regulate groundwater use and enhance social welfare (Brah and Jones, 1978; Tang, 1991). Some studies have focused on quantifying LS to better understand its extent and address its associated negative externalities. This review synthesizes previous research on LS, the health of groundwater-dependent ecosystems (GDEs), and groundwater overextraction, as well as their interconnections.

Systematic reviews by Herrera-García et al. (2021) and Bagheri-Gavkosh et al. (2021) highlight the global scope of land subsidence. Herrera-García et al. identified 200 cases of groundwater-related subsidence across 34 countries, while Bagheri-Gavkosh et al. documented 290 subsidence cases in 41 countries, with around 60% attributable to groundwater pumping and 41% linked specifically to agricultural extraction. Herrera-García et al. estimate that subsidence currently affects approximately 8% of the Earth's land surface, with some of the hugely affected regions being the Yazd-Ardakan aquifer and the California's Central Valley. Subsidence also threatens urban areas: their analysis suggests that 19% of the global population and 12% of global GDP are at high or very high potential risk, although only 1.6% of land is directly exposed. In response to these risks, the Indonesian government has announced plans to relocate the capital city to Borneo Island, more than 1,000 km inland (Cobourn, 2025).

Dinar et al. (2021) and Josset et al. (2024) developed indexes to measure the impacts of land subsidence, offering standardized approaches to monitor and inform policy decisions. Josset et al. proposed a multi-dimensional Land Subsidence Geospatial Risk Index (LSGRI), linking subsidence severity with direct damages to infrastructure and indirect damages from increased flood risk. Hu et al. (2013) combined physical modelling with a simplified calculation of monetary damages from subsidence, providing an initial quantitative assessment. Wade et al. (2018) examined the economic costs of LS caused by groundwater pumping by estimating the marginal damages from pumping in Virginia's southern Chesapeake Bay region. Shrestha et al. (2017) provided the first assessment of LS in Kathmandu Valley, Nepal, using a fully calibrated coupled surface-subsurface groundwater model. Their simulations showed that deep aquifer compaction from excessive groundwater abstraction drives LS. Managed aquifer recharge has been applied as a mitigation measure, successfully limiting subsidence in Las Vegas and Shanghai, although it proved less effective in Mexico City (Seidl et al., 2024).

Dinar et al. (2020) examined the use of Pigouvian taxes to internalize the external costs of land subsidence and aquifer storage loss caused by groundwater extraction. They showed that targeted taxation could prevent further compaction and water scarcity while aligning private extraction with socially optimal outcomes. Esteban et al. (2024) and Ndahangwapo et al. (2024) further examined the use of Pigouvian taxes on LS and aquifer storage capacity loss, showing that such taxes can significantly influence groundwater withdrawals, maintain higher water table levels, and prevent water scarcity. Ndahangwapo et al. (2024) also evaluated quota systems and combined tax-quota approaches, finding that while taxes alone reduce extractions, combining instruments through packaging and sequencing generates higher social benefits.

Ecosystem-related damages from groundwater depletion have been analysed in several studies. Roumasset and Wada (2013) demonstrated that payments for ecosystem services (PES) could incentivize groundwater conservation. Esteban and Dinar (2016) incorporated an ecosystem health function into groundwater models, showing that optimal extraction paths must reflect the economic value of ecosystem services. Esteban et al. (2021) extended this work by modelling regime shifts in GDEs, identifying tipping points beyond which ecosystem degradation becomes irreversible. Rohde et al. (2019) highlighted the importance of setting groundwater thresholds to secure environmental water needs for GDEs. Addressing data gaps in linking groundwater conditions to GDEs' health, they used geophysics alongside biological indicators of groundwater-dependent vegetation to assess GDEs' health. Their results showed that vegetation health indicators correlate strongly with subsurface hydrological conditions, offering a transdisciplinary framework that integrates hydrological, geophysical, and ecological data to improve monitoring and groundwater management. Esteban and Albiac (2011) proposed Pigouvian taxes based on ecosystem damage per unit of groundwater depletion, illustrating the role of economic instruments in preserving ecosystem health.

Brown and Deacon (1972) formulated a tax on groundwater pumping, showing that higher extraction costs encourage conservation. Maddock and Haimes (1975) developed a quadratic linear programming model combining taxes with quotas, with taxes applied to excess extraction and rebates for low extraction. Bredehoeft and Young (1970) compared taxes and quotas in a hypothetical basin, observing similar outcomes with only minor welfare improvements. Feinerman and Knapp (1983) reported that while users preferred quotas, the social welfare gains were limited. Weitzman (1974) highlighted that under uncertainty, neither taxes nor quotas alone achieve first-best outcomes. Choi and Feinerman (1995) applied these concepts to groundwater pollution, and Brozovic et al. (2004) found that quotas could achieve higher reductions under certain conditions. Duke et al. (2020) compared six tax policies using a coupled hydrologic-economic model, finding that social efficiency and earnings varied despite similar reductions in withdrawals.

To overcome the limitations of single instruments, studies have examined combined approaches. Maddock and Haimes (1975) showed that taxing excess extraction while subsidizing low extraction effectively reduced costs and promoted conservation. Lenouvel et al. (2011) developed a target-based mechanism combining ambient taxes with individual quotas, which reduced withdrawals in experiments despite informational limitations. Esteban and Dinar (2013) demonstrated in the Western La Mancha aquifer that sequencing tax and quota interventions can achieve more sustainable management than single policies, although determining optimal tax rates remains challenging under heterogeneous conditions. Costello and Karp (2004) found that dynamic taxes provide better regulatory information, enhancing social welfare compared to quotas.

Equity considerations are also crucial. Feinerman (1988) highlighted the need for stakeholder consensus to ensure fair adoption of groundwater policies. Sorensen and Herbertsson (1998) compared Pigouvian and flat-rate taxes, finding the former more efficient but challenging to implement due to information gaps.

Overall, the literature indicates that while taxes and quotas are effective for groundwater management, combining instruments and adapting policies over time generally yields superior social outcomes. Building on these insights, the present study examines both individual and combined policy instruments in mitigating groundwater externalities, with a particular focus on induced LS and its effects on GDE health. We develop a GDE health status function linking ecosystem condition with land subsidence to inform taxes and quotas designed to preserve ecosystem integrity and ensure sustainable groundwater use.

3. The model

We consider an aquifer system situated beneath a specific agricultural region, which is managed under the oversight of a regulatory authority. It is assumed, without loss of generality that all farmers in this region rely exclusively on groundwater extraction via water pumps, as no alternative water sources are available for irrigation purposes. Drawing on the framework established by Gisser and Sanchez (1980), the demand for irrigation water is expressed by Equation (1) below.

$$W(t) = g + kP(t),\ \ g > 0, k < 0. \tag{1}$$

The function $W(t)$ represents the groundwater extraction rate at time t, g and k are parameters of the demand function, and $P(t)$ is the price of irrigation water. The inverse demand function corresponding to Equation (1) is given by Equation (2) below.[2]

$$P = \frac{W}{k} - \frac{g}{k}. \tag{2}$$

As a standard in the literature, farmers' total revenue from groundwater use for irrigation is given by Equation (3) below.

$$\int_W P(W)\, dW = \frac{W^2}{2k} - \frac{gW}{k}. \tag{3}$$

The cost of groundwater extraction is defined by the function $\bar{P} = C_0 + C_1 H$, where $C_0 > 0$ represents fixed extraction costs and $C_1 < 0$ denotes marginal extraction costs. The depth to the water table is given by $S_l - H$, with S_l indicating the surface elevation of the irrigated field and H representing the water table height. Consequently, the private benefits derived from groundwater use are given by total revenue minus total extraction costs. The dynamics of groundwater are described by $\dot{H} = \frac{1}{AS}[R - (1-\alpha)W],\ \ 0 < t < +\infty$. Where A is the area of the aquifer system (m^2), S is the storativity coefficient (dimensionless), R is the natural recharge rate ($m^3/year$), and $0 \leq \alpha < 1$ represents the percolation return flow coefficient (dimensionless). Additionally, the change in water table height due to pumping is expressed as (Koundouri, 2004) $\Delta H = \frac{1}{AS}[R - (1-\alpha)W]$.

In this study, we model GDEs' health as a function of water table height coupled with a measure of LS extent, where a decline in water table height corresponds to a decline in GDEs'

[2] Omitting the operator t for simplicity (Ndahangwapo et al. (2024)).

health. A decrease in the water table height and a simultaneous increase in LS extent (when subsidence is occurring) jointly intensify stress on the aquifer system, thereby further reduce the health of the GDEs. We assume that the aquifer is at full capacity when the water table height equals the surface elevation, that is, $S_l = H$ (Esteban et al., 2021). A full aquifer implies that the GDEs' health is in its pristine state. Building on the framework proposed by Esteban et al. (2021), we define the GDEs' health over four distinct phases, as defined in the Introduction section (healthy, unhealthy, severe unhealthy, and critical unhealthy). The figure below illustrates the GDEs' health status (GDEsHS) given in Equation (4).

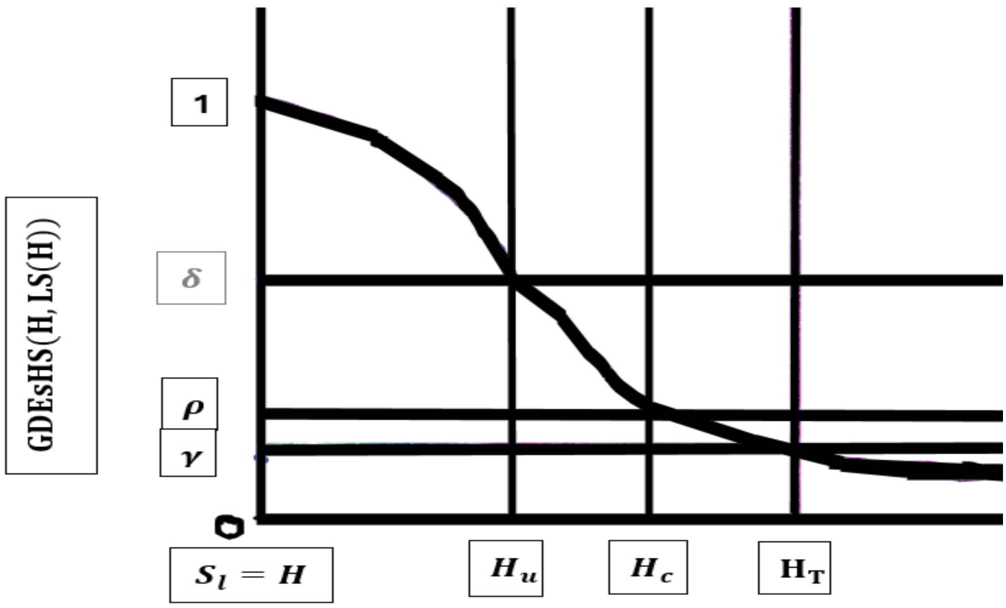

Figure 1. GDEs health status evolution.

We define three GDEs' health critical thresholds (or tipping points) that are governing the GDEs' health across the four phases: $0 < \gamma < \rho < \delta < 1$. The parameter δ marks the critical threshold beyond which ecosystem health switches into the unhealthy phase ($\rho \leq \text{Health} < \delta$), driven solely by a falling water table. Beyond ρ, ecosystem health enters the severe unhealthy phase ($\gamma \leq \text{Health} < \rho$), where both water table decline and elastic land subsidence contribute to the ecosystem health stress. When the health falls below γ, the system enters the critical unhealthy phase ($0 \leq \text{Health} < \gamma$), driven by a falling water table, both elastic and inelastic LS, and aquifer storage capacity loss. We assume that the health of the GDEs reaches zero when the water table falls to the aquifer bottom ($H = H_B$), regardless of the amount of LS experienced at that time.

In addition, we define three critical thresholds for the water table height: $H_T < H_c < H_u$. The threshold H_u marks the point beyond which the ecosystem health enters the unhealthy phase; that is, the healthy phase occurs when $H \geq H_u$, and the unhealthy phase begins when $H < H_u$. When the water table falls below H_c, elastic compaction begins, marking the start of the severe unhealthy phase. Thus, the unhealthy phase corresponds to $H_c \leq H < H_u$, and the severe unhealthy phase begins when $H < H_c$. Similarly, the threshold H_T represents the point below which inelastic compaction begins. Therefore, the critical unhealthy phase begins when $H < H_T$, and continues until the aquifer bottom H_B is reached. As a result, by modifying the evolution of the ecosystem health, dependent solely on the depth to water table, as suggested by Esteban et al. (2021), we define the GDEs' health status, $GDEsHS(H, LS(H))$ as presented in Equation (4) below (construction outlined in Appendix 1).

$$GDEsHS(H, LS(H)) = \begin{cases} \frac{\delta - 1}{(S_l - H_u)^2} \cdot (S_l - H)^2 + 1 & \text{if } H \geq H_u, \\ \frac{\delta - \rho}{(H_u - H_c)^2} \cdot (H - H_c)^2 + \rho & \text{if } H_c \leq H < H_u, \\ \frac{\rho - \gamma}{(d_c)^2} \cdot (H - LS(H) - H_T + LS(H_T))^2 + \gamma & \text{if } H_T \leq H < H_c, \\ \frac{\gamma}{(d_T)^2} \cdot (H - LS(H) - H_B + LS(H_B))^2 & \text{if } H < H_T. \end{cases} \quad (4)$$

where $d_c = H_c - LS(H_c) - H_T + LS(H_T)$, $d_T = H_T - LS(H_T) - H_B + LS(H_B)$, $LS(H_c) = LS(H(t_c))$, $LS(H_T) = LS(H(t_T))$, and $LS(H_B) = LS(H(t_B))$. The function, $LS(H) = -\eta \cdot \varepsilon \cdot b \cdot \psi \cdot (H - H_c)$, represents the cumulative LS (in m). The parameters η, b, ψ, and ε represent the density of water, the aquifer system's thickness, the aquifer system compressibility, and the acceleration due to gravity, respectively. Following Esteban et al. (2021), we further assume that at each critical threshold for the water table, the GDEs health status functional is continuous, taking the same value from both the left and right sides of the function. Phase one function is a downward opening parabola, where the GDEs' health status decreases from 1 towards δ as H reduces. Phase two function is an upward opening parabola, where the GDEs' health status decreases from δ towards ρ as H reduces.

In phase 3, GDEs' health stress is driven by a decreasing H and reversible $LS(H) \geq 0$ (see Appendix 1). The GDEs' health status decreases from ρ towards γ as H reduces and $LS(H)$ increases. In phase 4, GDEs' health decreases from γ to 0 as H reduces and $LS(H)$ increases.

Geological differences and withdrawal patterns explain variations in subsidence magnitude and spatial pattern (Zhang et al., 2007; Ha et al., 2021). Therefore, we assume one uniform aquifer system with evenly spread wells and effects. Finally, θ is a scaling parameter that translates GDEs' health into a monetary value of the ecosystem services. Thus, θ is defined as the maximum total economic value of ecosystem services when the GDEs are in a pristine health state. The model application is expected to serve as a robust tool for decision-making, providing quantitative insights into the interplay between groundwater use, LS, and ecosystem resilience, and helping identify policy options that achieve sustainable groundwater management while minimizing welfare and ecological risks.

4. Policy instruments

As previously stated, we examine several policy instruments: quotas and taxes. These policy instruments are chosen because they target different aspects of groundwater management, with quotas directly limiting the quantity of water extracted, while taxes provide economic incentives to reduce overuse. We also examine the performance of their joint implementation (packaging and sequencing) in affecting groundwater use and the health of GDEs. Testing multiple policy instruments allows us to identify which poicy instruments, individually or in combination, are most effective in sustaining both water resources and dependent ecosystems.

4.1 Implementation of taxes

Taxes will serve as the first policy intervention to be considered. A Pigouvian tax is aplicable when damages can be measured. Hence, taxing each unit of LS is reasonable. Although an alternative would be to tax the deterioration of GDEs' health directly, the monitoring cost of ecological health is likely much higher than the benefit of internalizing extraction externalities. By contrast, LS can be monitored relatively cheaply through satellite-based remote sensing and observation wells. The function $LS(W)$ represents the rate at which the land is sinking (m) due to pumping as suggested by Ndahangwapo et al. (2024): $LS(W) = -\eta \cdot \varepsilon \cdot b \cdot \psi \cdot \Delta H$. Where η, b, ψ, and ε represent the density of water, the aquifer system's thickness, the aquifer system compressibility, and the acceleration due to gravity, respectively.

Taxing ΔH (change in water table height due to pumping) instead would be less practical because its accurate measurement across space and time is costly and requires dense monitoring networks. Consequently, phases one and two will not be taxed since LS does not occur during these stages. Only phases three and four, where LS occurs, will be subject to taxation. Following Ndahangwapo et al. (2024), the parameter β represents the Pigouvian tax charged per meter of land sinking (in m). In addition, the regulator imposes a Pigouvian tax on each cubic meter of aquifer storage capacity lost, defined by $\phi(W,H) = \frac{W}{k} - \frac{g}{k} - (C_0 + C_1 H)$ (in $\$/m^3$). The volume of storage capacity lost due to inelastic compaction from groundwater pumping is calculated following Ndahangwapo et al. (2024).

$$p = -AS\psi b\pi(1 - n + n_w)\Delta H. \tag{5}$$

where, ψ denotes aquifer compressibility (ms^2/kg), π the unit weight of water (N/m^3), n the aquifer porosity (dimensionless), and n_w the moisture content in the unsaturated zone (fraction of total volume, dimensionless). Based on these formulations, farmers maximize private welfare subject to the tax policy, which leads to the following welfare maximization problem.

$$\max_{W,H,t_c,t_u,t_T} \int_0^{t_u} e^{-it}[\frac{W^2}{2k} - \frac{gW}{k} - (C_0 + C_1 H)W + \theta(\frac{\delta - 1}{(S_l - H_u)^2} \cdot (S_l - H)^2 + 1)]dt$$

$$+ \int_{t_u}^{t_c} e^{-it}[\frac{W^2}{2k} - \frac{gW}{k} - (C_0 + C_1 H)W + \theta(\frac{\delta - \rho}{(H_u - H_c)^2} \cdot (H - H_c)^2 + \rho)]dt$$

$$+ \int_{t_c}^{t_T} e^{-it}[\frac{W^2}{2k} - \frac{gW}{k} - (C_0 + C_1 H)W + \theta(\frac{\rho - \gamma}{(d_c)^2} \cdot (H - LS(H) - H_T + LS(H_T))^2 + \gamma)$$

$$-\beta \cdot LS(W)]dt$$

$$+ \int_{t_T}^{\infty} e^{-it}[\frac{W^2}{2k} - \frac{gW}{k} - (C_0 + C_1 H)W + \theta(\frac{\gamma}{(d_T)^2} \cdot (H - LS(H) - H_B + LS(H_B))^2)$$

$$-\beta \cdot LS(W) - \phi(W,H) \cdot p]dt, \tag{6}$$

subject to

$$\dot{H} = \begin{cases} \frac{1}{AS}[R - (1-\alpha)W], & \text{if } t \le t_u \\ \frac{1}{AS}[R - (1-\alpha)W], & \text{if } t_u < t \le t_c \\ \frac{1}{AS}[R - (1-\alpha)W], & \text{if } t_c < t \le t_T \\ \frac{1}{\Omega \cdot AS}[R - (1-\alpha)W], & \text{if } t > t_T. \end{cases} \tag{7}$$

and

$$H(t) > 0,\ H(t_0) = H_0,\ H(t_c) = H_c,\ H(t_u) = H_u,\ H(t_T) = H_T. \tag{8}$$

where i denotes the discount rate. The parameter $0 < \Omega \leq 1$ captures the impact of groundwater extraction on the aquifer system's storage capacity (Dinar et al., 2020). Following Ndahangwapo et al. (2024), we assume that the reduction in aquifer storage capacity is constant and independent of the aquifer system's volume. To solve the above multi-stage optimal control problem, the optimization is conceptually divided into four sub-problems, as in Kim et al. (1989). However, in this study, we employ a backward induction approach. The fourth sub-problem (SP4) is presented below.

$$\max_{W_4,H_4,t_T} \int_{t_T}^{\infty} e^{-it}[\frac{W_4^2}{2k} - \frac{gW_4}{k} - (C_0 + C_1H_4)W_4$$

$$+\theta(\frac{\gamma}{(d_T)^2} \cdot (H_4 - LS(H_4) - H_B + LS(H_B))^2) - \beta \cdot LS(W_4) - \phi(W_4, H_4) \cdot p]dt \quad (9)$$

subject to

$$\dot{H}_4 = \frac{1}{\Omega \cdot AS}[R - (1-\alpha)W_4], \quad (10)$$

$$H_4(t_T) = H_T \text{ given, } t_T \text{ free.} \quad (11)$$

The optimal solutions, $H_4^*(t)$ and $W_4^*(t)$, during the critical unhealthy phase, assuming that the severe unhealthy phase switches to the critical unhealthy phase when time t_T is surpassed, are determined by the following expressions.

$$W_4^*(t) = \frac{x_2 AS\Omega}{\alpha-1}[H_T - \frac{\frac{iR}{\alpha-1} - NN}{uu}]e^{x_2(t-t_T)} - \frac{R}{\alpha-1}, \quad (12)$$

$$H_4^*(t) = [H_T - \frac{\frac{iR}{\alpha-1} - NN}{uu}]e^{x_2(t-t_T)} + \frac{\frac{iR}{\alpha-1} - NN}{uu}, \quad (13)$$

where, $x_2 = \frac{i - \sqrt{i^2 + 4uu\frac{\alpha-1}{\Omega AS}}}{2} < 0$, $G_2 = \frac{\beta\eta\varepsilon b\psi}{AS}$, $G_3 = b\psi\pi(1 - n + n_w)$, $G_5 = \frac{RG_3}{k} + \frac{(1-\alpha)gG_3}{k} + G_3(1-\alpha)C_0 - G_2(1-\alpha)$, $G_6 = \frac{\theta\gamma}{[H_T - H_B]^2}$, $G_7 = G_3(1-\alpha) - 1$, $G_8 = 1 - 2G_3(1-\alpha)$, $uu = \frac{ikC_1G_7}{G_8} + \frac{2mkG_6}{\Omega G_8}$, and $NN = -\frac{ig}{G_8} - \frac{ikC_0}{G_8} + \frac{ikG_5}{G_8} - \frac{kG_7C_1R}{\Omega ASG_8} - \frac{mkG_3RC_1}{\Omega G_8} - \frac{2mkG_6H_B}{G_8}$.

The proof of sub-problem 4 can be found in Appendix 2. This paper is the first to explicitly link GDE health stress to the combined effects of LS and groundwater decline, establishing a dual-stressor framework for GDE vulnerability. From a policy perspective, this provides decision-makers with a new tool to internalize the ecological costs of unsustainable groundwater use.

While Ndahangwapo et al. (2024) examined taxes on LS and storage capacity loss, their framework did not incorporate GDE health. Similarly, Esteban and Albiac (2011) analyzed taxes targeting ecosystem damages from falling water tables but excluded the role of LS. The optimal solutions derived in this framework support the design of integrated groundwater governance strategies that better align hydrological management with GDE protection, particularly in regions where LS poses an additional threat to ecosystem viability.

Two types of Pigouvian taxes examined. The first is β, a Pigouvian tax charged per unit of land sinking, which directly internalizes the economic costs associated with LS. The second is a tax on each cubic meter of aquifer storage capacity lost, denoted by $\phi(W, H)$, which internalizes the storage capacity loss externality. Together, these taxes provide complementary approaches to incentivize sustainable groundwater use and mitigate damages to GDEs. In addition, Propositions 1-4 examine the impact of taxes on both groundwater extraction and GDEs' health. These combinations are analysed to illustrate how different Pigouvian taxes target specific ecological and hydrological externalities at various stages of ecosystem degradation, and to show how regulatory interventions can align private extraction decisions with social welfare objectives. By linking tax instruments to both water table levels and GDE health outcomes, the propositions demonstrate the effectiveness of these policies in mitigating LS, preserving aquifer storage capacity, and maintaining ecosystem function across different phases of ecosystem stress.

Proposition 1. *The Pigouvian tax per unit of land sinking (β) directly influences groundwater management in the critical unhealthy phase. A higher Pigouvian tax reduces the optimal level of groundwater extraction and raises the optimal water table level.*

The proof of Proposition 1 can be found in Appendix 3. In the critical unhealthy phase, irreversible ecological and hydrological damages emerge as external costs not borne by individual users. To correct this market failure, the regulator imposes a Pigouvian tax (β) on LS per unit of extraction. This raises the marginal cost of pumping, reduces optimal groundwater use, and maintains a higher water table. By internalizing the rising marginal damage from LS, the tax aligns private extraction decisions with social costs and helps prevent further ecological damages.

Proposition 2. *The Pigouvian tax per unit of aquifer system storage capacity loss ($\phi(W, H)$) directly influences groundwater management in the critical unhealthy phase. A higher Pigouvian tax reduces the optimal level of groundwater extraction and raises the optimal water table level.*

The proof of Proposition 2 can be found in Appendix 4. In this phase, groundwater pumping damages GDEs and reduces aquifer storage capacity. A Pigouvian tax ($\phi(W, H)$) internalizes the social cost of storage capacity loss, raising the marginal cost of extraction. This incentivizes users to pump less, maintaining a higher water table, slowing LS, and preserving aquifer capacity.

Since the solution to sub-problem 4 is obtained, we solve for a solution to sub-problem 3 (SP_3). Following Raouf et al., (2003); Boucekkine et al., (2004); and Dinar et al., (2020), we impose the following matching conditions for optimality and continuity.

$$\lambda_3^*(t_T, W_3^*(t_T), H_3^*(t_T)) = \lambda_4^*(t_T, W_4^*(t_T), H_4^*(t_T)) \tag{14}$$

$$\mathcal{H}_3^*(t_T) = \frac{\partial SP_4^*(t_T, W_4^*(t_T), H_4^*(t_T))}{\partial t_T}, \tag{15}$$

where $SP_4^*(\cdot)$ represents the optimal solution to sub-problem 4. The variable $\mathcal{H}_4$ represents the hamiltonian for sub-problem 4. As a result, sub-problem 3 is given by

$$\max_{W_3, H_3, t_c} \int_{t_c}^{t_T} e^{-it}[\frac{W_3^2}{2k} - \frac{gW_3}{k} - (C_0 + C_1 H_3)W_3$$

$$+\theta(\frac{\rho-\gamma}{(d_c)^2} \cdot (H_3 - LS(H_3) - H_T + LS(H_T))^2 + \gamma) - \beta \cdot LS(W_3)]dt + SP_4^*(H_T^*, t_T), \tag{16}$$

subject to

$$\dot{H}_3 = \frac{1}{AS}[R - (1-\alpha)W_3], \tag{17}$$

$$H_3(t_c) = H_c \text{ given}; \;\; H_3(t_T) = H_4(t_T) = H_T; \;\; t_T \text{ free}; \;\; t_c < t \leq t_T. \tag{18}$$

The optimal solutions, $H_3^*(t)$ and $W_3^*(t)$, during the severe unhealthy phase, assuming that the unhealthy phase switches to the severe unhealthy phase when time t_c is surpassed, are determined by the following expressions.

$$W_3^*(t) = \overline{DA}\mathrm{e}^{tz_1} + \overline{DB}\mathrm{e}^{tz_2} - \frac{R}{\alpha-1}, \tag{19}$$

$$H_3^*(t) = \frac{(\alpha-1)\overline{DA}}{ASz_1} \mathrm{e}^{tz_1} + \frac{(\alpha-1)\overline{DB}}{ASz_2} \mathrm{e}^{tz_2} + \frac{\frac{iR}{\alpha-1} - NNN}{uuu}. \quad (20)$$

where $z_{1,2} = \frac{i \pm \sqrt{i^2 + 4 \cdot uuu \cdot \frac{\alpha-1}{AS}}}{2}$, $G_2 = \frac{\beta\eta\varepsilon b\psi}{AS}$, $G_9 = \frac{\theta(\rho-\gamma)}{[H_T - H_c]^2}$, $uuu = 2mkG_9 - ikC_1$, $NNN = -ig - ikC_0 - ikG_2(1-\alpha) + \frac{C_1Rk}{AS} - 2mkG_9H_T$, and

$$\overline{DB} = \frac{z_2AS}{\alpha-1} \mathrm{e}^{-z_2t_c}[H_c - \frac{\frac{iR}{\alpha-1} - NNN}{uuu} - \frac{[H_T - \frac{\frac{iR}{\alpha-1} - NNN}{uuu}] - [H_c - \frac{\frac{iR}{\alpha-1} - NNN}{uuu}]\mathrm{e}^{z_2(t_T - t_c)}}{\mathrm{e}^{z_1(t_T - t_c)} - \mathrm{e}^{z_2(t_T - t_c)}}]. \quad (21)$$

$$\overline{DA} = \frac{z_1AS}{\alpha-1} [\frac{[H_T - \frac{\frac{iR}{\alpha-1} - NNN}{uuu}] - [H_c - \frac{\frac{iR}{\alpha-1} - NNN}{uuu}]\mathrm{e}^{z_2(t_T - t_c)}}{\mathrm{e}^{z_1t_T} - \mathrm{e}^{z_1t_c + z_2(t_T - t_c)}}]. \quad (22)$$

The proof of sub-problem 3 can be found in Appendix 5. For the first time, taxes on LS (β) are applied during the severe unhealthy phase of GDEs, where stress arises from both LS and a declining water table. Unlike prior studies, this framework treats these co-occurring stressors jointly, targeting a critical stage of ecosystem degradation. For policymakers, such taxes discourage harmful extraction after critical thresholds are crossed, signaling that urgent mitigation and restoration actions are needed in severely stressed aquifers.

Proposition 3. *The Pigouvian tax per unit of land sinking (β) directly influences groundwater management in the severe unhealthy phase. A higher Pigouvian tax reduces the optimal level of groundwater extraction and raises the optimal water table level.*

The proof of Proposition 3 can be found in Appendix 6. The Pigouvian tax (β) on LS internalizes the external cost of subsidence, raising the marginal cost of extraction and reducing groundwater pumping. This maintains a higher water table, preserves ecological function, and slows further subsidence. Since subsidence is still reversible in this phase, the tax provides a cost-effective intervention that prevents escalation into the critical unhealthy phase.

Proposition 4. *The Pigouvian tax per unit of land sinking (β) has a direct impact on the optimal*

GDEs' health in the severe unhealthy phase. The higher the Pigouvian tax the higher the optimal level of the GDEs' health.

The proof of Proposition 4 can be found in Appendix 7. Increasing the Pigouvian tax (β) on LS raises the marginal cost of pumping, reducing extraction, subsidence, and maintaining a higher water table. Because GDEs' health depends on groundwater depth, this leads to improved ecological outcomes and higher optimal GDE health. Thus, the tax acts as both a corrective and proactive tool, protecting ecosystem services efficiently before irreversible thresholds are crossed.

Since the solution to sub-problem 3 is obtained, we solve for a solution to sub-problem 2 (SP_2). Likewise, we impose the following matching conditions for optimality and continuity.

$$\lambda_2^*(t_c, W_2^*(t_c), H_2^*(t_c)) = \lambda_3^*(t_c, W_3^*(t_c), H_3^*(t_c)) \tag{23}$$

$$\mathcal{H}_2^*(t_c) = \frac{\partial SP_3^*(t_c, W_3^*(t_c), H_3^*(t_c))}{\partial t_c}, \tag{24}$$

where $SP_3^*(\cdot)$ represents the optimal solution to sub-problem 3. The variable $\mathcal{H}_3$ represents the hamiltonian for sub-problem 3. As a result, sub-problem 2 is given by

$$\max_{W_2, H_2, t_u} \int_{t_u}^{t_c} e^{-it}\left[\frac{W_2^2}{2k} - \frac{gW_2}{k} - (C_0 + C_1 H_2)W_2 + \theta\left(\frac{\delta-\rho}{(H_u-H_c)^2}\cdot(H_2-H_c)^2+\rho\right)\right]dt + SP_3^*(H_c^*, t_c), \tag{25}$$

subject to

$$\dot{H}_2 = \frac{1}{AS}[R - (1-\alpha)W_2], \tag{26}$$

$$H_2(t_u) = H_u \text{ given; } H_2(t_c) = H_3(t_c) = H_c; \; t_c \text{ free; } t_u < t \le t_c. \tag{27}$$

The optimal solutions, $H_2^*(t)$ and $W_2^*(t)$, during the unhealthy phase, assuming that the healthy phase switches to the unhealthy phase when time t_u is surpassed, are determined by the following expressions.

$$W_2^*(t) = \overline{EA}\mathrm{e}^{tq_1} + \overline{EB}\mathrm{e}^{tq_2} - \frac{R}{\alpha-1}, \tag{28}$$

$$H_2^*(t) = \frac{(\alpha-1)\overline{EA}}{ASq_1}\mathrm{e}^{tq_1} + \frac{(\alpha-1)\overline{EB}}{ASq_2}\mathrm{e}^{tq_2} + \frac{\frac{iR}{\alpha-1}-PPP}{ddd}. \tag{29}$$

where $q_{1,2} = \frac{i \pm \sqrt{i^2 + 4 \cdot ddd \cdot \frac{\alpha - 1}{AS}}}{2}$, $G_{10} = \frac{\theta(\delta - \rho)}{[H_u - H_c]^2}$, $ddd = 2mkG_{10} - ikC_1$, $PPP = -ig - ikC_0 + \frac{C_1 Rk}{AS} - 2mkG_{10}H_c$, and

$$\overline{EB} = \frac{q_2}{m} \mathrm{e}^{-q_2 t_u} [H_u - \frac{\frac{iM}{m} - PPP}{ddd} - \frac{[H_c - \frac{\frac{iM}{m} - PPP}{ddd}] - [H_u - \frac{\frac{iM}{m} - PPP}{ddd}] \mathrm{e}^{q_2(t_c - t_u)}}{\mathrm{e}^{q_1(t_c - t_u)} - \mathrm{e}^{q_2(t_c - t_u)}}]. \quad (30)$$

$$\overline{EA} = \frac{q_1}{m} [\frac{[H_c - \frac{\frac{iM}{m} - PPP}{ddd}] - [H_u - \frac{\frac{iM}{m} - PPP}{ddd}] \mathrm{e}^{q_2(t_c - t_u)}}{\mathrm{e}^{q_1 t_c} - \mathrm{e}^{q_1 t_u + q_2(t_c - t_u)}}]. \quad (31)$$

The proof of sub-problem 2 can be found in Appendix 8. These optimal solutions target the unhealthy phase of GDEs, where ecological damage is still highly reversible. This phase provides a narrow but critical window for intervention. The results guide policymakers to stabilize GDE health and slow progression toward severe degradation, offering timely, proactive strategies to prevent ecological collapse, especially in regions near tipping points.

We obtained the solution to sub-problem 2, we can solve for the solution to sub-problem 1 (SP_1). Likewise, we impose the following matching conditions for optimality and continuity.

$$\lambda_1^*(t_u, W_1^*(t_u), H_1^*(t_u)) = \lambda_2^*(t_u, W_2^*(t_u), H_2^*(t_u)) \quad (32)$$

$$\mathcal{H}_1^*(t_u) = \frac{\partial SP_2^*(t_u, W_2^*(t_u), H_2^*(t_u))}{\partial t_u}, \quad (33)$$

where $SP_2^*(\cdot)$ represents the optimal solution to sub-problem 2. The variable $\mathcal{H}_1$ represents the hamiltonian for sub-problem 1. As a result, sub-problem 1 is given by

$$\max_{W_1, H_1} \int_0^{t_u} e^{-it} [\frac{W_1^2}{2k} - \frac{gW_1}{k} - (C_0 + C_1 H_1) W_1$$

$$+ \theta(\frac{\delta - 1}{(S_l - H_u)^2} \cdot (S_l - H_1)^2 + 1)] dt + SP_2^*(H_u, t_u), \quad (34)$$

subject to

$$\dot{H}_1 = \frac{1}{AS}[R - (1 - \alpha) W_1], \quad (35)$$

$$H_1(t_0) = H_0 \text{ given}; \; H_1(t_u) = H_2(t_u) = H_u; \; t_u \text{ free}, \; 0 \le t \le t_u. \quad (36)$$

The optimal solutions, $H_1^*(t)$ and $W_1^*(t)$, during the healthy phase, are determined by the following expressions.

$$W_1^*(t) = \overline{A}e^{ty_1} + \overline{B}e^{ty_2} - \frac{R}{\alpha-1}, \tag{37}$$

$$H_1^*(t) = \frac{(\alpha-1)\overline{A}}{ASy_1}e^{ty_1} + \frac{(\alpha-1)\overline{B}}{ASy_2}e^{ty_2} + \frac{\frac{iR}{\alpha-1}-N}{u}. \tag{38}$$

Where $y_{1,2} = \frac{i \pm \sqrt{i^2+4u\frac{\alpha-1}{AS}}}{2}$, $u = 2mkG_{11} - ikC_1$, $N = -ig - ikC_0 + \frac{C_1Rk}{AS} - 2mkG_{11}S_l$, $G_{11} = \frac{\theta(\delta-1)}{[S_l-H_u]^2}$, and

$$\overline{B} = \frac{y_2AS}{\alpha-1}\left[H_0 - \frac{\frac{iR}{\alpha-1}-N}{u} - \frac{[H_u - \frac{\frac{iR}{\alpha-1}-N}{u}] - [H_0 - \frac{\frac{iR}{\alpha-1}-N}{u}]e^{y_2t_u}}{e^{y_1t_u} - e^{y_2t_u}}\right], \tag{39}$$

$$\overline{A} = \frac{y_1AS}{\alpha-1}\left[\frac{[H_u - \frac{\frac{iR}{\alpha-1}-N}{u}] - [H_0 - \frac{\frac{iR}{\alpha-1}-N}{u}]e^{y_2t_u}}{e^{y_1t_u} - e^{y_2t_u}}\right]. \tag{40}$$

The proof of sub-problem 1 can be found in Appendix 9. These results are crucial because few aquifers remain in the healthy phase, while most have already experienced irreversible LS and entered degraded states. For policymakers, this provides a rare opportunity to act proactively, maintaining the aquifer within safe ecological limits. The optimal solutions offer a preventive blueprint, enabling regions still in this phase to avoid delayed responses and stay ahead of ecological degradation. The quota system is analysed in the next subsection.

4.2 Implementation of the quotas system

An effective quota system limits groundwater extractions to remain within the aquifer's sustainable yield or ecological thresholds. To analyze its impact on GDE health and groundwater use, we introduce the constraint $W(t) \leq \widehat{W}$, with $\phi(W,H) = 0$, $\Omega = 1$, and $\beta = 0$, where $\widehat{W}$ is the quota level. The goal is to determine optimal extraction and water table levels that slow or prevent cumulative drawdown, internalizing externalities and aligning individual water use with aquifer and GDEs' health sustainability. If properly designed and enforced, the quota keeps the system in the healthy phase, preventing transition to unhealthy or critical phases. A quota is effective only if monitored, enforced, and based on ecological thresholds and realistic recharge rates. Farmers' welfare maximization is then solved subject to this quota policy.

$$\max_{W,H} \int_0^\infty e^{-it}[\frac{W^2}{2k} - \frac{gW}{k} - (C_0 + C_1 H)W + \theta(\frac{\delta-1}{(S_l - H_u)^2} \cdot (S_l - H)^2 + 1)]dt \quad (41)$$

subject to

$$\dot{H} = \frac{1}{AS}[R - (1-\alpha)W], \quad (42)$$

$$W(t) \leq \widehat{W}, \quad (43)$$

and

$$H(t) > 0;\ H(t_0) = H_0 \text{ and } H(t_u) = H_u \text{ given.} \quad (44)$$

The optimal solutions, $H^*(t)$ and $W^*(t)$, under quota restrictions to preserve the ecosystem health, are determined by the following expressions.

$$W^\star(t) = \begin{cases} \frac{r_2 AS}{\alpha-1}[H_0 - \frac{N_0 - i\frac{R}{\alpha-1}}{\overline{u}}]e^{r_2 t} - \frac{R}{\alpha-1} & N_0 \geq N_A(t) \\ \widehat{W} & N_0 < N_A(t) \end{cases} \quad (45)$$

and

$$H^\star(t) = \begin{cases} [H_0 - \frac{N_0 - i\frac{R}{\alpha-1}}{\overline{u}}]e^{r_2 t} + \frac{N_0 - i\frac{R}{\alpha-1}}{\overline{u}} & N_0 \geq N_A(t) \\ [H_0 - \frac{N_A(t) - i\frac{R}{\alpha-1}}{\overline{u}}]e^{r_2 t} + \frac{N_A(t) - i\frac{R}{\alpha-1}}{\overline{u}} & N_0 < N_A(t). \end{cases} \quad (46)$$

where $r_2 = \frac{i - \sqrt{i^2 - 4\overline{u}\frac{\alpha-1}{AS}}}{2}$, $\overline{u} = -2mkG_{11} + ikC_1$, $G_{11} = \frac{\theta(\delta-1)}{[S_l - H_u]^2}$, $N_0 = -ig - ikC_0 + \frac{C_1 Rk}{AS} - 2mkG_{11}S_l$, and $N_A(t) = H_0\overline{u} - \frac{\widehat{W}(\alpha-1)+R}{r_2 AS}e^{-r_2 t} \cdot \overline{u} + \frac{iR}{\alpha-1}$.

The proof of the quotas resolution can be found in Appendix 10. The optimal solutions illustrate the evolution of water table levels and extractions when quotas are applied early, during the healthy phase, and maintained through the planning period. By protecting GDEs from the outset, quotas can delay the system from entering unhealthy or irreversible states, ensuring sustainable groundwater use and preserving ecosystem health. This approach provides decision-makers with a strategy to maintain long-term ecological and hydrological balance, avoiding future trade-offs between water use and environmental protection. Ndahangwapo et al. (2024) showed that when a quota is applied, the planning period starts with a phase where $N_0 < N_A(t)$, followed by a phase where $N_0 \geq N_A(t)$. Since this result has already been established in the literature, proving it again here would be redundant. We therefore proceed to state the following propositions.

Proposition 5. *There exists a critical quota level $\widehat{W}_c$ such that if $\widehat{W} < \widehat{W}_c$ at the beginning of the planning period ($t = 0$), the quota remains binding ($N_0 < N_A(t)$) throughout the entire period. In contrast, if $\widehat{W} \geq \widehat{W}_c$ at the beginning of the planning period, the quota is initially non-binding ($N_0 \geq N_A(t)$), but the system eventually transitions into the binding quota phase at a finite time*

The proof of Proposition 5 can be found in Appendix 11. The quota binds when farmers want to extract more than the imposed level $\widehat{W}$, forcing their unconstrained optimum down to $\widehat{W}$, which occurs when the policy constraint is active ($N_0 < N_A(t)$). A non-binding quota occurs when the unconstrained optimum is already less than or equal to $\widehat{W}$, so the constraint is inactive ($N_0 \geq N_A(t)$). The critical quota level determines whether the quota affects optimum extractions, enabling regulators to control water use via the numerical level of the quota without heavy enforcement.

Proposition 6. *If the quota binds ($N_0 < N_A(t)$) at the start of the planning period, increasing the maximum total economic value (θ) of pristine GDEs' services lengthens the duration of the binding quota phase.*

The proof of Proposition 6 can be found in Appendix 12. A higher economic value of GDEs (θ) makes the quota more effective, causing it to bind for a longer period. In practice, if society increases θ (e.g., by legally recognising GDEs' values), the regulator can maintain the same conservation outcome with a less strict quota level.

Proposition 7. *When the quota is binding ($N_0 < N_A(t)$) for $t > 0$, there exists a maximum allowable quota level ($\widehat{W}_b$) that ensures the water table level remains above all critical thresholds for the water table height.*

The proof of Proposition 7 can be found in Appendix 13. The quota level ($\widehat{W}_b$) quantifies the maximum allowed extraction level that keeps the water table above all critical thresholds each year. In other words, ecological thresholds can be directly translated into clear, enforceable quota levels. The next subsection deals with the implementation of packaging and sequencing of policy instruments.

4.3 Packaging and sequencing of taxes and quotas

Adoption of quotas and taxes as standalone instruments has faced criticism due to high transaction costs, particularly for quotas, making them economically inefficient (Maddock and Haimes, 1975; Lenouvel et al., 2011; Esteban and Dinar, 2013). Combining quotas with taxes is often more efficient (Wetzman, 1974). For policy sequencing, one instrument may be applied first, the other later, or both simultaneously (packaging). Without intervention, optimal extraction initially exceeds steady-state levels and rises over time, making early quotas during the healthy phase effective, while taxes are not applied in the healthy and unhealthy phases. Mild taxes can signal risk and partially internalize ecological value in phase 2, but quotas are avoided in the unhealthy phase to preserve incentives for efficient water use. In the severe unhealthy phase, extraction above the quota is fully taxed, while amounts at or below the quota are untaxed. In the critical unhealthy phase, only quotas are applied to cap physical damage, since taxes alone cannot prevent collapse. Farmers, welfare is maximized as in Equation (6), subject to the new quota constraint.

$$\dot{H} = \begin{cases} \frac{1}{AS}[R-(1-\alpha)W], & \text{if } t \le t_u \\ \frac{1}{AS}[R-(1-\alpha)W], & \text{if } t_u < t \le t_c \\ \frac{1}{AS}[R-(1-\alpha)W], & \text{if } t_c < t \le t_T \\ \frac{1}{\Omega \cdot AS}[R-(1-\alpha)W], & \text{if } t > t_T. \end{cases} \tag{47}$$

$$\beta = \begin{cases} 0, & \text{if } W(t) \le \widehat{W} \text{ (and quota restriction applies)} \\ \text{tax}, & \text{if otherwise.} \end{cases} \tag{48}$$

$$\phi = \begin{cases} 0, & \text{if } W(t) \le \widehat{W} \text{ (and quota restriction applies)} \\ \text{tax}, & \text{if otherwise.} \end{cases} \tag{49}$$

$$\Omega = \begin{cases} 1, & \text{if } W(t) \le \widehat{W} \text{ (and quota restriction applies)} \\ 0 < \Omega \le 1, & \text{if otherwise.} \end{cases} \tag{50}$$

The optimal solutions to the objective function (47) and the constraints ((48), (49), and (50)) are given below.

$$W^*(t) = \begin{cases} \overline{A}\mathrm{e}^{ty_1} + \overline{B}\mathrm{e}^{ty_2} - \frac{R}{\alpha-1}, & \text{if } t \le t_u, \\ \overline{EA}\mathrm{e}^{tq_1} + \overline{EB}\mathrm{e}^{tq_2} - \frac{R}{\alpha-1}, & \text{if } t_u < t \le t_c, \\ \overline{DA2}\mathrm{e}^{tz_1} + \overline{DB2}\mathrm{e}^{tz_2} - \frac{R}{\alpha-1}, & \text{if } t_c < t \le t_T \,\&\, \overline{DA2} \le N_K(t), \\ \overline{DA}\mathrm{e}^{tz_1} + \overline{DB}\mathrm{e}^{tz_2} - \frac{R}{\alpha-1}, & \text{if } \square\square_c < t \le t_T \,\&\, \overline{DA2} > N_K(t), \\ \frac{a_2 AS\Omega}{\alpha-1}[H_T - \frac{\frac{iR}{\alpha-1}-N_1}{\overline{u1}}]\mathrm{e}^{a_2(t-t_T)} - \frac{R}{\alpha-1}, & \text{if } t > t_T \,\&\, N_1 \le N_B(t), \\ \widehat{W}, & \text{if } t > t_T \,\&\, N_1 > N_B(t). \end{cases} \tag{51}$$

$$H^*(t) = \begin{cases} \frac{(\alpha-1)\overline{A}}{ASy_1}\mathrm{e}^{ty_1} + \frac{(\alpha-1)\overline{B}}{ASy_2}\mathrm{e}^{ty_2} + \frac{\frac{iR}{\alpha-1}-N}{u}, & \text{if } t \le t_u, \\ \frac{(\alpha-1)\overline{EA}}{ASq_1}\mathrm{e}^{tq_1} + \frac{(\alpha-1)\overline{EB}}{ASq_2}\mathrm{e}^{tq_2} + \frac{\frac{iR}{\alpha-1}-PPP}{ddd}, & \text{if } t_u < t \le t_c, \\ \frac{(\alpha-1)\overline{DA2}}{ASz_1}\mathrm{e}^{tz_1} + \frac{(\alpha-1)\overline{DB2}}{ASz_2}\mathrm{e}^{tz_2} + \frac{\frac{iR}{\alpha-1}-PP}{uuu}, & \text{if } t_c < t \le t_T \,\&\, \overline{DA2} \le N_K(t), \\ \frac{(\alpha-1)\overline{DA}}{ASz_1}\mathrm{e}^{tz_1} + \frac{(\alpha-1)\overline{DB}}{ASz_2}\mathrm{e}^{tz_2} + \frac{\frac{iR}{\alpha-1}-NNN}{uuu}, & \text{if } t_c < t \le t_T \,\&\, \overline{DA2} > N_K(t), \\ [H_T - \frac{\frac{iR}{\alpha-1}-N_1}{\overline{u1}}]\mathrm{e}^{a_2(t-t_T)} + \frac{\frac{iR}{\alpha-1}-N_1}{\overline{u1}}, & \text{if } t > t_T \,\&\, N_1 \le N_B(t), \\ [H_T - \frac{\frac{iR}{\alpha-1}-N_B(t)}{\overline{u1}}]\mathrm{e}^{a_2(t-t_T)} + \frac{\frac{iR}{\alpha-1}-N_B(t)}{\overline{u1}}, & \text{if } t > t_T \,\&\, N_1 > N_B(t). \end{cases} \tag{52}$$

where, $a_2 = \frac{i-\sqrt{i^2+4\overline{u1}\frac{\alpha-1}{\Omega AS}}}{2}$ <0, $G_6 = \frac{\theta\gamma}{[H_T-H_B]^2}$, $\overline{u1} = -ikC_1 + \frac{2mkG_6}{\Omega}$, $N_1 = -ig - ikC_0 + \frac{kC_1R}{\Omega AS} - 2mkG_6H_B$, and $N_B(t) = \frac{\overline{u1}[\widehat{W}(\alpha-1)+R]}{a_2 AS\Omega}\mathrm{e}^{-a_2(t-t_T)} - H_T\overline{u1} + \frac{iR}{\alpha-1}$.

$$\overline{DB2} = \frac{z_2 AS}{\alpha-1}\mathrm{e}^{-z_2 t_c}[H_c - \frac{\frac{iR}{\alpha-1}-PP}{uuu} - \frac{[H_T-\frac{\frac{iR}{\alpha-1}-PP}{uuu}]-[H_c-\frac{\frac{iR}{\alpha-1}-PP}{uuu}]\mathrm{e}^{z_2(t_T-t_c)}}{\mathrm{e}^{z_1(t_T-t_c)}-\mathrm{e}^{z_2(t_T-t_c)}}]. \tag{53}$$

$$\overline{DA2} = \frac{z_1 AS}{\alpha-1}[\frac{[H_T-\frac{\frac{iR}{\alpha-1}-PP}{uuu}]-[H_c-\frac{\frac{iR}{\alpha-1}-PP}{uuu}]\mathrm{e}^{z_2(t_T-t_c)}}{\mathrm{e}^{z_1 t_T}-\mathrm{e}^{z_1 t_c+z_2(t_T-t_c)}}]. \tag{54}$$

The proof of the packaging and sequencing resolution can be found in Appendix 14. The rest of the parameters were defined in the previous sections. We present three propositions about packaging and sequencing of taxes and quotas.

Proposition 8. *There exists a critical quota level* $\widehat{W}_c$ *such that if* $\widehat{W} < \widehat{W}_c$ *at the beginning of the critically unhealthy phase (*$t = t_T$*), the system is initially binding (*$N_1 > N_B(t)$*), but the system eventually transitions into the non-binding quota phase at a finite time until the end of the planning period. If* $\widehat{W} > \widehat{W}_c$ *at the beginning of the critically unhealthy phase, the quota remains unbinding throughout the entire phase.*

The proof of Proposition 8 can be found in Appendix 15. This proposition shows that even in the critically unhealthy phase, a well-chosen quota level can prevent over-extraction. If the quota level is set below the critical level, the system starts under pressure but eventually relaxes, allowing recovery into a non-binding quota regime before the planning horizon ends.

Proposition 9. *When the quota is binding (*$N_1 > N_B(t)$*) for* $t > t_T$*, there exists a maximum allowable quota level (*$\widehat{W}_k$*) that ensures the water table level remains above the aquifer bottom level (*H_B*).*

The proof of Proposition 9 can be found in Appendix 16. This proposition implies that even in the critically unhealthy phase, groundwater use can be regulated to avoid complete GDEs collapse. By capping quotas at or below $\widehat{W}_k$, policymakers can guarantee that extraction never pushes the water table to the the aquifer bottom, thus preventing irreversible damage and securing minimum ecosystem survival.

Proposition 10. *If the quota binds (*$N_1 > N_B(t)$*) at the beginning of the critically unhealthy phase, increasing the maximum total economic value (*θ*) of pristine GDEs' services shortens the duration of the binding quota phase.*

The proof of Proposition 10 can be found in Appendix 17. This proposition shows how the economic valuation of GDEs (θ) directly affects water management outcomes. When θ increases, the regulator places greater weight on conserving GDEs, which tightens the optimal extraction path. As a result, even if the quota initially binds at the start of the critically unhealthy phase, the system exits the binding regime sooner, reducing ecological stress. The next section derives the optimal solutions when there is LS but no policy interventions are in place.

4.4 LS-GDE and No policy interventions

In the absence of any policy interventions and under conditions where LS is present, we add a new constraint to equations (7) and (8). That is, we assume $\beta = \phi(W, H) = 0$, meaning no tax policy is applied. Under these conditions, the optimal extraction and water table levels, denoted by $W^*(t)$ and $H^*(t)$, are given by the following expressions.

$$W^*(t) = \begin{cases} \overline{A}e^{ty_1} + \overline{B}e^{ty_2} - \frac{R}{\alpha-1}, & \text{if } t \le t_u \\ \overline{EA}e^{tq_1} + \overline{EB}e^{tq_2} - \frac{R}{\alpha-1}, & \text{if } t_u < t \le t_c \\ \overline{DA1}e^{tz_1} + \overline{DB1}e^{tz_2} - \frac{R}{\alpha-1}, & \text{if } t_c < t \le t_T \\ \frac{v_2 AS\Omega}{\alpha-1}[H_T - \frac{\frac{iR}{\alpha-1} - \overline{N}}{\overline{a}}]e^{v_2(t-t_T)} - \frac{R}{\alpha-1}, & \text{if } t > t_T. \end{cases} \quad (55)$$

$$H^*(t) = \begin{cases} \frac{(\alpha-1)\overline{A}}{ASy_1}e^{ty_1} + \frac{(\alpha-1)\overline{B}}{ASy_2}e^{ty_2} + \frac{\frac{iR}{\alpha-1} - N}{u}, & \text{if } t \le t_u \\ \frac{(\alpha-1)\overline{EA}}{ASq_1}e^{tq_1} + \frac{(\alpha-1)\overline{EB}}{ASq_2}e^{tq_2} + \frac{\frac{iR}{\alpha-1} - PPP}{ddd}, & \text{if } t_u < t \le t_c \\ \frac{(\alpha-1)\overline{DA1}}{ASz_1}e^{tz_1} + \frac{(\alpha-1)\overline{DB1}}{ASz_2}e^{tz_2} + \frac{\frac{iR}{\alpha-1} - NNN1}{uuu}, & \text{if } t_c < t \le t_T \\ [H_T - \frac{\frac{iR}{\alpha-1} - \overline{N}}{\overline{a}}]e^{v_2(t-t_T)} + \frac{\frac{iR}{\alpha-1} - \overline{N}}{\overline{a}}, & \text{if } t > t_T. \end{cases} \quad (56)$$

where, $v_2 = \frac{i - \sqrt{i^2 + 4\overline{a}\frac{\alpha-1}{\Omega AS}}}{2}$ <0, $G_6 = \frac{\theta\gamma}{[H_T - H_B]^2}$, $\overline{a} = -ikC_1 + \frac{2mkG_6}{\Omega}$, $\overline{N} = -ig - ikC_0 + \frac{kC_1R}{\Omega AS} - 2mkG_6H_B$, $MM = \frac{R}{\Omega AS}$, $z_{1,2} = \frac{i \pm \sqrt{i^2 + 4 \cdot uuu \cdot \frac{\alpha-1}{AS}}}{2}$, $G_9 = \frac{\theta(\rho-\gamma)}{[H_T - H_c]^2}$, $uuu = 2mkG_9 - ikC_1$, $NNN1 = -ig - ikC_0 + \frac{C_1Rk}{AS} - 2mkG_9H_T$, and

$$\overline{DB1} = \frac{z_2AS}{\alpha-1}e^{-z_2t_c}[H_c - \frac{\frac{iR}{\alpha-1} - NNN1}{uuu} - \frac{[H_T - \frac{\frac{iR}{\alpha-1} - NNN1}{uuu}] - [H_c - \frac{\frac{iR}{\alpha-1} - NNN1}{uuu}]e^{z_2(t_T - t_c)}}{e^{z_1(t_T - t_c)} - e^{z_2(t_T - t_c)}}]. \quad (57)$$

$$\overline{DA1} = \frac{z_1 AS}{\alpha-1}\left[\frac{\left[H_T - \frac{\frac{iR}{\alpha-1} - NNN1}{uuu}\right] - \left[H_c - \frac{\frac{iR}{\alpha-1} - NNN1}{uuu}\right]\mathrm{e}^{z_2(t_T - t_c)}}{\mathrm{e}^{z_1 t_T} - \mathrm{e}^{z_1 t_c + z_2(t_T - t_c)}}\right]. \tag{58}$$

The proof of the “LS-GDEs and no policy intervention” resolution can be found in Appendix 18. The rest of the parameters were defined in the previous sections. The theoretical findings are illustrated through an empirical application to the Dendron aquifer system in South Africa.

5. Application to the Dendron aquifer

The Dendron aquifer system in South Africa’s Hout River Catchment, part of the Limpopo River Basin, is a crucial water source in this semi-arid region, where average annual rainfall is only $407\ mm$. Since the 1970s, both commercial and non-commercial farmers have relied on this aquifer for irrigation, with groundwater withdrawals increasing significantly over time (Ndahangwapo et al., 2024). Between 1968 and 1986, irrigated land expanded by 170%, leading to a 133% rise in groundwater extraction (Masiyandima et al., 2002). Persistent droughts and weak enforcement of groundwater regulations have further exacerbated the depletion of water levels.

GDEs are recognized by the Water Research Commission in South Africa (Colvin et al., 2003), although they are not explicitly mentioned in the National Water Act of 1998. The Act ensures water is reserved for both human and environmental needs (Rohde et al., 2017). However, its emphasis on surface water and lack of clear distinction between surface and groundwater has limited effective consideration of GDEs in water management (Aldous and Bach, 2011). Land subsidence (LS), caused by excessive groundwater extraction, has been observed in Dendron, particularly in areas with clay sediments prone to compaction (Oosthuizen & Richardson, 2011). Over-extraction has also negatively affected groundwater-dependent ecosystems (GDEs), such as riparian forests in the Limpopo River's seasonal alluvial systems, which are highly sensitive to water table declines (Colvin et al., 2007). The region’s economy, heavily dependent on agriculture, faces rising irrigation costs as water tables drop. Though the National Water Act of 1998 mandates permits for borehole irrigation, weak enforcement has allowed over-extraction to persist (Fallon et al., 2018). Despite annual groundwater assessments, water levels continue to decline, further degrading GDEs.

The aquifer's vulnerability is compounded by its geology and hydrology. Fine-grained clay sediments make it particularly prone to subsidence under excessive pumping. The aquifer's estimated storage capacity is 124 million cubic meters, but most usable groundwater is found in the lower fractured zone, as the upper weathered zone has dried out (Jolly, 1986). This over-reliance on the deeper aquifer increases the risk of depletion. Without stricter enforcement of water regulations and sustainable management strategies, groundwater over-extraction, land subsidence, and ecosystem degradation will continue to threaten both the region's ecological health and its agricultural viability. Below is the table with the hydrological and economic values of the Dendron aquifer system as obtained from the mentioned sources.

Table 1. Hydrological and economic values of the Dendron aquifer system.

Parameter	Description	Units	Value	Source
k	Water demand slope	$\$/Mm^3$	-0.0425	Ndahangwapo et al. (2024)
g	Water demand intercept	$\$/Mm^3$	62	Ndahangwapo et al. (2024)
C_0	Pumping costs intercept	$\$/Mm^3$	5209.84	Ndahangwapo et al. (2024)
C_1	Pumping costs slope	$\$/Mm^3\ m$	-3.94	Ndahangwapo et al. (2024)
α	Return flow coefficient	dimensionless	0.2	Jolly (1986)
H_0	Current water table	m	1224.5	Fallon et al. (2018)
H_{T}	Critical water table level	m	1189.5	Ndahangwapo et al. (2024)
R	Natural recharge	$Mm^3/year$	7.35	Jolly (1986)
A	Aquifer system area	km^2	1600	Masiyandima et al. (2002)
S	Storativity coefficient	dimensionless	0.0025	Masiyandima et al.

				(2002)
i	Social discount rate	%	0.08	Conningarth Economists (2014, pp.69-70).
β	Pigouvian tax per unit of land sinking	$\$/\mathrm{m}$	1,245	Ndahangwapo et al. (2024)
η	Water density	Kg/m^3	1000	Wade et al. (2018)
b	Aquifer system's thickness	m	110	Masiyandima et al. (2002)
ψ	Aquifer system's compressibility	ms^2/kg	5.1×10^{-10}	Ndahangwapo et al. (2024)
n	Porosity	dimensionless	0.34	Woessner and Poeter (2020)
ε	Gravitational acceleration	m/s^2	9.81	Wade et al. (2018)
n_w	Vadose moisture/ Total volume	dimensionless	0.1	Jolly (1986)
π	Unit weight of water	N/m^3	9810	Poland and Davis (1969)
θ	Ecosystem services annual economic value	$Million$ $	2.53	Authors
H_B	Aquifer bottom	$m.a.s.l$	1169.5	Authors
H_u	Unhealthy phase critical threshold	$m.a.s.l$	1200.5	Authors
δ	Unhealthy phase critical threshold	dimensionless	0.5	Esteban et al. (2021)
ρ	Severe unhealthy phase critical threshold	dimensionless	0.35	Authors
γ	Critical unhealthy phase critical threshold	dimensionless	0.15	Authors
H_c	Severe unhealthy phase critical threshold	$m.a.s.l$	1191.5	Ndahangwapo et al. (2024)

H_T	Critical unhealthy phase critical threshold	$m.a.s.l$	1189.5	Authors

According to Ndahangwapo et al. (2024), the effective tax rate per unit of land sinking is $\beta = 1245$ US dollars, the empirical tax rate is $\beta = 3345$ US dollars, and the increase in the effective tax rate which is used for the sensitivity analysis is $\beta = 4\ Million$ US dollars. We make use of the ame values. Ndahangwapo et al. (2024) determined that the effective groundwater abstraction quota for the Dendron aquifer, when excluding the effects of land subsidence and ecosystem health considerations, is approximately $10\ Mm^3/year$. By contrast, the prevailing quota of $14\ Mm^3/year$ was found to be unsustainable and ineffective in safeguarding the long-term viability of the aquifer system. For the purposes of the sensitivity analysis, this existing quota level will be considered alongside an alternative quota of $20\ Mm^3/year$, consistent with the approach adopted by Ndahangwapo et al. (2024).

The aquifer bottom $H_B = 1169.5\ m.a.s.l$ (Jolly, 1986). level. There is little groundwater at heights below 1169.5 meters above sea level (Jolly, 1986). Since the aquifer thickness is 110 meters, the aquifer top water table height is $1279.5\ m.a.s.l$. We assume that the GDEs' health critical threshold beyond which the GDEs' health switches to the unhealthy phase is δ=0.5 (Esteban et al., 2021). In addition, without loss of generality, we assume that the GDEs' health critical threshold beyond which the GDEs' health switches to the severe unhealthy phase is ρ=0.35, and that the GDEs' health critical threshold beyond which the GDEs' health switches to the critical unhealthy phase is γ=0.15.

We further assume that the GDEs critical threshold for the water table height beyond which the GDEs' health switches to the severe unhealthy phase is $H_T = 1189.5\ m.a.s.l$, just 20 m before the aquifer bottom (Ndahangwapo et al., 2024). The GDEs critical threshold for the water table height beyond which the GDEs' health switches to the critical unhealthy phase is $H_c = 1191.5\ m.a.s.l$. We were unable to find an exact economic value of the ecosystem services provided by the Dendron Aquifer from the literature. Therefore, we used the carbon sequestration value from the Mogale's Gate Biodiversity Centre as a proxy. The Mogale's Gate

Biodiversity Centre, a game reserve in Gauteng province, South Africa, hosts approximately 702 plant species (Mudavanhu et al., 2017). The estimated economic value of carbon sequestration at the reserve is approximately 2,538,658 US dollars. GDEs, such as wetlands and riparian forests, play a key role in carbon sequestration. Their stable groundwater supports plant growth and the accumulation of carbon-rich soils, storing carbon for centuries. If groundwater is depleted, this stored carbon can be released as CO_2 and methane.

6. Results and discussions

This section compares three groundwater management policy instruments, Pigouvian taxes, withdrawal quotas, and their combined use involving the packaging and sequencing of taxes and quotas. The focus is on how each policy intrument affects groundwater conservation, farmers' welfare, and ecosystem health under land subsidence impacts.

6.1 Base case scenario (No LS, no GDEs scenario and no policy interventions)

A 600-year planning horizon is adopted, as the system converges to a steady state within this period. We observe (Figure 2) groundwater extractions rising sharply during the first 50 years. After that, there is a sharp decline for about 14 years, followed by a more gradual decline until the system eventually reaches a steady state. During the first 50 years, as groundwater extraction expands, water becomes physically scarcer. Extractions rise beyond the natural recharge rate of $7.35\,Mm^3$ per year, which means future groundwater use must fall. Economically, the falling water table pushes up pumping costs, continuously making groundwater increasingly expensive. At its highest, extraction peaks at $60\,Mm^3$ in year 50, then declines until stabilizing. Over the whole planning period, the water table keeps falling because the annual extractions are comparatively higher than the annual recharge. For example, in year 500 extraction is $9.32\,Mm^3$, above the $7.35\,Mm^3$ annual recharge. This reflects the over-exploitation of the aquifer, a finding also highlighted by Ndahangwapo et al. (2024).

Between years 50 and 64, extractions fall sharply. This is because the marginal cost of extraction (MEC) is rising rapidly as the water table falls steeply, making each unit of groundwater far more expensive to lift. Farmers respond by cutting back water use to avoid unprofitable costs. After year 64, the rise in extraction costs slows down. By then, the water table may have stabilized in a deeper zone, so additional declines are slower. That means the incremental cost of pumping (MEC) is still rising, but at a slower rate. This explains the gradual decline in extractions until the steady state is reached.

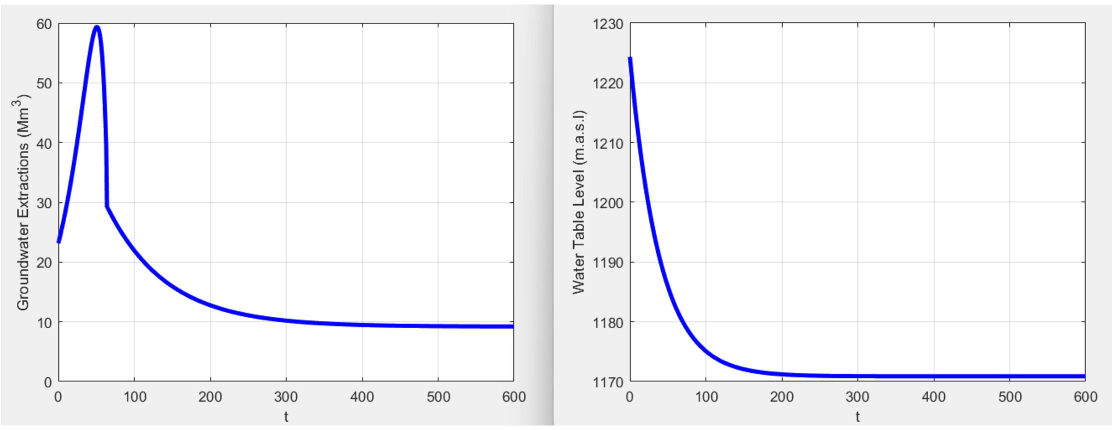

Figure 2 (a). Optimal paths of groundwater extractions and water table levels under the baseline scenario.

Under the current calibration, with a constant natural recharge of $R = 7.5Mm^3$ per year, the aquifer never recovers. The recharge is too small relative to the rate of pumping, causing $H(t)$ to continue declining over time. The water table begins to rise only when pumping is reduced to a level at which recharge plus return flow exceed total extraction. This condition is satisfied only when annual pumping declines below the equilibrium groundwater extraction level, $\frac{R}{\alpha-1}$. Thus, no increase in the water table level is observed throughout the planning horizon.

We account for uncertainty in the natural recharge rate ($R \approx 7.5\ Mm^3$) by conducting a Monte Carlo simulation in which R varies according to historical rainfall variability in the Dendron area. Gridded rainfall data (1900–2015), extracted using the area's geographic coordinates, were used to characterise this variability. A Gamma distribution was selected because it provided the best fit to the rainfall dataset and is widely applied in modelling rainfall and groundwater recharge (e.g., Husak et al., 2007; Bermudez et al., 2017; Martinez-Villalobos and Neelin, 2019; Sen, 2019; Ximenes et al., 2021). Further details on the simulation procedure and datasets are provided in Appendix 20. All the simulations were run 300 times in all sections.

Across 300 simulated recharge realizations, extraction initially rises sharply before declining toward a long-run level (Figure 2(b)). We observe (Figure 2(c)) that sample extraction paths (thin red lines) demonstrate that uncertainty in recharge generates a wide dispersion in short-run extraction rates, with some realizations showing rapid declines and others stabilizing more gradually. Despite this variability, the mean extraction path (thick red line) converges to approximately 9.6 Mm^3/year by around $t \approx 350 - 400$, indicating the system's long-run equilibrium in the absence of management. The spread of the simulated trajectories narrows over time, suggesting that extraction becomes less sensitive to recharge uncertainty as the system approaches equilibrium.

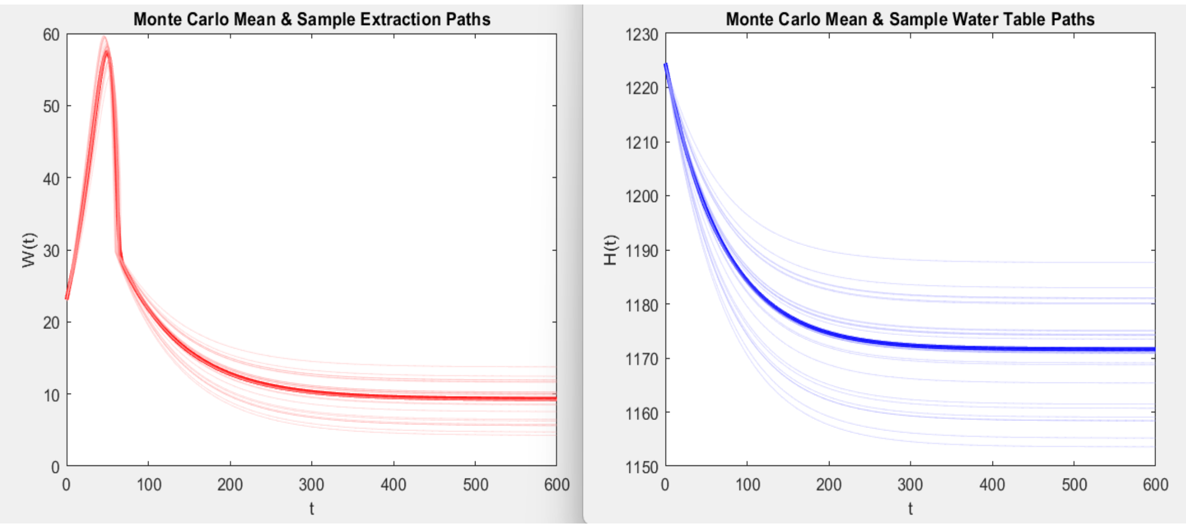

Figure 2 (b). Monte Carlo simulations of optimal groundwater extraction and water-table paths under the baseline scenario.

The simulated water-table trajectories (thin blue lines) reflect the same recharge-driven uncertainty (Figure 2(b)). Water levels decline steeply at first, with greater divergence in early periods, but gradually stabilize as the system converges toward its equilibrium level. The mean path (thick blue line) settles around $H \approx 1172.8\,m$ by $t \approx 350 - 400$. The wide initial spread reflects the dependence of early water-level dynamics on rainfall variability, whereas the later narrowing indicates that long-run groundwater conditions are more stable, even under significant recharge uncertainty when no policy constraints are present.

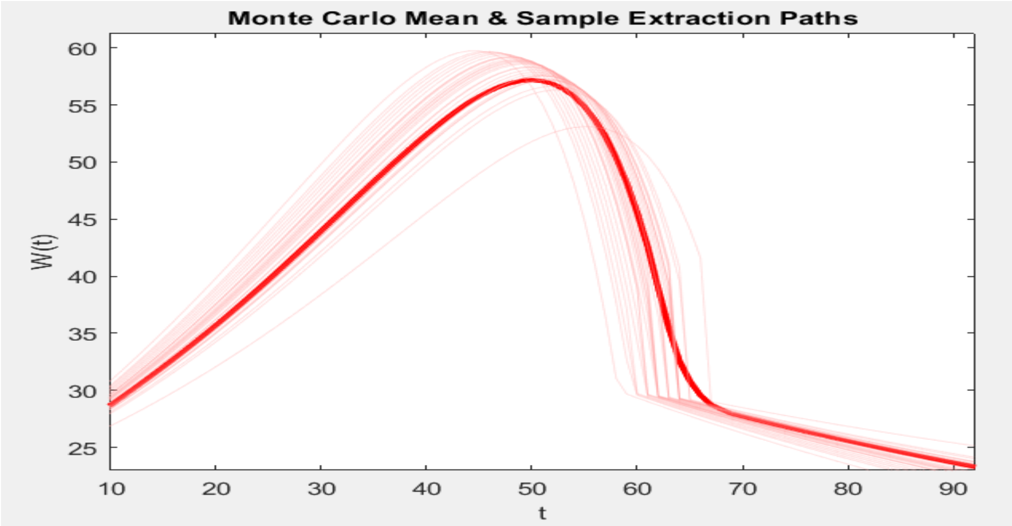

Figure 2 (c). A blow-out of the left panel of the graph in Figure 2(b) for years t = 10 to 90.

6.2 Scenario with Land Subsidence, GDEs, and No Policy Intervention

Without policy interventions under the LS and GDEs scenarios, farmers are directly affected by the loss of the aquifer system's storage capacity. We observe (Figure 3(a)) that in phase 1 (healthy phase), farmers pump aggressively because the water table is shallow, extraction costs are low, and there are no policy interventions. Extractions rise gradually to 64.5 Mm^3 (Ω = 0.4) and 59.5 Mm^3 (Ω = 0.49) before the system shifts into the unhealthy phase (phase 2), where Ω captures the impact of groundwater extraction on aquifer storage capacity. In phase 2, extractions continue increasing but now sharply, reaching peaks of 116 Mm^3 (Ω = 0.4) and 115 Mm^3 (Ω = 0.49). Entering phase 3 (severe unhealthy) in years 187 and 189, respectively, extractions fall to 101 Mm^3 (Ω = 0.4) and 94 Mm^3 (Ω = 0.49). As shown in Figure 3(b), extractions then begin to rise again once LS emerges, since LS starts in phase 3 and continues into phase 4. Even without taxes, extractions can decline in phase 3 because the system becomes more "expensive'' and "fragile'' when subsidence begins. Compaction amplifies depletion by reducing hydraulic conductivity and increasing pumping lift. Lower hydraulic conductivity slows the rate at which water can move through the aquifer, making it more difficult to sustain previous extraction levels without inducing additional drawdown. In the absence of policy intervention, farmers continue extracting heavily through phases 2 and 3 to maximize short-term profit, prioritizing immediate economic returns over long-term aquifer sustainability despite escalating ecological stress.

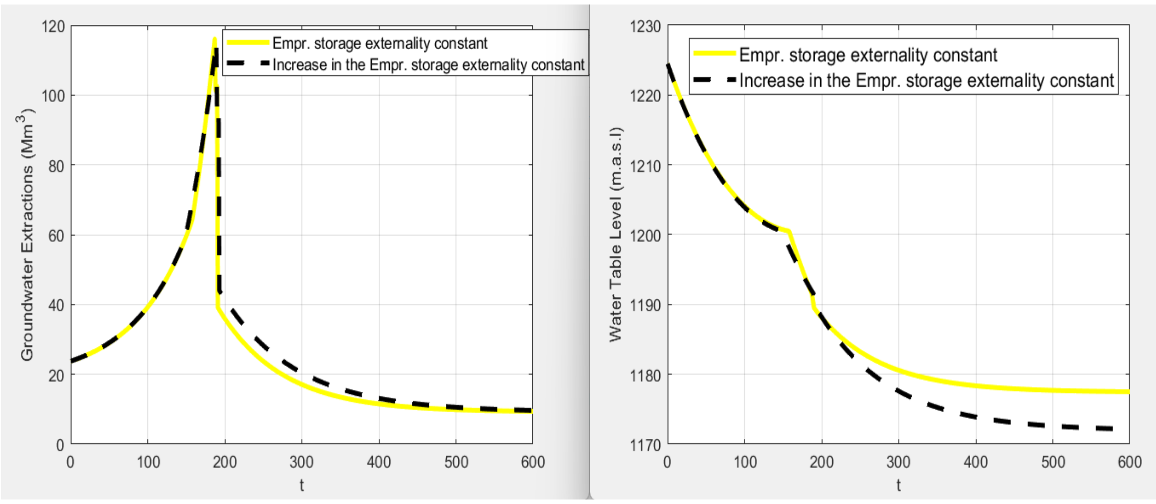

Figure 3(a). Optimal paths of groundwater extractions and water table levels under different values of the constant (Ω) representing the impact of groundwater extraction on the aquifer system's storage capacity.

Note: Yellow solid line shows the empirical constant ($\Omega = 0.4$), the black dotted line shows the increase in the empirical constant ($\Omega = 0.49$).

Inelastic compaction, which permanently reduces aquifer storage capacity, begins in phase 4 (critically unhealthy phase). The storage capacity of the aquifer system is affected by the size of the constant (Ω) in phase 4, and the larger it is, the more resistant/unaffected that area is to land sinking. This is because the smaller the LS impact, the larger the constant Ω is (Ndahangwapo et al., 2024). We observe (Figure 3(a)) that when the LS impact is small (large Ω), the aquifer is still able to release water more easily, even at deeper levels. Because the system can still supply water without severe permanent losses, the transition into the critical stage (phase 4) is delayed (Figure 3(b)). However, when the LS impact is big (small Ω), it signals that the aquifer's ability to release water has already been heavily damaged. This accelerates the system's transition into phase 4 (Figure 3(b)), because the system reaches the point of permanent compaction and reduced aquifer storage capacity much faster. With no policy interventions, farmers start with high extraction from year zero. But once storage capacity reduces, the water table falls, raising pumping costs. Farmers therefore reduce their extractions in phase 4.

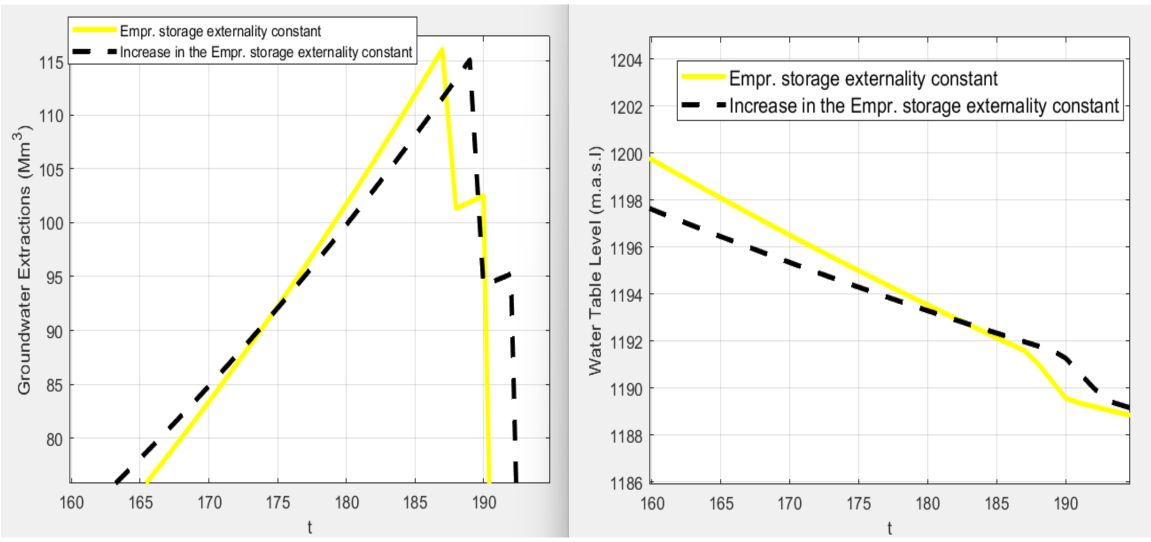

Figure 3(b). A blow-out of the graph in Figure 3(a) for years t = 160 to 190.

We observe (Figure 3(c)) that cumulative LS remains equal to zero in phases 1 and 2, regardless of the value of Ω. The reason is that in these phases, ecosystem stress comes only from declining groundwater levels since LS has not yet occurred. In phase 3, stress intensifies as it results from both further groundwater declines and rising LS caused by elastic compaction. In phase 4, stress is driven by groundwater declines, LS, and aquifer storage capacity loss.

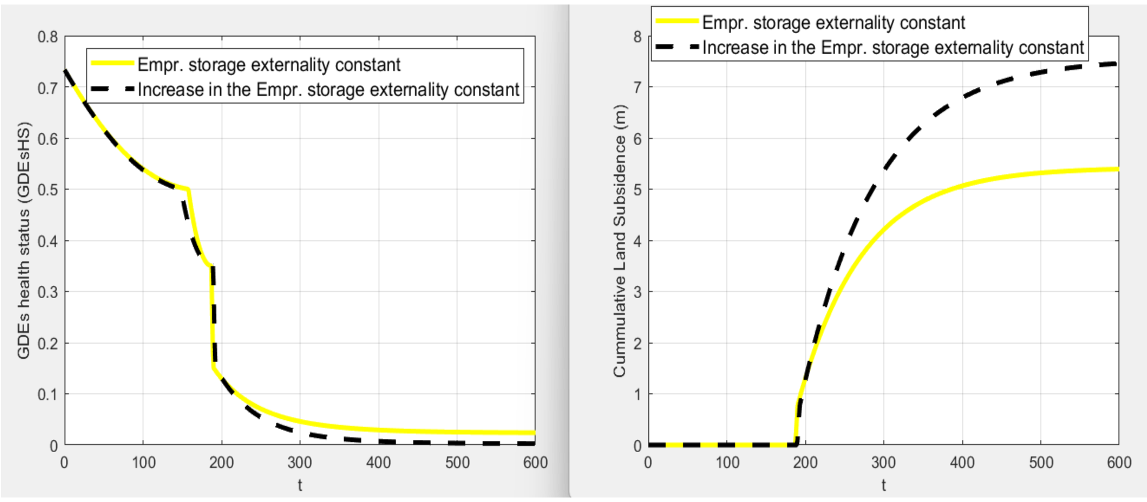

Figure 3(c). Ecosystem health status and cumulative LS under different values of the constant (Ω) representing the impact of groundwater extraction on the aquifer system's storage capacity.

Note: Yellow solid line shows the empirical constant ($\Omega = 0.4$), the black dotted line shows the increase in the empirical constant ($\Omega = 0.49$).

We observe (Figure 3(c)) that, in phase 1, when the LS impact is smaller (larger Ω), GDEs' health is similar to the case when the LS impact is larger. In phase 3, aquifer storage capacity is unaffected by LS, so the only LS effect comes through the *elastic* compaction term, which reduces the water table but does not amplify extraction costs via Ω. When Ω is small (large LS impact), the system already experienced faster drawdown and higher extraction costs in phase 2, leading to farmers reducing their extractions by the time phase 3 begins. Farmers extract more before the larger storage capacity is lost in phase 4, leading to higher extractions when Ω is small (large LS impact) compared to the case when Ω is large (small LS impact). This higher pumping increases water-table decline and rises cumulative LS, leaving GDEs' health lower in phase 3 for the larger LS-impact (small Ω) case (Figure 3(d)).

We further observe (Figure 3(d)) that the GDEs' health when the LS impact is larger (smaller Ω) suddenly rises above the health level for the case when the LS impact is smaller. This happens because extractions are lower when the LS impact is larger throughout phase 4 (Figure 3(b)). With a small Ω, the extraction costs rise rapidly as LS erodes aquifer storage capacity, causing farmers to significantly reduce pumping in phase 4. In contrast, when Ω is large and the impact of LS on aquifer storage capacity is small, extraction remains relatively inexpensive, allowing farmers to maintain higher pumping levels. Likewise, cumulative LS when the LS impact is larger is lower compared to the case when the LS impact is smaller in phase 4.

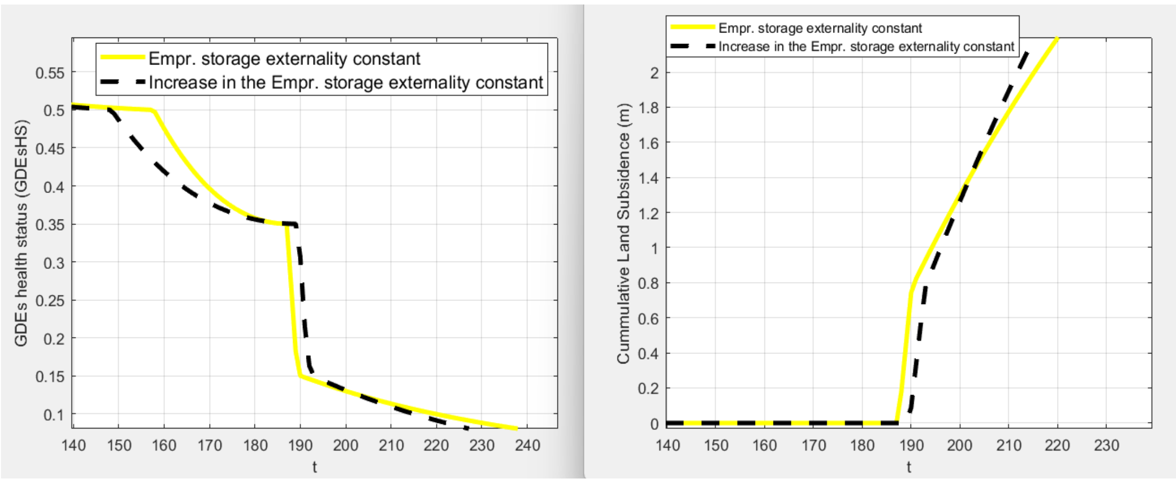

Figure 3(d). A blow-out of the right panel of the graph in Figure 3(c) for years t = 140 to 240.

We observe (Figure 3(e)) that when LS reduces the aquifer's storage capacity, the Monte Carlo results indicate that the system transitions into unhealthy ecological conditions with notable variability driven by recharge uncertainty. The mean switching time to the unhealthy phase is ≈177 years, with a relatively widespread (std = 20.3). The 10th–90th percentile range (145–198 years) shows that under some recharge realizations the system degrades much sooner, while in others the transition is delayed by several decades. This sensitivity reflects the strong influence of recharge variability when storage capacity is reduced. The transition to the severe unhealthy phase occurs shortly thereafter, with a mean of ≈191 years and lower variability (std = 8.3). The narrower percentile range (185–201 years) indicates that once the system enters the unhealthy regime, its progression toward the severe phase is much less sensitive to recharge uncertainty. Reduced storage amplifies the pace at which degradation unfolds. The shift into the critically unhealthy phase occurs at a mean of ≈208 years, again with substantial variability (std = 21.8). The 10th–90th percentile interval (188–239 years) shows that in some realizations the system reaches critical conditions soon after entering the severe phase, while in others the transition is more gradual. This reflects the combined influence of declining water-table levels and accumulating LS on GDEs' health.

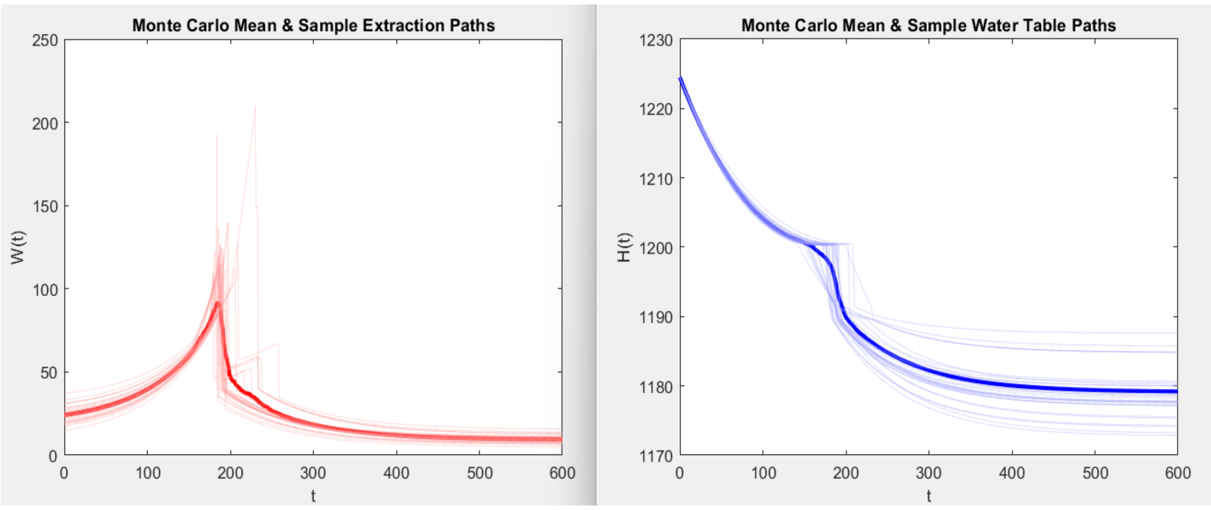

Figure 3(e). Monte Carlo simulations of optimal paths of groundwater extractions and water table levels under the effective constant ($\Omega = 0.4$) representing the impact of groundwater extraction on the aquifer system's storage capacity.

To assess how the magnitude of LS impacts on aquifer storage capacity influences the timing of ecological degradation (Figure 3(f)), we compare the mean Monte Carlo switching times for the two scenarios: (i) large LS impact on aquifer storage capacity and (ii) small LS impact. In both cases, switching times represent transitions between the unhealthy (t_u), severe unhealthy (t_c), and critically unhealthy (t_T) ecological phases. Under the small LS impact, the mean switching times occur at 176.99 years for entry into the unhealthy phase, 191.49 years for the severe unhealthy phase, and 207.65 years for the critically unhealthy phase. When the LS impact is larger, these transitions occur at 175.99 years, 190.85 years, and 203.90 years, respectively. Comparing the two scenarios shows that a larger LS impact leads to earlier switching for the first two thresholds, but importantly, an earlier transition into the critically unhealthy phase. The differences are small for t_u (≈1 year earlier) and t_c (≈0.6 years earlier), indicating that moderate improvements in aquifer storage capacity delay the onset of early ecological degradation. However, the mean t_T shifts from 207.65 years (small LS) to 203.90 years (large LS), indicating that when LS impact is smaller, the system reaches the critically unhealthy phase ~3.7 years later.

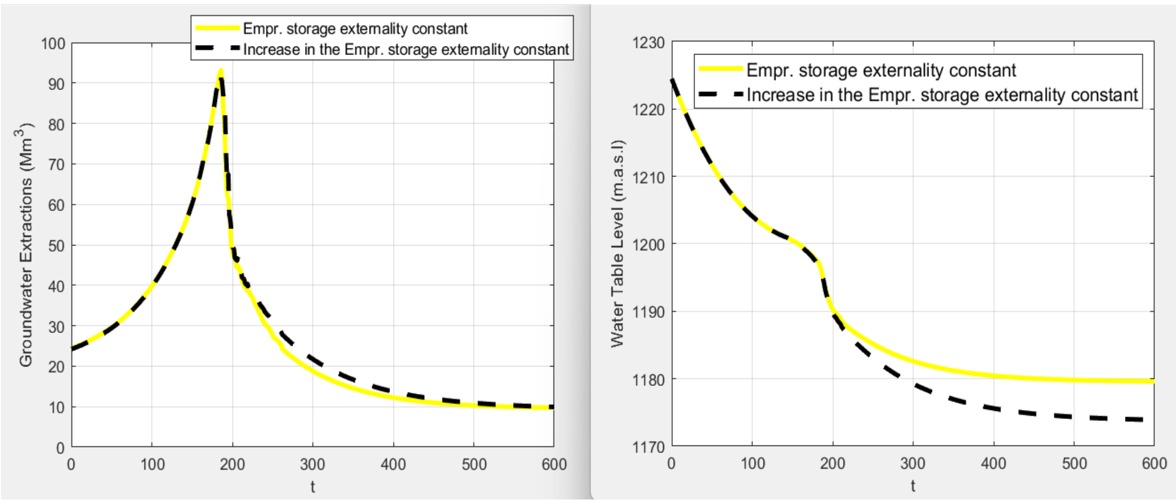

Figure 3(f). Mean Monte Carlo simulations of optimal paths of groundwater extractions and water table levels under different values of the constant (Ω) representing the impact of groundwater extraction on the aquifer system's storage capacity.

<u>Note</u>: Yellow solid line shows the empirical constant ($\Omega = 0.4$), the black dotted line shows the increase in the empirical constant ($\Omega = 0.49$).

6.3 LS - GDEs Scenario with Taxes

In our model, the parameter β represents the Pigouvian tax per unit of land sinking. This tax directly targets LS caused by farmers' groundwater extractions. We observe (Figure 4(a)) that a small increase in β do not significantly change the optimal extraction paths because of the very low compressibility of the Dendron aquifer. For illustration, a very high tax rate of $\beta = 4\ Million$ is used, following Ndahangwapo et al. (2024). We observe (Figure 4(a)) that in phase 1 (healthy phase), farmers pump aggressively throughout. Extractions rise gradually to $68.3\ Mm^3$ ($\beta = 1245$), $67.4\ Mm^3$ ($\beta = 3345$), and $30.8\ Mm^3$ ($\beta = 4\ Million$). The system shifts into phase 2 (unhealthy) in years 163 ($\beta = 1245$), 170 ($\beta = 3345$), and 207 ($\beta = 4\ Million$), where withdrawals rise sharply to $132.4\ Mm^3$ ($\beta = 1245$), $125.1\ Mm^3$ ($\beta = 3345$), and $102.1\ Mm^3$ ($\beta = 4\ Million$). The continuous increase in extractions happens because there are no policy interventions, as the tax policy applies only in phases 3 and 4 when LS begins. The severe unhealthy phase (phase 3) is entered in years 197 ($\beta = 1245$), 200 ($\beta = 3345$), and 214 ($\beta = 4\ Million$).

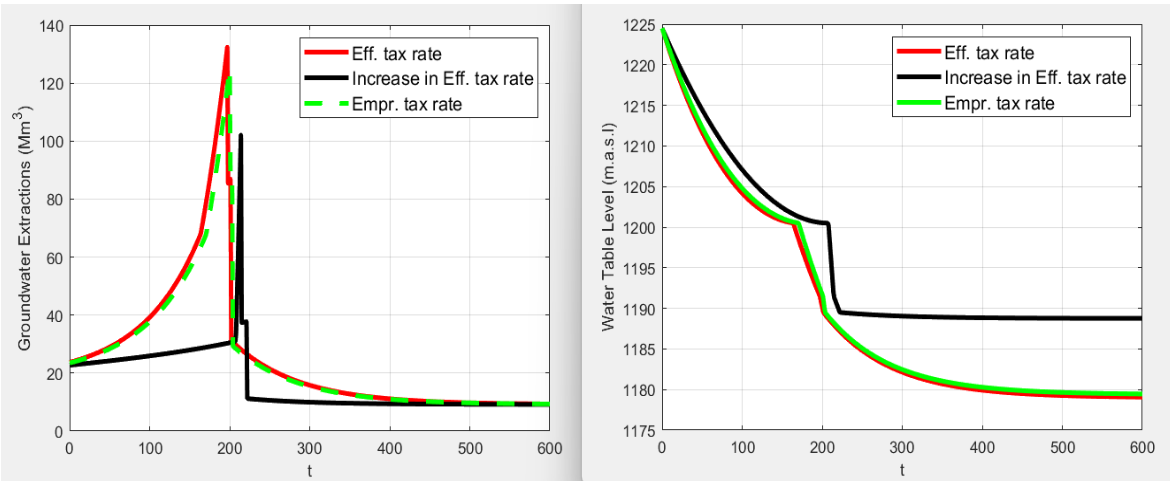

Figure 4(a). Optimal paths of groundwater extractions and water table levels under different Pigouvian tax rates per unit of land sinking.

Note: Red solid line shows the effective tax rate per unit of land sinking ($\beta = 1{,}245$), the black solid line shows the increase in the effective tax rate ($\beta = 4$ Million), and the green dotted line shows the empirical tax rates ($\beta = 3{,}345$).

We further observe (Figure 4(a) and Figure 4(b)) that higher tax rates reduce extractions and delay aquifer storage capacity loss. At the start of phase 3, with a higher tax rate ($\beta = 4\ Million$), extractions drop by $64.8\ Mm^3/year$ (from 102.1 to $37.3\ Mm^3/year$), compared to 47 $Mm^3/year$ (from 132.4 to $85.4\ Mm^3/year$) with a lower tax ($\beta = 1245$). The critical unhealthy phase (phase 4) is reached later in year 222 with a high tax ($\beta = 4\ Million$), versus year 201 with a low tax ($\beta = 1245$), delaying permanent aquifer storage loss. We also observe (Figure 4(b)) that the water table stays higher from phase 3 under a higher tax, which is good for groundwater conservation. At the start of phase 4, with a higher tax ($\beta = 4\ Million$), extractions fall to $11.2\ Mm^3/year$, compared to $31.1\ Mm^3/year$ under a lower tax rate ($\beta = 1245$). The results show that higher tax rates lead to lower extraction levels and help maintain a higher water table over time. By reducing pumping, the Pigouvian tax slows groundwater declines and delays the onset of permanent aquifer storage loss. Economically, the tax is efficient because it internalizes the external costs of land subsidence, aligning farmers' decisions with the long-term sustainability of the aquifer.

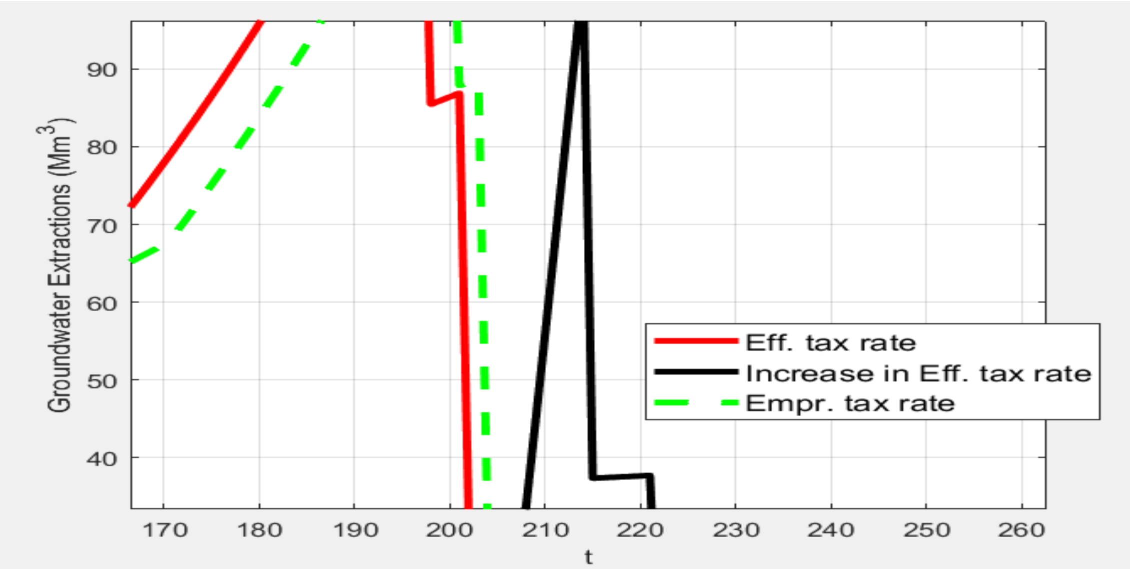

Figure 4(b). A blow-out of the left panel of the graph in Figure 4(a) for years t = 170 to 260.

The tax per unit of land sinking (β) directly targets the LS caused by farmers' groundwater extractions, which also leads to further degradation of GDEs' health. By imposing β, farmers are encouraged to reduce groundwater withdrawals, which mitigates LS and slows the decline in GDEs' health. We observe (Figure 4(c)) that GDEs' health is higher when a higher tax rate per unit of land sinking ($\beta = 4\,Million$) is applied compared to a lower tax rate ($\beta = 1245$). A higher tax rate also delays GDEs' health from entering the critically unhealthy phase. Likewise, cumulative LS is lower under a higher tax rate ($\beta = 4\,Million$) compared to the case with a lower tax ($\beta = 1245$). In conclusion, higher tax rates minimize cumulative LS, postpone the shift into the critically unhealthy phase, and lead to a higher long-run equilibrium level of ecosystem health compared to lower tax scenarios. Economically, this shows that well-calibrated Pigouvian taxes can align private incentives with ecological sustainability, preserving both aquifer function and GDEs' health while moderating long-term extraction costs.

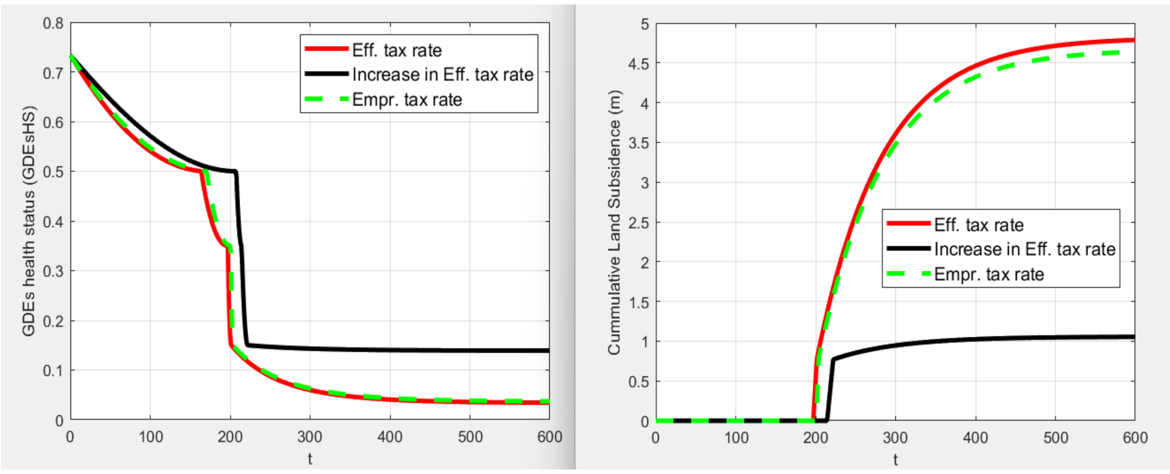

Figure 4(c). Ecosystem health status and cumulative LS under different Pigouvian tax rates per unit of land sinking.

Note: Red solid line shows the effective tax rate per unit of land sinking ($\beta = 1{,}245$), the black solid line shows the increase in the effective tax rate ($\beta = 4\ Million$), and the green dotted line shows the empirical tax rates ($\beta = 3{,}345$).

The Monte Carlo results show (Figure 4(d)) that the switching time to the unhealthy phase occurs, on average, at 188.08 years, with a standard deviation of 18.54 years. This indicates moderate variability across simulations, and the 10th–90th percentile range (159–207 years) shows that most realizations fall within this interval. The transition to the severe unhealthy phase has a mean switching time of 201.25 years and a much smaller standard deviation (8.14 years), meaning this threshold is reached within a relatively narrow window across simulations. The 10th–90th percentiles (195–208 years) confirm this tight clustering. The critically unhealthy phase occurs at a mean of 215.36 years, with a larger standard deviation (21.64 years) and a broader 10th–90th percentile range (198–247 years), reflecting greater dispersion in outcomes.

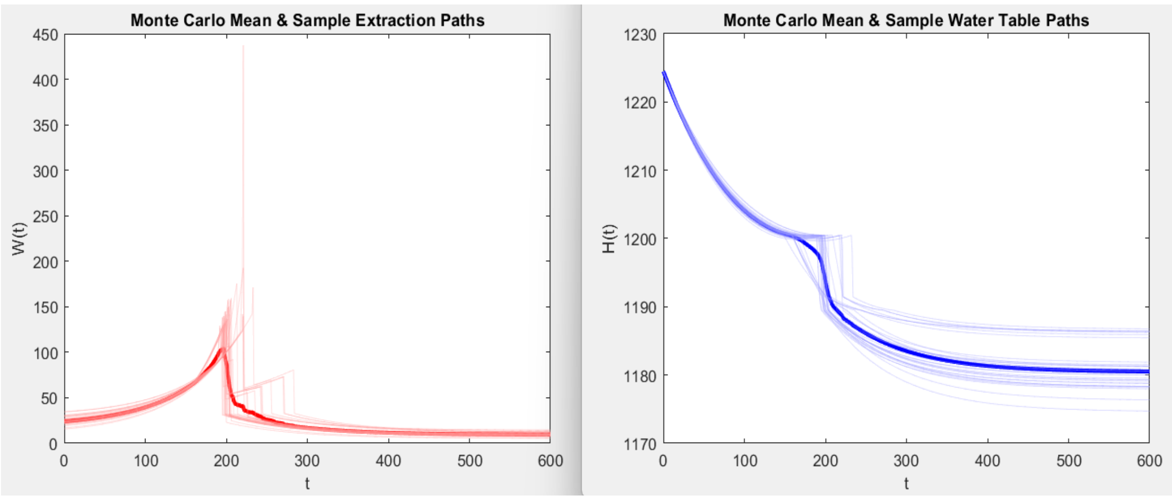

Figure 4(d). Monte Carlo simulations of optimal paths of groundwater extractions and water table levels under the effective Pigouvian tax rate per unit of land sinking ($\beta = 1{,}245$).

The switching-time statistics show that higher tax rates per unit of land sinking systematically delay the onset of ecological degradation across all three thresholds (Figure 4(e)). For β = 1245, the transition to the unhealthy phase occurs at a mean of 158.02 years (std 18.03), with the 10th–90th percentile range spanning 133–178 years. The severe unhealthy threshold is reached at a mean of 200.42 years (std 7.46), with a relatively narrow percentile interval (195–208 years), indicating low variability across simulations. The critically unhealthy transition occurs at a mean of 213.59 years, exhibiting greater dispersion (std 20.08) and a percentile range of 198–247 years.

For the much higher tax level β = 4 Million, all switching times are substantially delayed. The unhealthy-phase transition shifts to a mean of 211.29 years (std 13.62, percentiles 191–227), indicating later onset and reduced uncertainty. The transition to the severe unhealthy phase occurs at 220.22 years (std 8.10, percentiles 213–231), again showing a tightly clustered distribution. The critically unhealthy threshold is reached at a mean of 238.86 years, with a larger spread (std 19.84, percentiles 222–271), reflecting the increasing influence of recharge variability at later stages. The case β = 3345 produces the same statistical outcomes as β = 1245. Taken together, the statistics show that only the largest tax rate (β = 4 Million) generates a significant delay in switching times across all phases, whereas moderate tax levels (β = 1245 and β = 3345) yield nearly identical outcomes. This demonstrates that substantial tax strength is required to produce meaningful postponement of ecological degradation under recharge uncertainty.

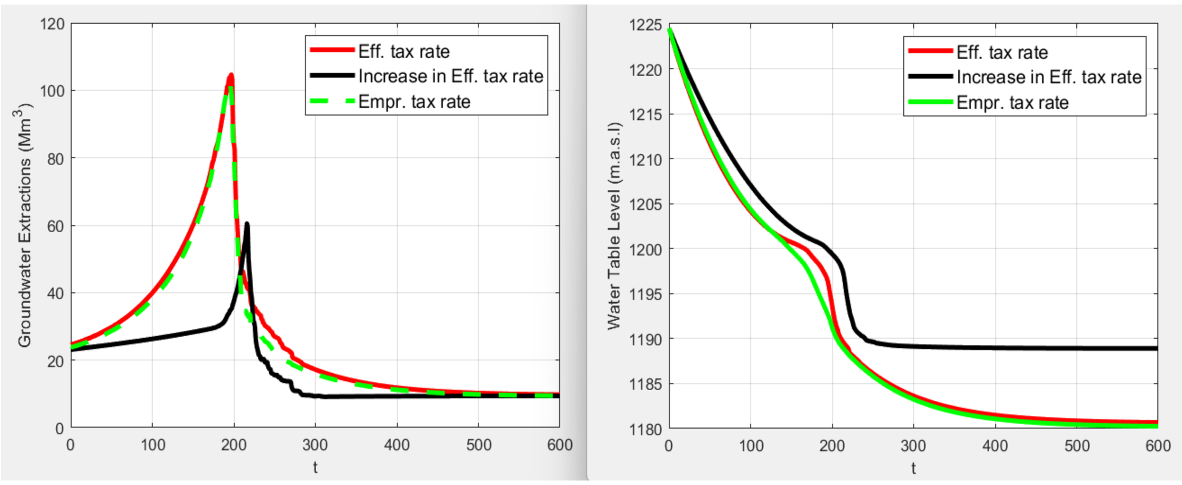

Figure 4(e). Mean Monte Carlo simulations of optimal paths of groundwater extractions and water table levels under different Pigouvian tax rates per unit of land sinking.

<u>Note</u>: Red solid line shows the effective tax rate per unit of land sinking ($\beta = 1{,}245$), the black solid line shows the increase in the effective tax rate ($\beta = 4$ Million), and the green dotted line shows the empirical tax rates ($\beta = 3{,}345$).

6.4 LS - GDEs scenario and quotas

Under the LS-GDEs scenario, groundwater extraction quotas act as a regulatory tool to control LS and safeguard ecosystem health over time. When an effective quota is applied, water table levels are better conserved compared to lower quota levels, since very reduced extractions can directly lower crop yields or livestock numbers, leading to lower revenue. Setting the quota too high is ineffective, as it permits excessive extraction, causing lower water table levels, greater LS, and faster GDEs' health degradation. We observe (Figure 5(a)) that a quota of $10\ Mm^3/year$ is the effective quota level for the Dendron aquifer, consistent with Ndahangwapo et al. (2024) findings under the LS scenario alone. These results indicate that well-calibrated groundwater quotas are essential for mitigating aquifer damage and promoting groundwater conservation, and policymakers should use localized quota thresholds to balance groundwater use with long-term ecological sustainability.

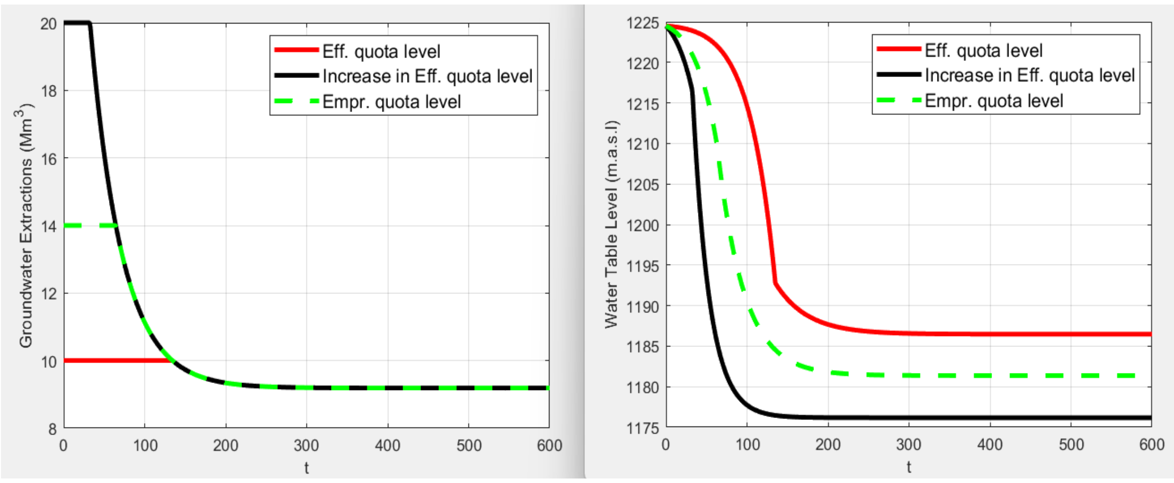

Figure 5(a). Optimal paths of groundwater extractions and water table levels under different quota levels.

<u>Note</u>: Red solid line shows the effective quota level ($\widehat{W} = 10$), the black solid line shows the increase in the effective quota level ($\widehat{W} = 20$), and the green dotted line shows the empirical quota level ($\widehat{W} = 14$).

Let us recall that the GDEsHS ranges from 0 to 1. From 1 to 0.5, GDEs are in the healthy phase; from below 0.5 to 0.35, they are in the unhealthy phase; from below 0.35 to 0.15, they are in the severe unhealthy phase; and below 0.15, they are in the critically unhealthy phase. We observe (Figure 5(b)) that applying the effective quota level ($\widehat{W} = 10$) delays the onset of both the severe and critical unhealthy phases, while maintaining a higher ecosystem health status over time. The critically unhealthy phase is reached in year 158 with $\widehat{W} = 10$, in year 105 with $\widehat{W} = 14$, and in year 65 with $\widehat{W} = 20$. Furthermore, we observe that the higher the quota level, the lower the GDEs' health level. The onset of cumulative LS marks the beginning of the severe unhealthy phase (phase 3), where LS starts to occur. Thus, we also observe that applying the effective quota level delays the onset of cumulative LS, and that higher quota levels lead to higher levels of cumulative LS.

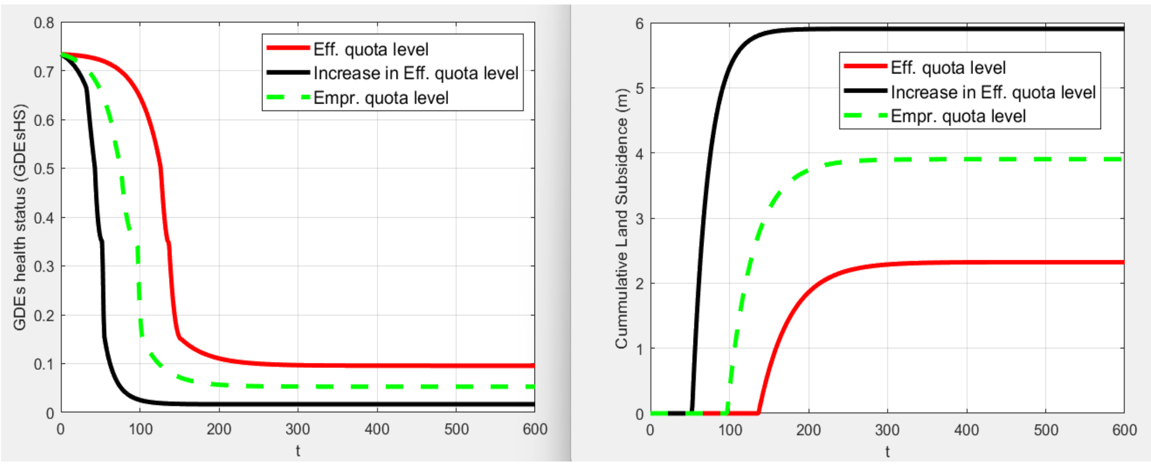

Figure 5(b). Ecosystem health status and cumulative LS under different quota levels.

Note: Red solid line shows the effective quota level ($\widehat{W} = 10$), the black solid line shows the increase in the effective quota level ($\widehat{W} = 20$), and the green dotted line shows the empirical quota level ($\widehat{W} = 14$).

The results demonstrate that stricter and effective groundwater quotas (e.g., $\widehat{W} = 10$) are economically efficient in sustaining ecosystem health and delaying costly LS. Higher quota levels accelerate ecological decline and increase cumulative subsidence, raising long-term economic damages. Thus, from a policy perspective, effective quotas not only safeguard GDEs' health but also reduce future remediation costs, making them a welfare-enhancing instrument for managing groundwater resources.

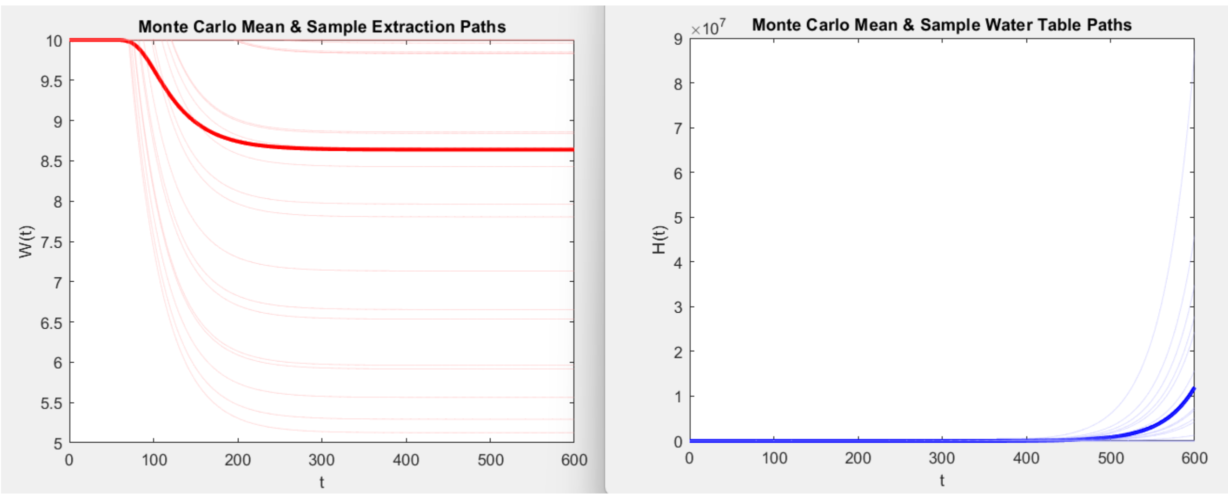

Figure 5(c). Monte Carlo simulations of optimal paths of groundwater extractions and water table levels under the effective quota level ($\widehat{W} = 10$).

The Monte Carlo results for the quota scenario show (Figure 5(c)) that the water table does not approach an equilibrium level within the 600-year simulation horizon, nor even within 2,000 years. Instead, the simulated water table height increases continuously, and by the end of the plotted period it exceeds the irrigation surface level of 1289.5 m a.s.l. This behaviour arises because groundwater extractions are constrained by the imposed quota (10 Mm^3 per year in this case). Whenever a Monte Carlo draw produces a natural recharge rate that exceeds this quota, the model's equilibrium extraction level shifts upward. Since the actual extraction remains fixed at the quota, the system removes less water than it receives, causing a net accumulation of groundwater over time. This dynamic explains the persistent upward drift in the water-table paths observed in the figure. This occurs for all quota levels considered in this paper.

6.5 LS - GDEs scenario and packaging and sequencing of taxes and quotas

The packaging and sequencing of taxes and quotas provides a refined tool for managing groundwater. It helps to limit LS and sustain GDEs' health over time. In the severe unhealthy phase (phase 3), all extractions above the quota are fully taxed. Extractions at or below the quota remain untaxed. In the critical unhealthy phase (phase 4), only quotas are used. Once a quota is imposed in phase 3, it remains in place until the end of the planning horizon. Firstly, we observe (Figure 6(a)) that under all scenarios of packaging and sequencing, extractions always exceeded the quota levels in phase 3. As a result, taxes were applied in phase 3 across all tax–quota combinations. Quotas, in contrast, were only enforced at the start of phase 4. We further observe that, throughout the planning period, the best combination is a high tax rate with a low quota level. This combination produces higher water table levels than all other tax–quota combinations. In the long run, the second best combination is the effective tax rate and effective quota level, followed by the combination of an increase in the effective tax rate and effective quota level. In the short run, the second best combination is the increase in the effective tax rate and effective quota level. We futher observe that after quotas are implemented (for both tax–quota combinations), the water table drops very gradually (from $H = 1189.5$ to the equlibirum level) when both the effective tax rate and low quota level are applied. This shows that the aquifer is responding to the quota policy, so the water table does not fall sharply as it does when a higher qupta level is applied (or the effective quota level increased).

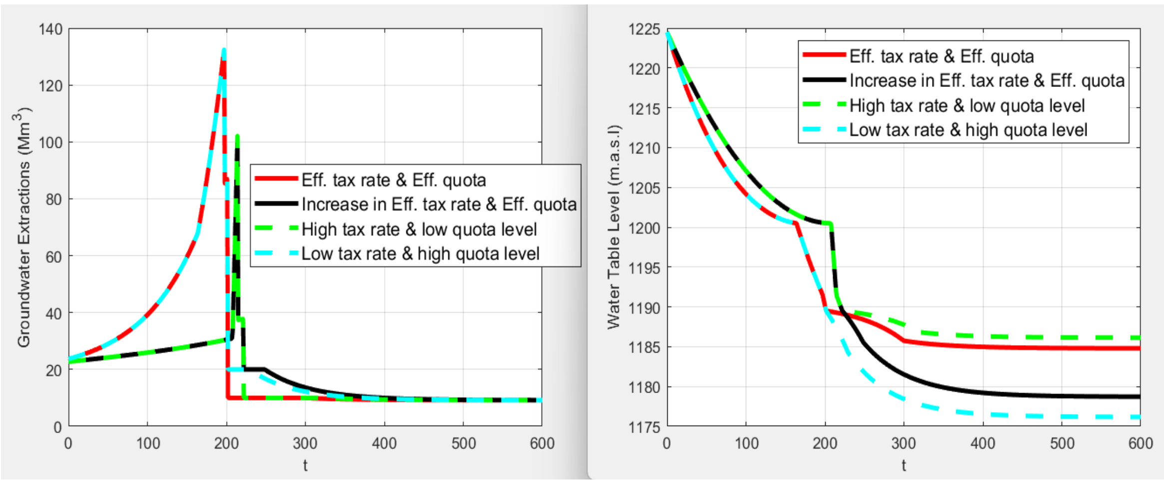

Figure 6(a). Optimal paths of groundwater extractions and water table levels when taxes and quotas are combined (under different tax rates and quota levels).

Note: Red solid line shows the effective tax rate and effective quota ($\beta = 1245, \widehat{W} = 10$), the black solid line shows the increase in the effective tax rate and effective quota level ($\beta = 4 \text{ Million}, \widehat{W} = 20$), the green dotted line shows a combination of higher tax rate and a low quota ($\beta = 4 \text{ Million}, \widehat{W} = 10$), and the light blue dotted line shows a combination of low tax rate and a higher quota ($\beta = 1245, \widehat{W} = 20$).

In addition, we observe (Figure 6(b)) that the high-tax–low-quota combination provides the highest GDEs' health over time. This combination also best delays the onset of the critically unhealthy phase. Additionally, the same combination results in the lowest cumulative LS levels over time. The results show that combining a high tax rate with a low quota is the most effective approach for protecting GDEs and limiting LS in the Dendron aquifer. Economically, this combination aligns farmers' private incentives with long-term aquifer sustainability by discouraging excessive pumping. Policy-wise, it delays the onset of critical ecological stress and permanent storage loss, reducing future remediation costs. Thus, well-designed tax–quota policies can simultaneously preserve ecosystem health and maintain groundwater resources.

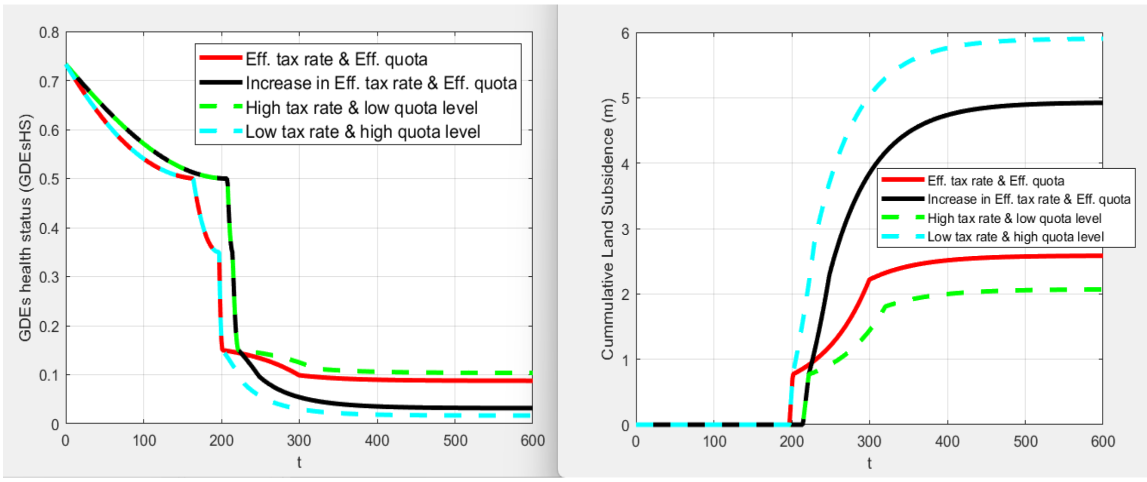

Figure 6(b). Ecosystem health status and LS when taxes and quotas are combined (under different tax rates and quota levels).

<u>Note</u>: Red solid line shows the effective tax rate and effective quota ($\beta = 1245, \widehat{W} = 10$), the black solid line shows the increase in the effective tax rate and effective quota level ($\beta =$ 4 Million, $\widehat{W} = 20$), the green dotted line shows a combination of higher tax rate and a low quota ($\beta = 4$ Million, $\widehat{W} = 10$), and the light blue dotted line shows a combination of low tax rate and a higher quota ($\beta = 1245, \widehat{W} = 20$).

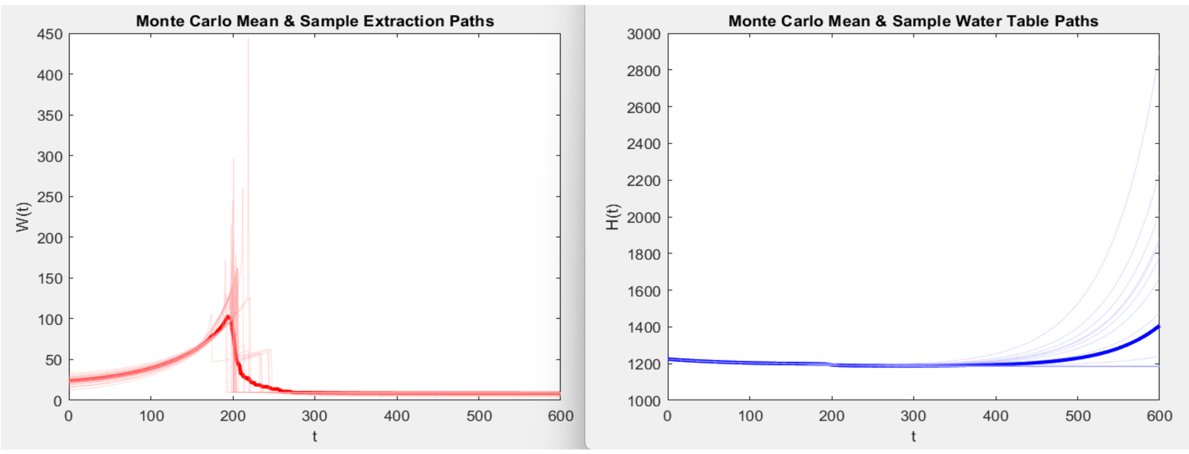

Figure 6(c). Monte Carlo simulations of optimal paths groundwater extractions and water table levels when the effective tax and the effective quota level are combined ($\beta =$ $1245, \widehat{W} = 10$).

The same results as in the Monte Carlo results for the quota scenario (Figure 5(c)) occurs here. We observe (Figure 6(c)) that the water table does not approach an equilibrium level. This behaviour arises because, in phase 4, groundwater extractions are constrained by the imposed quota level. This behaviour makes Monte Carlo simulation unsuitable for the comparative policy analysis conducted in the remaining sections of the paper. Those sections require a consistent evaluation of all policy instruments under identical hydrological conditions, including the ability to identify equilibrium water-table levels and switching times. For this reason, the subsequent sections of the paper rely solely on deterministic simulations, where equilibrium dynamics are well-defined and comparable across all management instruments.

6.6 Comparison of several policy instruments and the associated farmers' welfare

In this section, we compare different policy instruments, Pigouvian taxes, extraction quotas, and the combined approach of packaging and sequencing of taxes and quotas, against the baseline scenario and the LS with GDEs scenario without any policy intervention. Comparisons focus on effective tax rates and quota levels, as other values are non-viable. We observe (Figure 7(a)) that quotas alone are the most effective in reducing extractions and keeping higher water table levels over the planning period. Before $t = 126$, the quota policy is the best policy instrument as it outperform all other policy instruments considered by keeping higher water table levels. From $t = 126$ to $t = 201$, taxes alone and the packaging and sequencing of taxes and quotas are the best instruments. In addition, from $t = 201$ to $t = 285$, packaging and sequencing of taxes and quotas outperforms other considered policy intruments. After $t = 285$, quotas becomes the best policy instrument by keeping higher equilibrium water table levels than all other policy instruments considered.

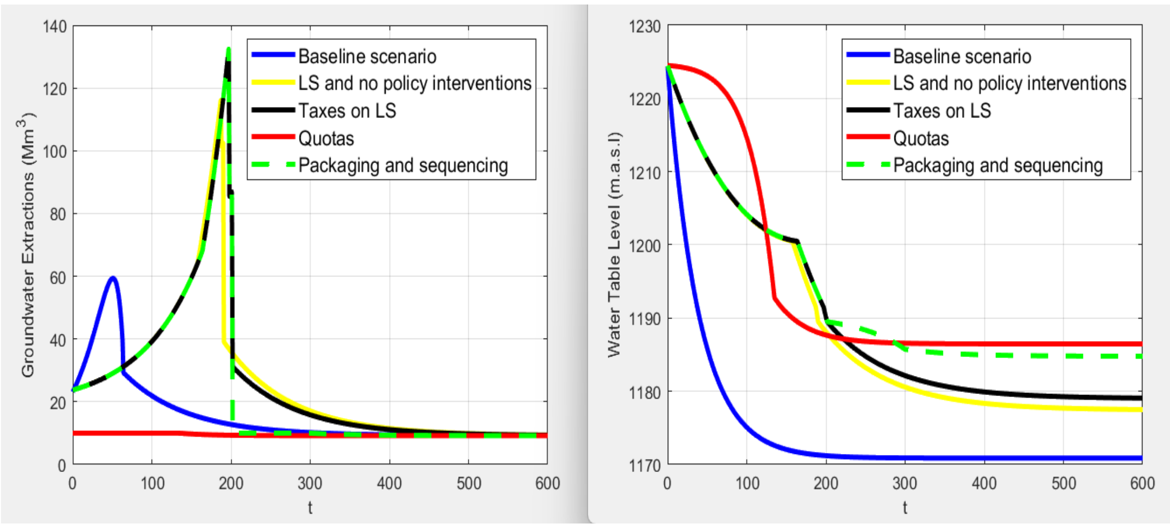

Figure 7(a). Optimal paths of groundwater extractions and water table levels under different policy instruments and scenarios (quotas, taxes, packaging and sequencing, LS and no policy interventions, and the baseline scenario).

Note: Blue solid line shows the baseline scenario. Green solid line shows the scenario for packaging and sequencing. The yellow solid line shows the scenario for LS and no policy interventions. The red solid line shows the scenario for quotas, and the black solid line shows the scenario for taxes.

We futher observe (Figure 7(a)) that some policy instruments may show lower extraction levels when approaching the steady state, but if the aquifer was exploited in the past under those policies, water table levels may still end up lower at steady state. Thus, the baseline scenario performs the worst in conserving groundwater. This outcome reflects the natural response time of aquifers. Ndahangwapo et al. (2024) explain that aquifers have a natural response time, meaning it takes time for recharge or discharge changes to affect water table levels.

From Figure 7(b), we oberve that the same ranking applies to ecosystem health and cummulative LS outcomes. Quotas help sustain ecosystem health initially by limiting over-extraction, but taxes alone and the combined tax-quota approach becomes superior after $t =$ 126 to $t = 201$, effectively minimizing LS and preserving GDEs' health. After $t = 285$, quotas becomes the best policy instrument by keeping higher GDEs' health levels than all other policy instruments considered. In addition, the quota policy results in the lowest levels of cummulative LS in the long run. From $t = 200$ to $t = 300$, combining taxes with quotas outperforms single instruments, sustaining lower levels of cummulative LS. These results demonstrate that the quota policy provide a more robust policy instrument, balancing economic and ecological objectives by reducing extraction pressures, delaying critical ecosystem stress, and delaying the onset of land subsidence over time. The results suggest that quotas alone are effective in reducing extractions and maintaining water table levels in the long term. Policies applied after heavy aquifer exploitation will not fully recover to lower levels of cummulative LS due to the aquifer's natural response time, emphasizing the need for proactive intervention. Overall, the quota policy offer the most robust approach for long-term groundwater, LS and GDEs' health management.

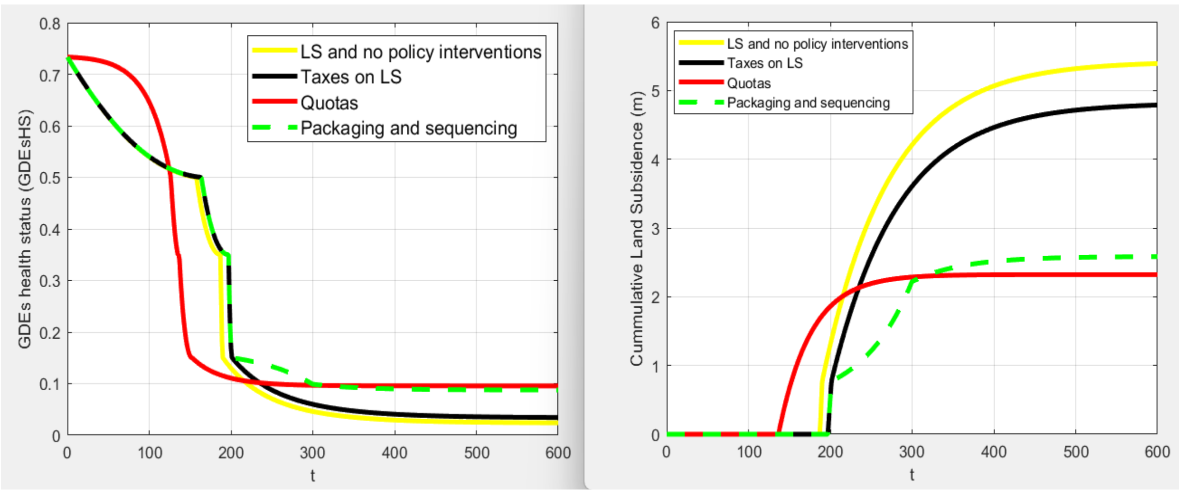

Figure 7(b). Ecosystem health status and LS under different policy instruments and scenarios (quotas, taxes, packaging and sequencing, LS and no policy interventions, and the baseline scenario).

Note: Blue solid line shows the baseline scenario. Green solid line shows the scenario for packaging and sequencing. The yellow solid line shows the scenario for LS and no policy interventions. The red solid line shows the scenario for quotas, and the black solid line shows the scenario for taxes.

The farmers' private welfare is represented by the private net benefit in the baseline scenario, where only the depth externality is considered. We observe (Figure 8) that farmers obtain positive net benefits under all three policy instruments, meaning that revenues exceed costs across the planning period. Economically, this highlights that policy interventions do not eliminate profitability but rather redistribute incentives to balance private gains with groundwater sustainability. The baseline scenario delivers the highest profit to farmers (0.4032 Million US dollars). Because there are no ecological feedbacks or policy constraints, farmers extract aggressively to maximize short-run revenue. There are no penalties from LS or GDEs' degradation, so private profit is maximized. The second-highest welfare occurs under the LS–GDEs scenario with no policy interventions (0.3415 Million US dollars). In this case, farmers still face no policy restrictions, but ecological feedbacks (LS and GDEs) reduce the effective productivity of pumping by increasing extraction costs. Profit is therefore lower than in the baseline, but still relatively high because farmers remain unconstrained by regulation.

The third-highest welfare arises under taxes alone and under packaging and sequencing of taxes and quotas (0.3414 Million US dollars). Taxation internalizes part of the ecological externality by making extraction more expensive. Farmers optimally reduce pumping to avoid high extraction or subsidence costs, leading to slightly lower profit. Packaging/sequencing has similar effects, so welfare aligns closely with taxes alone. The lowest welfare is observed under the quota policy (0.1395 Million US dollars). Quotas impose a hard cap on extraction regardless of farmers' willingness to pay and regardless of short-run profitability. This strict quantity constraint severely reduces groundwater use, limiting crop production and yielding the lowest farmers' welfare among all scenarios.

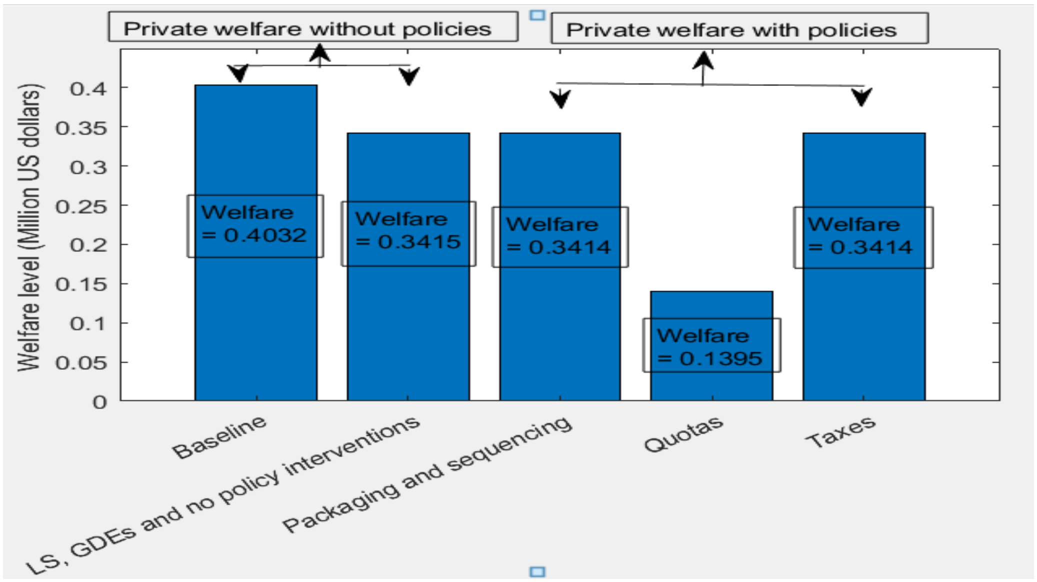

Figure 8. Farmers' private welfare under different policy instruments (taxes, quotas, packaging and sequencing, LS and no policy interventions scenario, and the private welfare (baseline) scenario).

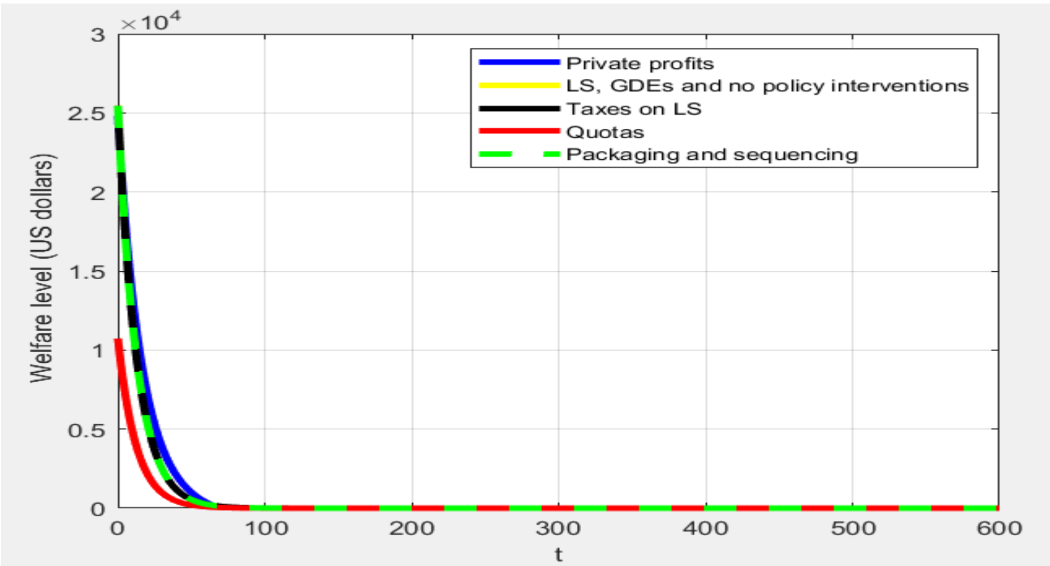

Figure 9. Farmer Disaggregated farm profits time paths under different scenarios (quotas, taxes, packaging and sequencing, LS-GDEs and no policy interventions scenario, and the private profits (No LS and no policy interventions) scenario).

<u>Note</u> Blue solid line shows the baseline scenario. Green solid line shows the scenario for packaging and sequencing. The yellow solid line shows the scenario for LS and no policy interventions. The red solid line shows the scenario for quotas, and the black solid line shows the scenario for taxes

We observe (Figure 9(a)) that across all scenarios, total economic benefits decline over time, as rising extraction costs make it harder for revenues to exceed costs. Extraction costs rise as the aquifer becomes more depleted and compaction increases pumping lift, so farm revenues increasingly fail to keep pace with rising marginal extraction costs. In the long run, the baseline scenario yields the highest total private economic benefit. Quotas produce the lowest farm profit. Binding extraction caps limit groundwater use regardless of farmers' willingness to pay, reducing crop output and leading to the lowest private economic returns among all scenarios.

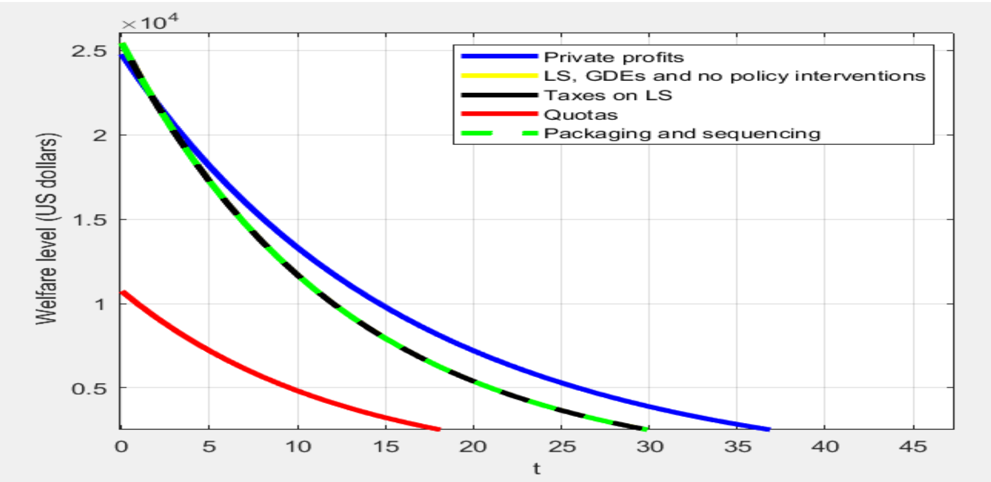

Figure 9(b). A blow-out of of the graph in Figure 9(a) for years t = 0 to 45.

We further observe (Figure 9(b)) that, in the first two years, farmers profit more under the Tax scenario, the LS–GDEs and no policy intervention scenario, and the packaging-and-sequencing approach. In early years, the aquifer is still relatively productive, and taxes or ecological feedbacks do not yet impose sufficiently large extraction costs. Farmers therefore maintain high pumping and enjoy strong short-run profits.

6.7 Sensitivity analysis (farmers' welfare)

To see how policy changes affect farmers' welfare, we run a sensitivity analysis on quotas and taxes designed to prevent LS, aquifer storage capacity loss, and GDEs' health deterioration. Using different values from earlier sections, we observe (Figure 10) that farmers' welfare rises when the quota is set at 14 Mm^3 and even more at 20 Mm^3. However, as shown in Figure

5(a), very high quotas like 20 Mm^3 do not conserve groundwater, even though they raise farmer profits. This result highlights an economic trade-off. Higher quotas benefit farmers in the short term but damage aquifers and ecosystems in the long run. For policymakers, especially in South Africa, the key challenge is to set quota levels that balance private welfare with groundwater conservation, ensuring sustainable resource use and long-term economic efficiency.

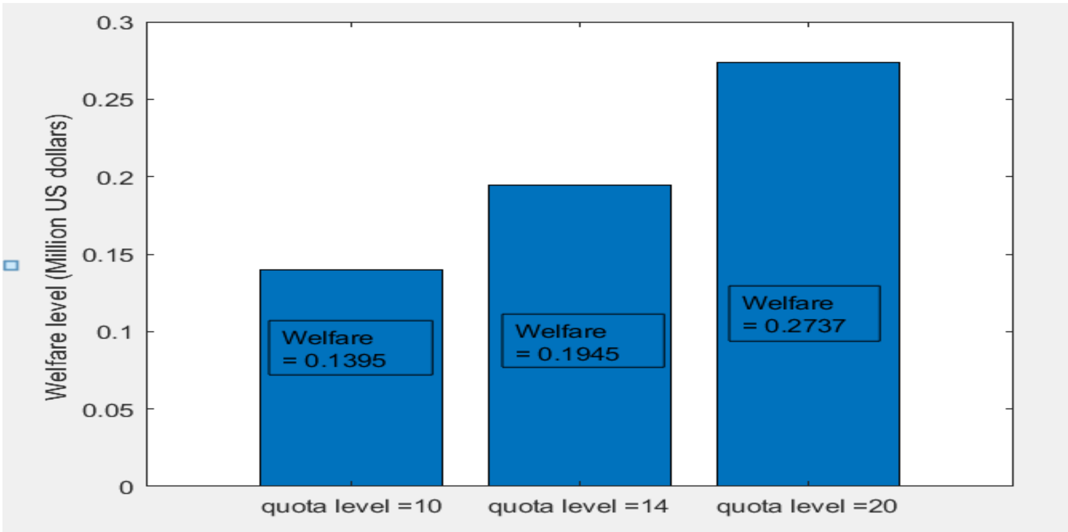

Figure 10. Farmers' private welfare under different quota levels; the effective quota level ($\widehat{W} = 10$), the empirical quota level ($\widehat{W} = 14$), and the increase in the effective quota level ($\widehat{W} = 20$).

A higher Pigouvian tax increases the marginal cost of groundwater extraction by penalizing LS more heavily. We observe (Figure 11) that, as the tax (β) rises, farmers reduce pumping earlier and more aggressively to avoid higher tax payments. This reduction in extraction lowers agricultural output and farm revenues, which outweighs the ecological benefits captured in the welfare measure. Consequently, farmers' welfare falls from 0.3414 Million US dollars ($\beta = 1245$ US dollars) to 0.3376 Million US dollars ($\beta = 3345$ US dollars) and further to 0.3189 Million US dollars ($\beta = 4$ Million US dollars), because the tax burden and loss in production dominate any gains from reduced subsidence.

Figure 11. Farmers' private welfare under different values of the Pigouvian tax per unit of land sinking (β); the effective tax rate ($\beta = 1{,}245$), the increase in the Pigouvian tax per unit of land sinking ($\beta = 4$ Million), and the empirical tax rate per unit of land sinking ($\beta = 3{,}345$).

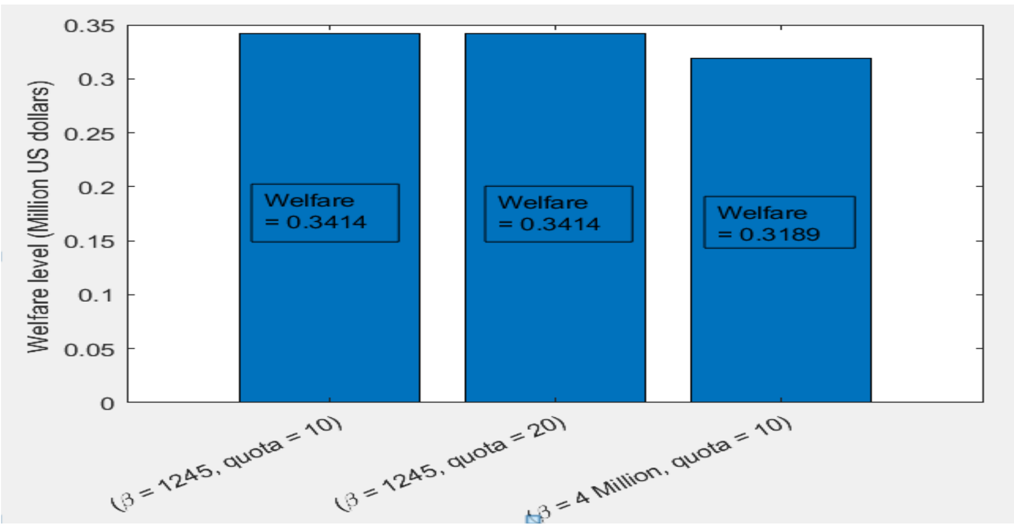

Figure 12. Farmers' private welfare when taxes and quotas are combined (under different tax rates and quota levels). The effective tax rate and effective quota level ($\beta = 1245, \widehat{W} = 10$), the increase in the Pigouvian tax per unit of land sinking ($\beta = 4$ Million$, \widehat{W} = 10$), and the increase in the effective quota level ($\beta = 1245, \widehat{W} = 20$).

We observe (Figure 12) that when taxes and quotas are combined, farmers' private welfare (0.4032 Million US dollars) declines as the Pigouvian tax per unit of land sinking increases. Therefore, farmers benefit from this combination only when the Pigouvian tax equals the effective tax rate. Economically, this indicates that excessively high Pigouvian taxes lower farmers' welfare without providing extra benefits. From a policy perspective, it suggests that combining taxes and quotas is most effective when the tax is set at the optimal effective rate, balancing private welfare with sustainable groundwater use and ecosystem health.

6.8 Social welfare with respect to LS-based externalities' costs

Social welfare is defined as the net benefit once all the negative externalities from LS are included. To measure this effect under different policy settings, we apply a damage function that monetarizes LS impacts, meaning it assigns a social cost to the environmental damages caused by LS. The damage function must be written in terms of the water table changes (ΔH, positive when the water table rises, negative when it falls). A negative change leads to LS, while a positive change means there is no LS. In our model, we adopt the quadratic damage function from Ndahangwapo et al. (2024): $D(\Delta H) = \delta \cdot \Delta H + \frac{\tau}{2}(\Delta H)^2 = \frac{\delta}{AS}(R - (1 - \alpha)W) + \frac{\tau}{2}(\frac{1}{AS}(R - (1 - \alpha)W))^2$, with $\delta > 0$ and $\tau > 0$. Here, δ and τ are scaling parameters that represent how LS externalities grow as ΔH become larger. When the change in water table is positive, the monetarized environmental damage $\Delta H + \frac{\tau}{2}(\Delta H)^2$ is also positive. When the change is negative, the outcome depends on the relative size of δ and τ. Specifically, δ must be substantially larger than τ for $\delta > \frac{\tau}{2}\Delta H$ to hold. The social benefits during the four phases of the GDEs' health are then given by the modified equation below.

$$\frac{(W^*)^2}{2k} - \frac{gW^*}{k} - (C_0 + C_1 H^*)W^* + \theta(GDEsHS(H, LS(H))) + \frac{\delta}{AS}(R - (1 - \alpha)W^*) + \frac{\tau}{2}(\frac{R - (1 - \alpha)W^*}{AS})^2 \quad (59)$$

Once calibrated, we found through simulation that social welfare is always lower than private welfare, with $\delta = 3\ Million$ and $\tau = 0.00000002$. The results (Figure 13) show that as the effective tax rate per unit of land sinking rises, social welfare falls significantly below private welfare. This indicates that a higher tax amplifies the social costs associated with LS externalities faced by farmers. This finding suggests that tax instruments need careful calibration. Excessively high tax rates may discourage efficient groundwater use without necessarily improving welfare, as they increase the burden on farmers while amplifying measured social costs. Policymakers should therefore balance tax rates to internalize externalities while still maintaining incentives for sustainable extraction.

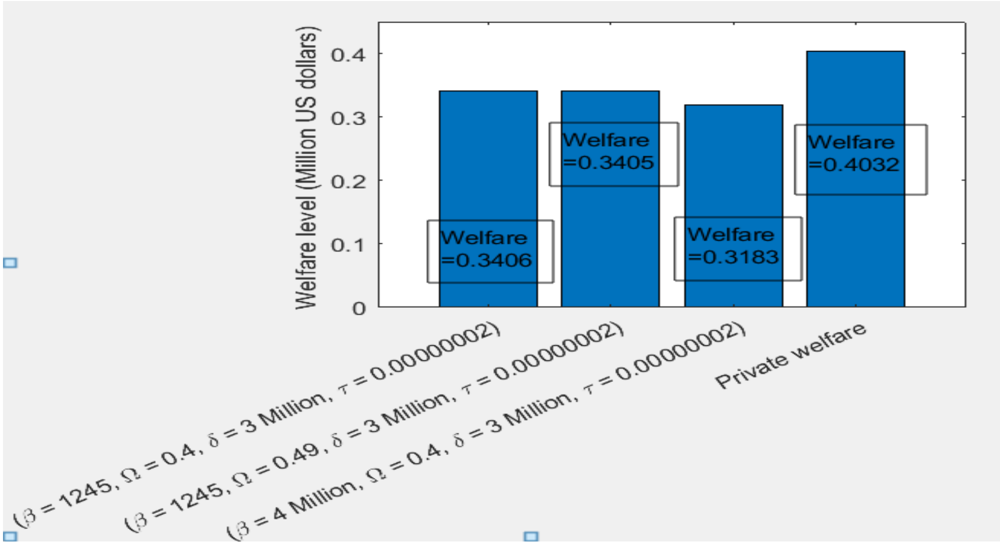

Figure 13. Private welfare (No LS, GDEs and no policy interventions), and social welfare under different values of the Pigouvian tax per unit of land sinking (β) and the constant (Ω) representing the impact of groundwater extraction on the aquifer system's storage capacity; the effective tax rate per unit of land sinking and the effective constant (Ω) ($\beta = 1{,}245$, $\Omega = 0.4$, $\delta = 5\ Million$ and τ =0.00000004), the increase in the effective tax rate per unit of land sinking ($\beta = 4\ Million$, $\Omega = 0.4$, $\delta = 5\ Million$ and τ =0.00000004), and the effective tax rate per unit of land sinking and the increase in the constant (Ω) ($\beta = 1{,}245$, $\Omega = 0.49$, $\delta = 5\ Million$ and τ =0.00000004).

When the effective constant (Ω), which represents the impact of groundwater extraction on the aquifer system's storage capacity increases, social welfare reduces by 0.0001 Million US dollars (from 0.3406 Million US dollars to 0.3405 Million US dollars) (Figure 13). A higher value of Ω implies a smaller LS – impact on aquifer storage capacity. Therefore, the more the storage capacity is not affected by LS, societal welfare reduces slightly. When LS has little effect on aquifer storage capacity (large Ω), extraction remains relatively cheap because subsidence does not significantly reduce the aquifer's ability to store and transmit water. Farmers therefore extract more groundwater, generating higher cumulative LS and greater long-term ecological damage to GDEs. Although short-term extraction profits may rise slightly, the increased ecological degradation reduces total social welfare, leading to a small overall decline in welfare when the aquifer is less sensitive to subsidence like the Dendron aquifer.

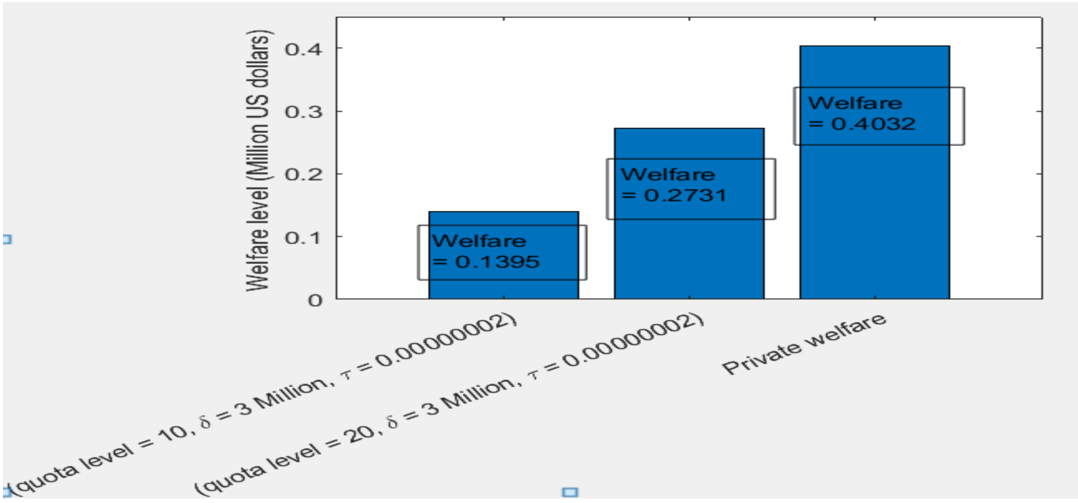

Figure 14. Private welfare (No LS, GDEs and no policy interventions), and social welfare under different quota levels; the effective quota level ($\widehat{W} = 10$, $\delta = 5\ Million$ and τ =0.00000004), and the increase in the effective quota level ($\widehat{W} = 20$, $\delta = 5\ Million$ and τ =0.00000004).

For the quota policy, we observe (Figure 14) that social welfare increases by $0.1336\ Million$ USD, rising from $0.1395\ Million$ USD to $0.2731\ Million$ US dollars, when the effective quota level is raised. This improvement occurs because the additional water allocation is directed toward higher-value agricultural uses, which enhances overall productivity. These results highlight that well-calibrated quota adjustments can generate significant welfare gains by ensuring that scarce groundwater is allocated more efficiently. In addition, a balanced approach, linking quota levels to aquifer and GDEs' health indicators or coupling them with incentives for adopting water-efficient farming technologies could maximize welfare while maintaining sustainability.

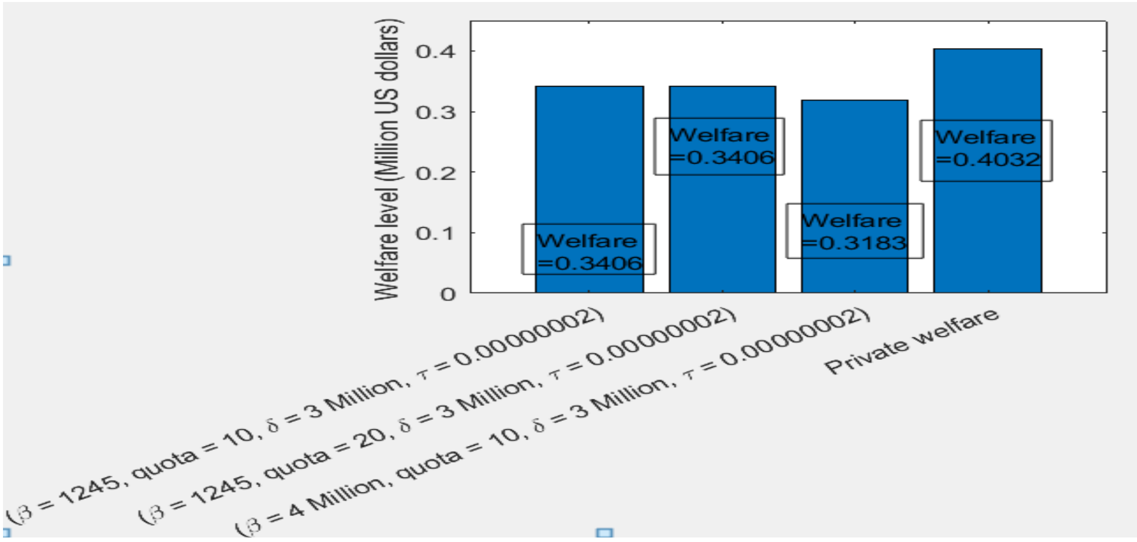

Figure 15. Social welfare when taxes and quotas are combined (under different tax rates and quota levels). The effective tax rate and effective quota level ($\beta = 1245, \widehat{W} = 10,\ \delta = 5\ Million$ and τ =0.00000004), the increase in the Pigouvian tax per unit of land sinking ($\beta = 4$ Million, $\widehat{W} = 10,\ \delta = 5\ Million$ and τ =0.00000004), and the increase in the effective quota level ($\beta = 1245, \widehat{W} = 20,\ \delta = 5\ Million$ and τ =0.00000004).

For packaging and sequencing of taxes and quotas, we observe (Figure 15) that when taxes and quotas are combined, social welfare (from $0.3406\ Million$ US dollars to $0.3183\ Million$ US dollars) decreases as the Pigouvian tax per unit of land sinking increases. This decline indicates that the interaction between the quota constraint and rising Pigouvian taxes generates additional economic inefficiencies, reducing overall welfare instead of improving it. These results suggest that layering taxes on top of quotas without proper calibration can undermine social welfare, as the two policies may overlap in their corrective function. Policymakers should therefore carefully evaluate whether combining instruments is necessary. In contexts where quotas already constrain water extraction effectively, additional Pigouvian taxation may not only be redundant but also welfare-reducing.

7. Extension of the model (change of the threshold tipping points)

A key element of our groundwater-GDEs modeling framework lies in the specification of the critical thresholds for ecosystem health (δ, ρ, γ) and for the water table height (H_u, H_c, H_T). These critical thresholds determine the timing of phase transitions in the aquifer–ecosystem system and, consequently, shape the dynamics of groundwater extraction, LS, and ecosystem health outcomes. However, these parameters are inherently uncertain, both empirically and ecologically, as they depend on site-specific hydrological conditions, ecosystem resilience, and the socio-economic valuation of ecosystem services. Conducting sensitivity analysis is therefore essential to assess the robustness of our results. By varying the critical thresholds around their empirical baseline values, we can evaluate how shifts in ecosystem resilience (health tipping points) and hydrological stress points (water table thresholds) alter the timing of regime shifts, the path of extractions, aquifer depletion, and ultimately the evolution of GDEs' health.

7.1 sensitivity analysis of the critical thresholds

In general, we expect that increasing the values of the GDEs' health thresholds, i.e., assuming ecosystems are more fragile, will lead to earlier onset of unhealthy, severe unhealthy, and critical unhealthy phases, reducing the time horizon for sustainable groundwater use. Conversely, lowering these thresholds, implying greater resilience, should prolong the healthy phase, delay transitions, and sustain higher levels of social welfare over time. Similarly, higher values of the water table thresholds are expected to accelerate compaction processes and health deterioration, whereas lower thresholds should delay these transitions and moderate the severity of ecosystem stress. Overall, this sensitivity analysis allows us to test the stability and robustness of our optimal paths' results, highlight the importance of ecological resilience for groundwater policy design, and identify which parameters exert the strongest influence on long-run aquifer-ecosystem sustainability.

For the sensitivity analysis, we only use the effective quota level, effective tax rate, and the empirical constant ($\Omega = 0.4$). We set a short horizon of 250 years to estimate aquifer depletion. This longer horizon is more useful for policymakers to understand differences between scenarios (Esteban et al., 2021). Our policy instruments, tax, packaging and sequencing, and the LS-GDEs and no policy intervention, show similar water table and extraction levels within the 20-year period used by Esteban et al. (2021), necessitating our extended horizon.

7.1.1 Scenario with Land Subsidence, GDEs, and No Policy Intervention

Table 2 (in Appendix 19) shows how varying the GDEs' health thresholds and water-table thresholds affects the optimal outcomes under the LS–GDEs–no-policy scenario. Under the empirical thresholds (δ = 0.5, ρ = 0.35, γ = 0.15; H_u = 1200.5, H_c = 1191.5, H_T = 1189.5), the equilibrium water table height is 1177.53 m.a.s.l, aquifer depletion is 164.8 Mm³, and total social welfare is 0.3415 Million US dollars. Lowering the GDEs' health thresholds (δ = 0.4, ρ = 0.3, γ = 0.1) yields a slightly higher water table (1177.65 m.a.s.l), slightly lower depletion (164 Mm³), and a small welfare gain (0.3419 Million US dollars), while delaying the severe and the critically unhealthy phases because more resilient ecosystems tolerate drawdown for longer. Raising the health thresholds (δ = 0.7, ρ = 0.4, γ = 0.2) produces a marginally lower water table (1177.4 m.a.s.l), higher depletion (165.68 Mm³), and slightly lower welfare (0.3414 Million US dollars), with earlier switching time for the critically unhealthy phase, and delayed unhealthy phase. Lowering the water-table thresholds (H_u = 1195.5, H_c = 1190.5, H_T = 1184.5) raises welfare to 0.3482 Million US dollars and reduces depletion to 162.3 Mm³, with delayed unhealthy phase and the critically unhealthy phase, as well as an early severe unhealthy phase. Conversely, raising the thresholds (H_u = 1205.5, H_c = 1196.5, H_T = 1192.5) yields the lowest welfare (0.3349 Million US dollars) and the lowest depletion (150.64 Mm³), with delayed transitions into the GDEs' health phases.

7.1.2 LS - GDEs Scenario with Taxes

Table 3 (in Appendix 19) shows tah the empirical critical thresholds (δ = 0.5, ρ = 0.35, γ = 0.15; H_u = 1200.5, H_c = 1191.5, H_T = 1189.5) yield an equilibrium water-table height of 1179.10 m.a.s.l, aquifer depletion of 158 Mm³, and social welfare of 0.3414 Million US dollars. Lowering the GDEs' health thresholds (δ = 0.4, ρ = 0.3, γ = 0.1) produces nearly identical outcomes, 1179.04 m.a.s.l, 159 Mm³, and 0.3415 Million US dollars. The switching times shift only minimally, indicating that under a tax regime ecological resilience has very small leverage over long-run hydrology or welfare. Raising the health thresholds (δ = 0.7, ρ = 0.4, γ = 0.2) similarly produces only slight changes, 1178 m.a.s.l, 160 Mm³, and 0.3413 Million US dollars, with switching times again showing negligible movement. Adjusting the water-table thresholds yields somewhat more visible effects: lowering them (H_u = 1195.5, H_c = 1190.5, H_T = 1184.5) increases welfare to 0.3477 Million US dollars and yields 160 Mm³ depletion, while raising them (H_u = 1205.5, H_c = 1196.5, H_T = 1192.5) lowers welfare to 0.3347 Million US dollars and reduces depletion to 146 Mm³. Across all cases, the switching times change only marginally, confirming that Pigouvian taxes dominate the timing of transitions, and adjusting the ecological thresholds produces small, second-order variations. Economically, the tax internalises subsidence damage so strongly that the system's optimal path is governed primarily by the tax rate itself; changes in ecological fragility only slightly perturb the timing of transitions and long-run welfare.

7.1.3 LS - GDEs scenario and quotas

Table 4 (in Appendix 19) shows that under the quota policy, the imposed extraction cap dominates system behaviour, resulting in almost identical long-run hydrological and economic outcomes across all sensitivity cases. With the empirical thresholds (δ = 0.5; H_u = 1200.5), the equilibrium water table height is 1186.47 m.a.s.l, aquifer depletion is 150.8 Mm^3, and total welfare is 0.1395 Million US dollars. The switching times are t_u = 126, t_c = 155, and t_T = 161.

It is worth mentioning that the optimal solutions only contains δ and H_u, and not other critical thresholds. Lowering the GDE health thresholds (δ = 0.4) does not change any optimal outcomes: the equilibrium water table remains 1186.47 m.a.s.l, depletion remains 150.7 Mm^3, welfare stays at 0.1395 Million US dollars, and all switching times shift only slightly to t_u = 126, t_c = 144, ans t_T = 161. This occurs because δ affects only the ecological penalty term in phase 1, but the quota binds extraction so tightly that behaviour cannot adjust in response. Raising the GDE health thresholds (δ = 0.7) also produces identical hydrological and economic outcomes, equilibrium water table 1186.47 m.a.s.l, depletion 150.7 Mm^3, welfare 0.1395 Million US dollars, with almost unchanged switching times (126, 145, 163). Since the quota fixes total pumping throughout, farmers cannot respond to ecosystem fragility by reducing extraction; thus only the timing of ecological transitions shifts slightly. The water-table threshold cases show the same rigidity. Lowering the water table thresholds (H_u = 1195.5) leaves the equilibrium water table (1186.47 m.a.s.l) and welfare (0.1395 Million US dollars) unchanged, with switching times moving to t_u = 132, t_c = 151, while t_T is not reported (because the quota-driven trajectory never reaches inelastic compaction). Raising the thresholds (H_u = 1205.5 m.a.s.l) yields a nearly identical equilibrium (1186.5 m.a.s.l), depletion (150.7 Mm^3), and welfare (0.1395 Million US dollars), with earlier transitions (t_u = 119, t_c =

131, t_T = 136) because the system crosses the higher thresholds sooner.

7.1.4 LS - GDEs scenario and packaging and sequencing of taxes and quotas

Table 5 (in Appendix 19) shows that, with the empirical thresholds (δ = 0.5, ρ = 0.35, γ = 0.15; H_u = 1200.5, H_c = 1191.5, H_T = 1189.5), imposing the quota only in phase 4 produces a much higher equilibrium water table (1184.8 m.a.s.l), lower depletion (144.6 Mm³), and lower welfare (0.3414 Million US dollars). Varying the GDEs' health thresholds has only small changes from the lone tax policy results because the quota policy in phase 4 depends only on γ. Lowering the thresholds (δ = 0.4, ρ = 0.3, γ = 0.1) keeps the equilibrium water table (1184.8 m.a.s.l) and depletion (144.6 Mm³) almost unchanged and slightly increases welfare to 0.3415 Million US dollars. The switching times also shift only marginally: the unhealthy phase occurs earlier, and the severe unhealthy phases occur slightly later.

Raising the GDEs' health thresholds (δ = 0.7, ρ = 0.4, γ = 0.2), making ecosystems more fragile, produces almost no change in the equilibrium water table (1184.7 m.a.s.l), slightly increases depletion (145 Mm³), and reduces welfare slightly to 0.3413 Million US dollars. Here, the switching times adjust modestly in the opposite direction: the severe unhealthy and critically unhealthy phases begin slightly earlier. Changing the water-table thresholds has clearer effects because these thresholds determine when compaction begins and, crucially, when the phase-4 quota is activated. Lowering the thresholds (H_u = 1195.5, H_c = 1190.5, H_T = 1184.5) brings earlier the onset of elastic compaction and delays inelastic compaction. As a result, farmers can pump more before entering phase 4, causing depletion to rise to 160 Mm³ and welfare to increase to 0.3477 Million US dollars, while the equilibrium water table declines slightly to 1182.53 m.a.s.l. Conversely, raising the thresholds (H_u = 1205.5, H_c = 1196.5, H_T = 1192.5) makes the aquifer more fragile to compaction and triggers the unhealthy phase earlier. The severe unhealthy and the critically unhealthy phases are delayed. As a result, depletion falls sharply to 132 Mm³, welfare decreases to 0.3347 Million USD, and the equilibrium water table becomes higher (1187.8 m.a.s.l).

8 Conclusion and Policy Implications

This study assessed the performance of Pigouvian taxes, extraction quotas, and the packaging and sequencing of taxes and quotas in managing land subsidence (LS) and sustaining groundwater-dependent ecosystems (GDEs) in the Dendron aquifer under a unified LS–GDEs framework. The results reveal clear and policy-relevant trade-offs between private welfare, social welfare, aquifer depletion, and ecosystem health. Across all scenarios, the baseline (no LS and no GDE feedbacks) generates the highest private welfare but also the lowest long-run water table levels and the greatest aquifer depletion, confirming that unregulated pumping is incompatible with long-term hydrological and ecological sustainability.

Quotas, applied throughout the horizon, remain the most effective instrument for maintaining higher water table levels and substantially reducing aquifer depletion, although they impose the largest private welfare losses relative to alternative policies. Taxes alone generate higher short-run private benefits but do not reduce extractions sufficiently to prevent long-run declines in the water table. The analysis shows that Pigouvian taxes internalise LS damages, but large tax increases depress both private and social welfare without corresponding ecological gains.

The packaging and sequencing of taxes and quotas with Pigouvian taxes in phases 1–3 and quotas only in phase 4, consistently emerges as the most balanced policy option. This combined approach delivers higher welfare than quotas alone, prevents the sharp long-run declines observed under taxes alone, and yields intermediate extraction and water-table paths that stabilise earlier than in the single-instrument cases. Importantly, because the quota binds only in phase 4, welfare losses are moderated while long-run groundwater protection is preserved. The switching-time patterns observed in the sensitivity analysis qualify and refine the policy comparison rather than overturning it. Changes in the GDEs' health thresholds and water-table thresholds shift the timing of entry into the unhealthy, severe-unhealthy, and critical phases in non-linear ways, but the combined tax–quota policy continues to deliver balanced extraction and water-table paths and to prevent persistent, deep declines in groundwater levels. In particular, the phase-4 quota consistently acts as a hard cap on extractions once the system enters the critical unhealthy phase, even when ecological and hydrological thresholds are perturbed.

The sensitivity analysis of the GDEs' health thresholds (δ, ρ, γ) and the water-table thresholds

(H_u, H_c, H_T) further shows that relatively small changes in these critical values can generate noticeable shifts in long-run welfare, and aquifer depletion. Depending on the parameter configuration, transitions into stressed phases can be brought forward or pushed back, and welfare can rise or fall, underscoring the importance of ecological resilience and aquifer morphology in shaping optimal policy design. Across all scenarios and parameter variants, equilibrium social welfare remains systematically lower than private welfare because LS–GDE damages impose external costs not internalised by individual farmers, reinforcing the case for regulatory intervention through taxes, quotas, or their combination.

Taken together, the results demonstrate that no single policy dominates across all metrics, but integrated and adaptive approaches, particularly the packaging and sequencing of taxes and quotas—offer the strongest long-term protection against aquifer depletion, LS, and GDE degradation while maintaining reasonable welfare outcomes. For South African groundwater governance, these findings emphasise the importance of calibrating Pigouvian taxes at effective levels, setting quotas within sustainable bounds, and coordinating instruments across ecological phases. Such targeted and combined policies provide the most sustainable and welfare-preserving pathway for managing the Dendron aquifer and similar groundwater systems facing coupled hydrological–ecological risks.

Appendix

Appendix 1. Construction of the GDEs' health status (GDEsHS) function

The health of GDEs depends on one key groundwater attribute, among others: depth to the water table (Clifton and Evans, 2001). Depth to the water table is quantified as the difference between the elevation of the irrigated field surface and the height of the water table, $S_l - H$. Several papers have defined ecosystem health as a function of the depth to the water table (Esteban et al., 2021; Esteban and Dinar, 2016). The higher the depth to the water table, the lower the health level of the GDEs. Alternatively, GDEs health can be expressed as a function of the water table height (Esteban et al., 2021). In this study, we examine GDEs health as a function of water table height, where a decline in water table height corresponds to a decline in ecosystem health. We assume the aquifer is at full capacity when the water table height equals the surface elevation, that is, $S_l = H$ (Esteban et al., 2021). Intuitively, a full aquifer implies that the GDEs' health is in its pristine (unaltered or undisturbed) state. Building on the framework proposed by Esteban et al. (2021), we define GDEs' health as occurring in four distinct phases. Phase 1 is the healthy phase, during which GDEs are fully functional, and all ecological and hydrological processes are functioning in a stable, undisturbed, and ecologically ideal state, supporting long-term sustainability without intervention. Ecological processes are the natural interactions and functions that sustain ecosystems and the organisms within them. Phase 2, the unhealthy phase, reflects a state where some ecological processes are not efficient or disrupted. In Phase 3, the severe unhealthy phase, GDEs experience major or severe functional impairment, with key or essential ecological processes significantly compromised. Finally, Phase 4, the critical unhealthy phase, represents a state in which essential ecological processes have largely ceased or critically impaired, indicating that the GDE is on the verge of complete failure. The GDEs' health status (GDEsHS) functional represents the condition or level of health of GDEs.

We have four parameters that define the GDEsHS functional throughout the aforementioned four phases, $0 < \gamma < \rho < \delta < 1$. We define the health level 1 as the pristine state of the GDEs, corresponding to their condition when the aquifer is full (Esteban et al., 2021). Between 1 and δ, the GDEs are relatively healthy (healthy phase). The parameter δ represents the

GDEs' health critical threshold (or tipping point) beyond which the GDEs' health switches to the unhealthy phase. Between δ and ρ, the GDEs are unhealthy (unhealthy phase), during which a decreasing water table height caused by groundwater extraction is the sole driver of GDEs' health stress.

The parameter ρ represents the GDEs' health critical threshold beyond which the GDEs' health switches to the severe unhealthy phase, where land subsidence is occurring due to elastic compaction. Between ρ and γ, the GDEs are severely unhealthy (severe unhealthy phase), during which a decreasing water table height coupled with LS (elastic compaction), both caused by groundwater extraction, simultaneously drive GDEs' health stress.

The parameter γ represents the GDEs' health critical threshold beyond which the GDEs' health switches to the critical unhealthy phase, where land subsidence is occurring due to both elastic and inelastic compaction. Between γ and zero, the GDEs are critically unhealthy (critical unhealthy phase), during which a decreasing water table height, coupled with LS (both elastic and inelastic compaction) and aquifer system storage capacity loss, all caused by groundwater extraction, simultaneously drive the GDEs' health stress. We assume that the GDEs' health level must drop to zero when the aquifer is fully depleted ($H = H_B$), regardless of the level of LS experienced at that point in time t. That is, GDEs extinguish when the water table height is equal to the bottom (H_B) of the aquifer. Following Esteban et al. (2021), we further assume that at each critical threshold, the GDEs health status functional is continuous, taking the same value from both the left and right sides of the function.

In addition, we have three critical thresholds for the water table height that define the GDEsHS functional throughout the aforementioned four phases: $H_T < H_c < H_u$. The water table height H_u represents the critical threshold for the water table height beyond which the GDEs' health switches to the unhealthy phase. Between H_u and H_c, decreasing water table height, which is caused by groundwater extraction, is the sole driver of GDEs' health stress. The water table height H_c represents the critical threshold for the water table height beyond which the elastic compaction phase begins. That is, land subsidence caused solely by elastic compaction begins when H_c is surpassed. Between H_c and H_T, the GDEs' health stress is simultaneously driven by decreasing water table height and land subsidence caused by elastic compaction. The water table height H_T represents the critical threshold for the water table height beyond which the inelastic compaction phase begins. Below H_T, the GDEs' health stress is simultaneously driven by decreasing water table height, land subsidence caused by both elastic and inelastic compaction, as well as aquifer system storage capacity loss. The water table height H_B represents the bottom of the aquifer. As a results, we define the GDEs health status functional for the healthy phase (phase 1) as suggested by Esteban et al. (2021) as follows below.

$$GDEsHS(H) = \frac{\delta - 1}{(S_l - H_u)^2} \cdot (S_l - H)^2 + 1, \quad H \geq H_u. \tag{60}$$

Since $\delta < 1$, then $\delta - 1 < 0$, and we observe that the denominator in the expression is also strictly greater than zero since $S_l > H_u$. Therefore, the GDEs' health status is a negative quadratic in H. The above function is a downward opening parabola, decreasing gradually as the water table height decreases. When the water table height is equal to S_l (no water stress as the aquifer is full), the GDEs' health is in its pristine state with a health level equal to 1. As H reduces, the GDEs' health status decreases quadratically from 1 towards δ. When the water table height reaches H_u, the GDEs' health state is equal to δ. We define the GDEs health status functional for the unhealthy phase (phase 2) as follows below.

$$\begin{aligned} GDEsHS(H) &= \frac{\delta - \rho}{(H_u - H_c)^2} \cdot (S_l - H_c - (S_l - H))^2 + \rho \\ &= \frac{\delta - \rho}{(H_u - H_c)^2} \cdot (H - H_c)^2 + \rho, \quad H_c \leq H < H_u. \end{aligned} \tag{61}$$

Since $\delta > \rho$, then $\delta - \rho > 0$, and we observe that the denominator in the expression is also strictly greater than zero since $H_u > H_c$. Therefore, the GDEs' health status is a positive quadratic in H. The function decreases as the water table height decreases. The GDEs' health status decreases from δ towards ρ as H reduces. When the water table height is equal to H_u, the GDEs' health level is equal to δ. When the water table height is equal to H_c, the GDEs' health state is equal to ρ.

The GDEs' health status functionals for both phase 1 and phase 2 are not affected by LS. The depth to the water table used to construct their health functionals is defined by: $\text{Depth} = S_l - H$, where S_l is the irrigation surface elevation, and H is the water table height. In phase 3 and phase 4, GDEs' health stress is simultaneously driven by a decreasing water table height and LS. When LS occurs, the ground surface physically lowers. That is, the value of S_l changes (decreases) as LS progresses. Therefore, if S_l is dynamically updated to reflect the current ground surface elevation (i.e., to include the effect of LS), the effective depth to the water table at any time is given as follows below.

$$\text{Depth} = S_l - LS(H) - H. \tag{62}$$

This formulation reflects that even if H_t remains constant, an increase in $LS(H)$ results in a larger effective depth, which imposes stress on GDEs. The function $LS(H)$ represents the cumulative LS (in meters) that has occurred since surpassing the critical threshold H_c up to and including time t.

$$LS(H) = -\eta \cdot \varepsilon \cdot b \cdot \psi \cdot (H - H_c),\ H < H_c. \tag{63}$$

Where H, η, b, ψ, and ε represent the water table height at time t, the density of water, the aquifer system's thickness, the aquifer system compressibility, and the acceleration due to gravity. As H decreases, $H - H_c < 0$ and $LS(H) > 0$, which reflects a positive cumulative LS. Subsidence begins only once the H_c is surpassed and increases as H falls farther below H_c. Take note that the cumulative LS is always greater than or equal to zero. If $LS(H) = 0$, it means that there is no cumulative LS from the onset of compaction (i.e., from when H first dropped below H_c) up to the current time t. Either previously induced land sinking has been completely offset by land uplift, or the land surface elevation has returned to its original (pre-compaction) level, i.e., the elevation at the time H was equal to H_c. The latter can only happen if all the compaction was elastic (i.e., reversible), and the water table has recovered back to H_c or higher. Even if water returns to pre-extraction levels, it is difficult to fully recover previously induced land sinking in most aquifers. In some regions, even when groundwater levels rise, the land surface does not immediately rebound, but continues to subside (Wang et al., 2013; Zhang et al., 2013). Even if groundwater returns to pre-extraction levels, the uplift is usually small and does not fully reverse the previous LS (Zhang et al., 2012; 2015a). This delayed response of land uplift relative to water table recovery is influenced by the geological properties of the soil and aquifer system (Jin et al., 2014). If any inelastic compaction has occurred, $LS(H) = 0$ is no longer physically possible. If $LS(H) < 0$, the land uplifted beyond its original elevation because $LS(H)$ moved from being equal to zero (when all the cumulative land sinking experienced in the past were offset to no land sinking occurred before) to negative, which is not physically realistic in most real-world aquifer systems (Wang et al., 2013; Zhang et al., 2013). Therefore, the maximum amount of $LS(H)$ the aquifer system can experience is less than or equal to $H_c - H$ at any time time step. Land compaction is caused by a reduction in H. Even if delayed compaction occurs, it still originates from past drops in H, not independently.

In phase 3 (the severe unhealthy phase), GDEs' health stress is simultaneously driven by a decreasing water table height and LS caused by elastic compaction. As a result, we define the GDEs health status functional for the severe unhealthy phase as follows below.

$$GDEsHS(H, LS(H)) = \frac{\rho-\gamma}{(d_c)^2} \cdot (H - LS(H) - H_T + LS(H_T))^2 + \gamma,\ H_T \leq H < H_c. \quad (64)$$

Where $d_c = H_c - LS(H_c) - H_T + LS(H_T)$, $LS(H_c) = LS(H(t_c))$, and $LS(H_T) = LS(H(t_T))$. Since $\rho > \gamma$, then $\rho - \gamma > 0$, and we observe that the denominator in the expression is also strictly greater than zero. Therefore, the GDEs' health status is a positive quadratic in $H - LS(H)$. The function decreases as the water table height decreases and cumulative LS increases. The GDEs' health status decreases from ρ towards γ as H reduces and cumulative LS increases. When the water table height is equal to H_c and cumulative LS is equal to $LS(H_c)$, the GDEs' health level is equal to ρ. When the water table height and cumulative LS are equal to H_T and $LS(H_T)$, respectively, the GDEs' health state is equal to γ.

In phase 4 (the critical unhealthy phase), GDEs' health stress is simultaneously driven by a decreasing water table height and LS caused by both elastic and inelastic compaction. Another extra factor that adds on the GDEs' health stress in this phase is aquifer system storage capacity loss. We define the GDEs health status functional for the critical unhealthy phase as follows below.

$$GDEsHS(H, LS(H)) = \frac{\gamma}{(d_T)^2} \cdot (H - LS(H) - H_B + LS(H_B))^2,\ H < H_T. \quad (65)$$

Where $d_T = H_T - LS(H_T) - H_B + LS(H_B)$, $LS(H_B) = LS(H(t_B))$, and $LS(H_T) = LS(H(t_T))$. Since $\gamma > 0$, and we observe that the denominator in the expression is also strictly greater than zero. Then, the GDEs' health status is a positive quadratic in $H - LS(H)$. The function decreases as the water table height decreases and cumulative LS increases. The GDEs' health status decreases from γ towards zero as H reduces and cumulative LS increases. When the water table height is equal to H_T and cumulative LS is equal to $LS(H_T)$, the GDEs' health level is equal to γ. When the water table height and cumulative LS are equal to H_B and $LS(H_B)$, respectively, the GDEs' health state is equal to zero.

Storage capacity loss does not affect GDEs' health directly like depth to water table or land subsidence. But it undermines the aquifer system's ability to sustain water availability, making ecosystems more vulnerable. In phase 4 of the GDEs' health state functional, there is no explicit parameter representing aquifer system storage capacity loss. However, this loss naturally coincides with permanent land subsidence due to inelastic compaction, which occurs when collapsed pore spaces are permanently lost. Notably, in this phase, inelastic compaction contributes to land subsidence that is several times greater than that caused by elastic compaction (Sneed, 2001; Smith et al., 2017; Smith and Majumdar, 2020). It is, however, worth mentioning that inelastic compaction, measured as vertical ground deformation in meters, is not an exact measure of aquifer system storage capacity loss, which is measured in cubic meters. As a result, storage capacity cannot be directly incorporated into the GDEs' health functional, which is based on vertical measures such as H and LS. Instead, the precise representation of storage capacity loss will be introduced later in the model, particularly in the groundwater dynamics equation of phase 4, where storage capacity is a key component. Moreover, the economic value of this storage loss will be accounted for in the sections on taxes, as well as the packaging and sequencing of taxes and quotas.

Appendix 2. Detailed solution of the fourth sub-problem on taxes

The hamiltonian function of the system (9), (10), (11) is given as follows

$$\mathcal{H}_4(t, W_4, H_4, \lambda_4) = -\mathrm{e}^{-it}[\frac{W_4^2}{2k} - \frac{gW_4}{k} - (C_0 + C_1 H_4)W_4 + \theta[\frac{\gamma}{((1+\eta\varepsilon b\psi)(H_T - H_B))^2} \cdot (H_4 + \eta\varepsilon b\psi(H_4 - H_c) - H_B - \eta\varepsilon b\psi(H_B - H_c))^2] + \frac{\beta\eta\varepsilon b\psi}{AS}[R - (1-\alpha)W_4] + b\psi\pi(1 - n + n_w)[R - (1-\alpha)W_4] \cdot (\frac{W_4}{k} - \frac{g}{k} - C_0 - C_1 H_4)] + \lambda_4 \cdot \frac{[R + (\alpha - 1)W_4]}{\Omega \cdot AS} \quad (66)$$

Equation (66) can be rewritten as follows.

$$\mathcal{H}_4(t, W_4, H_4, \lambda_4) = -\mathrm{e}^{-it}[\frac{W_4^2}{2k} - \frac{gW_4}{k} - (C_0 + C_1 H_4)W_4 + G_6(H_4 - H_B)^2 + G_5 W_4 - G_3 \frac{(1-\alpha)W_4^2}{k} - G_3 R C_1 H_4 + G_3(1-\alpha)C_1 W_4 H_4 + G_4]$$

$$+\lambda_4 \cdot \frac{[R+(\alpha-1)W_4]}{\Omega \cdot AS} \quad (67)$$

Where

$$G_2 = \frac{\beta\eta\varepsilon b\psi}{AS}. \quad (68)$$

$$G_3 = b\psi\pi(1-n+n_w). \quad (69)$$

$$G_4 = -\frac{RgG_3}{k} - RC_0G_3 + G_2R. \quad (70)$$

$$G_5 = \frac{RG_3}{k} + \frac{(1-\alpha)gG_3}{k} + G_3(1-\alpha)C_0 - G_2(1-\alpha). \quad (71)$$

$$G_6 = \frac{\theta\gamma}{[H_T-H_B]^2}. \quad (72)$$

Hence, the first order conditions are as follows

$$\frac{\partial\mathcal{H}_4}{\partial W_4} = -\mathrm{e}^{-it}[(\frac{1-2G_3(1-\alpha)}{k})W_4 - \frac{g}{k} - C_0 - C_1H_4 + G_5 + G_3(1-\alpha)C_1H_4]$$
$$+\lambda_4[\frac{(\alpha-1)}{\Omega \cdot AS}] = 0. \quad (73)$$

$$\dot{\lambda}_4 = -\frac{\partial\mathcal{H}_4}{\partial H_4}. \quad (74)$$

$$\dot{H}_4 = \frac{1}{\Omega \cdot AS}[R + (\alpha-1)W_4]. \quad (75)$$

The transversality condition is given by $\lim_{t\to\infty}\lambda_4(t) = 0$. From Equation (73), we obtain the value for the costate variable λ_4 as follows.

$$\lambda_4 = \frac{\Omega}{m}\mathrm{e}^{-it}[(\frac{1-2G_3(1-\alpha)}{k})W_4 - \frac{g}{k} - C_0 - C_1H_4 + G_5 + G_3(1-\alpha)C_1H_4], \quad (76)$$

where $m = \frac{(\alpha-1)}{AS}$. The derivative of λ_4 with respect to t is given by

$$\dot{\lambda}_4 = \frac{\Omega}{m}\mathrm{e}^{-it}[-\frac{iG_8W_4}{k} + \frac{ig}{k} + iC_0 - iG_7C_1H_4 - iG_5$$
$$+\frac{G_7C_1R}{\Omega \cdot AS} + \frac{G_7C_1m}{\Omega}W_4 + \frac{G_8\dot{W}_4}{k}]. \quad (77)$$

Where,

$$G_7 = G_3(1-\alpha) - 1 \quad (78)$$

$$G_8 = 1 - 2G_3(1-\alpha) \quad (79)$$

The derivative of $\mathcal{H}_4$ with respect to the water table height H_4 is given by

$$-\frac{\partial \mathcal{H}_4}{\partial H_4} = -\mathrm{e}^{-it}[G_3RC_1 - G_7C_1W_4 + 2G_6H_B - 2G_6H_4]. \quad (80)$$

From Equation (74) and (77), we obtain the following equation.

$$-G_3RC_1 + G_7C_1W_4 - 2G_6H_B + 2G_6H_4 = \frac{\Omega}{m}[-\frac{iG_8W_4}{k} + \frac{ig}{k} + iC_0 - G_7iC_1H_4 - iG_5$$

$$+\frac{G_7C_1R}{\Omega \cdot AS} + \frac{G_7C_1m}{\Omega}W_4 + \frac{G_8\dot{W}_4}{k}]. \quad (81)$$

Solving for $\dot{W}_4$ in the above equation we get the following equations.

$$\frac{\Omega G_8\dot{W}_4}{mk} = \frac{\Omega G_8 iW_4}{mk} + \frac{\Omega C_1G_7iH_4}{m} + 2G_6H_4 - \frac{\Omega ig}{mk} - \frac{\Omega iC_0}{m} + \frac{\Omega iG_5}{m}$$

$$-\frac{G_7C_1R}{ASm} - G_3RC_1 - 2G_6H_B \quad (82)$$

$$\frac{G_8\dot{W}_4}{k} = \frac{G_8iW_4}{k} + C_1G_7iH_4 + \frac{2mG_6H_4}{\Omega} - \frac{ig}{k} - iC_0 + iG_5 \; -\frac{G_7C_1R}{AS\Omega} - \frac{mG_3C_1R}{\Omega} - \frac{2mG_6H_B}{\Omega} \quad (83)$$

$$\dot{W}_4 = iW_4 + \frac{ikC_1G_7H_4}{G_8} + \frac{2mkG_6H_4}{\Omega G_8} - \frac{ig}{G_8} - \frac{ikC_0}{G_8} + \frac{ikG_5}{G_8} - \frac{G_7kC_1R}{\Omega ASG_8} \; - \frac{mkG_3RC_1}{\Omega G_8} + \frac{2mkG_6H_B}{G_8} \quad (84)$$

$$\dot{W}_4 = iW_4 + [\frac{ikC_1G_7}{G_8} + \frac{2mkG_6}{\Omega G_8}]H_4 + [-\frac{ig}{G_8} - \frac{ikC_0}{G_8} + \frac{ikG_5}{G_8} - \frac{kG_7C_1R}{\Omega ASG_8} \; - \frac{mkG_3RC_1}{\Omega G_8} - \frac{2mkG_6H_B}{G_8}] \quad (85)$$

Likewise, the value for $\dot{H}_4$ can be rewritten as

$$\dot{H}_4 = \frac{(\alpha-1)W_4}{\Omega \cdot AS} + \frac{R}{\Omega \cdot AS}. \quad (86)$$

Consequently, we now have to solve the two simultaneous differential equations ((85) and (86)). Thus, by letting $mm = \frac{(\alpha-1)}{\Omega AS}$, $uu = \frac{ikC_1G_7}{G_8} + \frac{2mkG_6}{\Omega G_8}$, $NN = -\frac{ig}{G_8} - \frac{ikC_0}{G_8} + \frac{ikG_5}{G_8} - \frac{kG_7C_1R}{\Omega ASG_8} - \frac{mkG_3RC_1}{\Omega G_8} - \frac{2mkG_6H_B}{G_8}$ and $MM = \frac{R}{\Omega AS}$, we get the following system of differential equations.

$$\dot{W}_4 = iW_4 + uu \cdot H_4 + NN. \quad (87)$$

$$\dot{H}_4 = mm \cdot W_4 + MM. \quad (88)$$

Putting the above system of differential equations in a D operator format (where $D = \frac{d}{dt}$), and solving for W_4 yields the following second order linear non-homogeneous differential equation.

$$[(D^2 - Di) - uu \cdot mm]W_4 = uu \cdot MM. \quad (89)$$

The particular solution of the above differential equation is given by: $-\frac{MM}{mm}$ and the solution to the homogeneous differential equation ($[(D^2 - Di) - uu \cdot mm]W_4 = 0$) by

$$W_3(t) = \overline{MA}\mathrm{e}^{tx_1} + \overline{MB}\mathrm{e}^{tx_2}, \quad (90)$$

where $x_{1,2} = \frac{i \pm \sqrt{i^2 + 4uumm}}{2}$ are the characteristic roots. The parameters $\overline{MA}$ and $\overline{MB}$ are constants to be determined by imposing the initial conditions. Substituting the right hand side (RHS) of (90) for $W_4(t)$ in the homogenous DE ($\dot{H}_4 = mm \cdot W_4$) and integrating gives the solution for the water table level $H_4(t)$ as follows.

$$H_4(t) = \frac{mm \cdot \overline{MA}}{x_1}\mathrm{e}^{tx_1} + \frac{mm \cdot \overline{MB}}{x_2}\mathrm{e}^{tx_2}. \quad (91)$$

Furthermore, the steady state level water table is given by

$$H_4^* = [\frac{i\frac{MM}{mm} - NN}{uu}] \quad (92)$$

Hence, the solution for $W_4^*(t)$ and $H_4^*(t)$ are given as follows, respectively.

$$W_4^*(t) = \overline{MA}\mathrm{e}^{tx_1} + \overline{MB}\mathrm{e}^{tx_2} - \frac{MM}{mm}, \quad (93)$$

$$H_4^*(t) = \frac{mm \cdot \overline{MA}}{x_1}\mathrm{e}^{tx_1} + \frac{mm \cdot \overline{MB}}{x_2}\mathrm{e}^{tx_2} + \frac{i\frac{MM}{mm} - NN}{uu}. \quad (94)$$

Similarly to Gisser and Sanchez (1980) results, it is worth mentioning that $+4uumm > 0$ since $k < 0, C_1 < 0, i > 0, A > 0, S > 0, \Omega > 0, H_B > 0, H_T > 0, \psi > 0, \theta > 0, \gamma > 0, \eta > 0, \varepsilon > 0$, $b > 0$, $\beta > 0$, $\pi > 0$, $n > 0$, $n_w > 0$, $G_3 > 0$, $G_7 < 0$, $G_8 > 0$, $G_6 > 0$, $\alpha < 1 \Longrightarrow (\alpha - 1) < 0$ or $(1 - \alpha) > 0$, and $m < 0$. Furthermore, we observe that $\frac{ikC_1G_7(\alpha-1)}{\Omega ASG_8} > 0$ and $\frac{2mkG_6(\alpha-1)}{\Omega^2 ASG_8} < 0$. It can also be proved that $\frac{ikC_1G_7(\alpha-1)}{\Omega ASG_8} > \frac{2mkG_6(\alpha-1)}{\Omega^2 ASG_8}$. Hence, $+4uu \cdot mm = 4[\frac{ikC_1G_7(\alpha-1)}{\Omega ASG_8} + \frac{2mkG_6(\alpha-1)}{\Omega^2 ASG_8}] > 0$. This implies that $x_1 > i$ and $x_2 < 0$. Therefore, x_2 is the stable characteristic root. Likewise, similarly to Gisser and Sanchez (1980), we obtained that the transversality condition is only satisfied when $\overline{MA} = 0$. By imposing the initial conditions of the sub problem ($H_4(t_T) = H_T$), we obtain the constant $\overline{MB}$ as follows below.

$$\overline{MB} = \frac{x_2}{mm}[H_T - \frac{i\frac{MM}{mm} - NN}{uu}]\mathrm{e}^{-x_2 t_T}. \quad (95)$$

Therefore, the optimal solutions for $W_4^*(t)$ and $H_4^*(t)$ are given as follows below, respectively.

$$W_4^*(t) = \frac{x_2}{mm}[H_T - \frac{i\frac{MM}{mm} - NN}{uu}]\mathrm{e}^{x_2(t-t_T)} - \frac{MM}{mm}. \quad (96)$$

$$H_4^*(t) = [H_T - \frac{i\frac{MM}{mm} - NN}{uu}]\mathrm{e}^{x_2(t-t_T)} + \frac{i\frac{MM}{mm} - NN}{uu}. \quad (97)$$

Because $x_2 < 0$ and $i > 0$, the functional defined in (9) is verified to be a convergent integral.

Appendix 3. Proof of Proposition 1.

To determine the impact of the tax per unit of land sinking on optimal solutions, we differentiate the optimal solutions with respect to β.

$$\frac{\partial W^*}{\partial \beta} = -[\frac{i(1-\alpha)\eta\varepsilon b\psi AS\Omega^2 x_2}{[\Omega ASiC_1G_7 + 2(\alpha-1)G_6](\alpha-1)}]\mathrm{e}^{x_2(t-t_T)} \quad (98)$$

We observe that $i(1-\alpha)\eta\varepsilon b\psi AS\Omega^2 x_2 < 0$ since $x_2 < 0$, $i > 0$, $(1-\alpha) > 0$, $\eta > 0$, $\varepsilon > 0$,$b > 0$,$\psi > 0$, $AS > 0$, and $\Omega^2 > 0$. We also observe that $\mathrm{e}^{x_2(t-t_T)} > 0$ and $\mathrm{e}^{x_2(t-t_T)} < 1$ always since $x_2 < 0$ and $t > t_T$. Likewise, $\Omega ASiC_1G_7(\alpha-1) < 0$ since $\Omega > 0$, $AS > 0$, $i > 0$, $C_1 < 0$, $(\alpha-1) < 0$, and $G_7 < 0$. The term $2(\alpha-1)G_6(\alpha-1) > 0$ since $2(\alpha-1)^2 > 0$, and $G_6 > 0$. Therefore, the sign of the derivative depends on sign of the denominator, if $\Omega ASiC_1G_7(\alpha-1) > 2(\alpha-1)G_6(\alpha-1)$ the the derivative is negative. Thus, $\Omega ASiC_1G_7(\alpha-1) > 2(\alpha-1)G_6(\alpha-1) \Longrightarrow i > \frac{2(\alpha-1)G_6}{\Omega ASC_1G_7}$ always since $i > 0$ and $\frac{2(\alpha-1)G_6}{\Omega ASC_1G_7} < 0$. The case $\Omega ASiC_1G_7(\alpha-1) \leq 2(\alpha-1)G_6(\alpha-1)$ can not occur since it will imply that $i \leq \frac{2(\alpha-1)G_6}{\Omega ASC_1G_7}$ which is impossible since $i > 0$ and $\frac{2(\alpha-1)G_6}{\Omega ASC_1G_7} < 0$. In addition, the derivative of the optimal water table height with respect to β is given below.

$$\frac{\partial H^*}{\partial \beta} = [\frac{i(1-\alpha)\eta\varepsilon b\psi\Omega}{\Omega ASiC_1G_7 + 2(\alpha-1)G_6}](1 - \mathrm{e}^{x_2(t-t_T)}). \quad (99)$$

We observe that $i(1-\alpha)\eta\varepsilon b\psi\Omega > 0$ since $i > 0$, $(1-\alpha) > 0$, $\eta > 0$, $\varepsilon > 0$,$b > 0$,$\psi > 0$, and $\Omega^2 > 0$. We also observe that $\mathrm{e}^{x_2(t-t_T)} > 0$ and $\mathrm{e}^{x_2(t-t_T)} < 1$ always since $x_2 < 0$ and $t > t_T$, hence $(1 - \mathrm{e}^{x_2(t-t_T)}) > 0$. Likewise, $\Omega ASiC_1G_7 > 0$ since $\Omega > 0$, $AS > 0$, $i > 0$, $C_1 < 0$, and $G_7 < 0$. The term $2(\alpha-1)G_6 < 0$ since $2(\alpha-1) < 0$, and $G_6 > 0$. Therefore, the sign of the derivative depends on sign of the denominator, if $\Omega ASiC_1G_7 > 2(\alpha-1)G_6$ the the derivative is positive. Thus, $\Omega ASiC_1G_7 > 2(\alpha-1)G_6 \Longrightarrow i > \frac{2(\alpha-1)G_6}{\Omega ASC_1G_7}$ always since $i > 0$ and $\frac{2(\alpha-1)G_6}{\Omega ASC_1G_7} < 0$. The case $\Omega ASiC_1G_7 \leq 2(\alpha-1)G_6$ can not occur since it will imply that $i \leq \frac{2(\alpha-1)G_6}{\Omega ASC_1G_7}$ which is impossible since $i > 0$ and $\frac{2(\alpha-1)G_6}{\Omega ASC_1G_7} < 0$. Therefore, a higher Pigouvian tax reduces the optimal level of groundwater extraction and raises the optimal water table level.

Appendix 4. Proof of Proposition 2.

To determine the impact of aquifer storage capacity reduction on optimal solutions, we differentiate the expression for the economic cost $\phi(W,H)$ of losing the aquifer systems' storage capacity with respect to the optimal water table level and extractions. This proof is the same as that of Ndahangwapo et al. (2024).

$$\frac{\partial\phi(W^*,H^*)}{\partial W^*} = \frac{1}{k} \tag{100}$$

The derivative is negative since $k < 0$.

$$\frac{\partial\phi(W^*,H^*)}{\partial H^*} = -C_1 \tag{101}$$

The derivative is positive since $C_1 < 0$. Therefore, a higher Pigouvian tax reduces the optimal level of groundwater extraction and raises the optimal water table level.

Appendix 5. Detailed solution of the third sub-problem on taxes

We can now solve for the third sub-problem since we have the solution (SP_4^*) to the fourth sub-problem. The hamiltonian function of the system (16), (17), (18) is given as follows

$$\begin{aligned}\mathcal{H}_3(t,W_3,H_3,\lambda_3) = -\mathrm{e}^{-it}\Big[\frac{W_3^2}{2k} - \frac{gW_3}{k} - (C_0 + C_1H_3)W_3 + \\ \theta\Big[\frac{\gamma}{((1+\eta\varepsilon b\psi)(H_T-H_c))^2} \\ \cdot (H_3 + \eta\varepsilon b\psi(H_3-H_c) - H_T - \eta\varepsilon b\psi(H_T-H_c))^2 + \gamma\Big] \\ + \frac{\beta\eta\varepsilon b\psi}{AS}[R-(1-\alpha)W_3]\Big] + \lambda_3 \cdot \frac{[R+(\alpha-1)W_3]}{AS}\end{aligned} \tag{102}$$

Equation (102) can be rewritten as follows.

$$\mathcal{H}_3(t, W_3, H_3, \lambda_3) = -\mathrm{e}^{-it}[\frac{W_3^2}{2k} - \frac{gW_3}{k} - (C_0 + C_1H_3)W_3 + G_9(H_3 - H_T)^2$$

$$+\theta\gamma + G_2[R - (1-\alpha)W_3]] + \lambda_3 \cdot \frac{[R + (\alpha-1)W_3]}{AS} \quad (103)$$

Where

$$G_2 = \frac{\beta\eta\varepsilon b\psi}{AS}. \quad (104)$$

$$G_9 = \frac{\theta(\rho-\gamma)}{[H_T - H_c]^2}. \quad (105)$$

Hence, the first order conditions are as follows

$$\frac{\partial\mathcal{H}_3}{\partial W_3} = -\mathrm{e}^{-it}[\frac{W_3}{k} - \frac{g}{k} - C_0 - C_1H_3 - G_2(1-\alpha)] + \lambda_3[\frac{(\alpha-1)}{AS}] = 0. \quad (106)$$

$$\dot{\lambda}_3 = -\frac{\partial\mathcal{H}_3}{\partial H_3}. \quad (107)$$

$$\lambda_3^*(t_T, W_3^*(t_T), H_3^*(t_T)) = \lambda_4^*(t_T, W_4^*(t_T), H_4^*(t_T)) \quad (108)$$

$$\mathcal{H}_3^*(t_T) = \frac{\partial SP_4^*(t_T, W_4^*(t_T), H_4^*(t_T))}{\partial t_T}, \quad (109)$$

$$\dot{H}_3 = \frac{1}{AS}[R + (\alpha-1)W_3]. \quad (110)$$

The transversality condition is given by $\lim_{t\to\infty}\lambda_3(t) = 0$. From Equation (106), we obtain the value for the costate variable λ_3 as follows.

$$\lambda_3 = \frac{1}{m}\mathrm{e}^{-it}[\frac{W_3}{k} - \frac{g}{k} - C_0 - C_1H_3 - G_2(1-\alpha)], \quad (111)$$

where $m = \frac{(\alpha-1)}{AS}$. The derivative of λ_3 with respect to t is given by

$$\dot{\lambda}_3 = \frac{1}{m}\mathrm{e}^{-it}[-\frac{iW_3}{k} + \frac{ig}{k} + iC_0 + iC_1H_3 + iG_2(1-\alpha)$$

$$-\frac{C_1R}{AS} - C_1mW_3 + \frac{\dot{W}_3}{k}]. \quad (112)$$

The derivative of $\mathcal{H}_3$ with respect to the water table height H_3 is given by

$$-\frac{\partial\mathcal{H}_3}{\partial H_3} = -\mathrm{e}^{-it}[C_1W_3 - 2G_9H_3 + 2G_9H_T]. \quad (113)$$

From Equation (107) and (112), we obtain the following equation.

$$-C_1W_3 + 2G_9H_3 - 2G_9H_T = \frac{1}{m}[-\frac{iW_3}{k} + \frac{ig}{k} + iC_0 + iC_1H_3 + iG_2(1-\alpha)$$
$$-\frac{C_1R}{AS} - C_1mW_3 + \frac{\dot{W}_3}{k}]. \qquad (114)$$

Solving for $\dot{W}_3$ in the above equation we get the following equations.

$$\frac{\dot{W}_3}{mk} = \frac{iW_3}{mk} - \frac{ig}{mk} - \frac{iC_0}{m} - \frac{iC_1H_3}{m} - \frac{iG_2(1-\alpha)}{m}$$
$$+\frac{C_1R}{ASm} + 2G_9H_3 - 2G_9H_T \qquad (115)$$

$$\frac{\dot{W}_3}{k} = \frac{iW_3}{k} - \frac{ig}{k} - iC_0 - iC_1H_3 - iG_2(1-\alpha)$$
$$+\frac{C_1R}{AS} + 2mG_9H_3 - 2mG_9H_T \qquad (116)$$

$$\dot{W}_3 = iW_3 - ig - ikC_0 - ikC_1H_3 - ikG_2(1-\alpha)$$
$$+\frac{C_1Rk}{AS} + 2mkG_9H_3 - 2mkG_9H_T \qquad (117)$$

$$\dot{W}_3 = iW_3 + [2mkG_9 - ikC_1]H_3 + [-ig - ikC_0 - ikG_2(1-\alpha)$$
$$+\frac{C_1Rk}{AS} - 2mkG_9H_T] \qquad (118)$$

Likewise, the value for $\dot{H}_3$ can be rewritten as

$$\dot{H}_3 = \frac{(\alpha-1)W_3}{AS} + \frac{R}{AS}. \qquad (119)$$

Consequently, we now have to solve the two simultaneous differential equations ((118) and (119)). Thus, by letting $m = \frac{(\alpha-1)}{AS}$, $uuu = 2mkG_9 - ikC_1$, $NNN = -ig - ikC_0 - ikG_2(1-\alpha) + \frac{C_1Rk}{AS} - 2mkG_9H_T$ and $M = \frac{R}{AS}$, we get the following system of differential equations.

$$\dot{W}_3 = iW_3 + uuu \cdot H_3 + NNN. \qquad (120)$$

$$\dot{H}_3 = m \cdot W_3 + M. \qquad (121)$$

Putting the above system of differential equations in a D operator format (where $D = \frac{d}{dt}$), and solving for W_3 yields the following second order linear non-homogeneous differential equation.

$$[(D^2 - Di) - uuu \cdot m]W_3 = uuu \cdot M. \quad (122)$$

The particular solution of the above differential equation is given by: $-\frac{M}{m}$ and the characteristic roots by $z_{1,2} = \frac{i \pm \sqrt{i^2 + 4uuu \cdot m}}{2}$. Furthermore, the steady state level water table is given by

$$H_3^* = [\frac{i\frac{M}{m} - NNN}{uuu}] \quad (123)$$

Hence, the solution for $W_3^*(t)$ and $H_3^*(t)$ are given as follows, respectively.

$$W_3^*(t) = \overline{DA}\mathrm{e}^{tz_1} + \overline{DB}\mathrm{e}^{tz_2} - \frac{M}{m}, \quad (124)$$

$$H_3^*(t) = \frac{m \cdot \overline{DA}}{z_1}\mathrm{e}^{tz_1} + \frac{m \cdot \overline{DB}}{z_2}\mathrm{e}^{tz_2} + \frac{i\frac{M}{m} - NNN}{uuu}. \quad (125)$$

Where $\overline{DA}$ and $\overline{DB}$ are obtained by imposing the initial conditions.

$$\overline{DB} = \frac{z_2}{m}\mathrm{e}^{-z_2 t_c}[H_c - \frac{\frac{iM}{m} - NNN}{uuu} - \frac{[H_T - \frac{\frac{iM}{m} - NNN}{uuu}] - [H_c - \frac{\frac{iM}{m} - NNN}{uuu}]\mathrm{e}^{z_2(t_T - t_c)}}{\mathrm{e}^{z_1(t_T - t_c)} - \mathrm{e}^{z_2(t_T - t_c)}}]. \quad (126)$$

$$\overline{DA} = \frac{z_1}{m}[\frac{[H_T - \frac{\frac{iM}{m} - NNN}{uuu}] - [H_c - \frac{\frac{iM}{m} - NNN}{uuu}]\mathrm{e}^{z_2(t_T - t_c)}}{\mathrm{e}^{z_1 t_T} - \mathrm{e}^{z_1 t_c + z_2(t_T - t_c)}}]. \quad (127)$$

Therefore, the functional defined in (16) is verified to be a convergent integral.

Appendix 6. Proof of Proposition 3.

To determine the impact of the tax per unit of land sinking on optimal solutions, we differentiate the optimal solutions with respect to β.

$$\frac{\partial W^*}{\partial \beta} = \frac{ik(1-\alpha)\eta\varepsilon b\psi}{mAS[2mkG_9 - ikC_1]} \times [\frac{(\mathrm{e}^{z_2(t_T - t_c)} - 1)\mathrm{e}^{tz_1}z_1}{\mathrm{e}^{t_T z_1} - \mathrm{e}^{z_1 t_c + z_2(t_T - t_c)}} - z_2\mathrm{e}^{z_2(t - t_c)} - \frac{(\mathrm{e}^{z_2(t_T - t_c)} - 1)\mathrm{e}^{z_2(t - t_c)}z_2}{\mathrm{e}^{t_T z_1} - \mathrm{e}^{t_c z_1 + z_2(t_T - t_c)}}]. \quad (128)$$

We observe that $\mathrm{e}^{z_2(t_T - t_c)} - 1 < 0$ since $\mathrm{e}^{z_2(t_T - t_c)} \in (0,1)$ because$z_2 < 0$ and $t_T > t_c$. In addition, $e^{z_1 t} > 1$ since $t > 0$ and $z_1 > 0$. In addition, $e^{z_1 t_T} > 1$. Therefore, $(e^{z_2(t_T - t_c)} - 1)e^{z_1 t} z_1 < 0$, and $e^{z_1 t_T} - e^{z_1 t_c + z_2(t_T - t_c)} > 0$ because $e^{z_1 t_T} > e^{z_1 t_c + z_2(t_T - t_c)}$ implies $e^{z_1} > e^{z_2}$ always which is true since $e^{z_1} > 0$ and $e^{z_2} \in (0,1)$. Therefore, $\frac{(e^{z_2(t_T - t_c)} - 1)e^{t z_1} z_1}{e^{t_T z_1} - e^{z_1 t_c + z_2(t_T - t_c)}} < 0$. Furthermore, $z_2 e^{z_2(t - t_c)} < 0$ since $z_2 < 0$, and $e^{z_2(t - t_c)} \in (0,1)$ because $z_2 < 0$ and $t > t_c$. In addition, the final term in the bracket is $\frac{(e^{z_2(t_T - t_c)} - 1)e^{z_2(t - t_c)} z_2}{e^{t_T z_1} - e^{t_c z_1 + z_2(t_T - t_c)}} < 0$. The terms $2m^2 ASkG_9 < 0$, $mASikC_1 < 0$, and $mAS[2mkG_9 - ikC_1] < 0$ since $2m^2 kG_9 AS > mASikC_1$ implies $\frac{2mG_9}{C_1} > i$ where $i \in (0,1)$ and $G_9 > 0$ implies $\frac{2mG_9}{C_1} > 0$. The whole derivative is negative because

$$\frac{(e^{z_2(t_T - t_c)} - 1)e^{t z_1} z_1}{e^{t_T z_1} - e^{z_1 t_c + z_2(t_T - t_c)}} > z_2 e^{z_2(t - t_c)} + \frac{(e^{z_2(t_T - t_c)} - 1)e^{z_2(t - t_c)} z_2}{e^{t_T z_1} - e^{t_c z_1 + z_2(t_T - t_c)}} \quad (129)$$

The Left Hand Side (LHS) is less than zero and the Right Hand Side (RHS) is also less than zero, but the RHS is more negative than the other because

$$\frac{z_2 e^{z_2(t - t_c)}}{e^{z_1 t} z_1} > \frac{(e^{z_2(t_T - t_c)} - 1)e^{z_2(t - t_c)} z_2}{e^{t_T z_1}}. \quad (130)$$

We now differentiate the optimal water table level with respect to β.

$$\frac{\partial H^*}{\partial \beta} = \frac{ik(1-\alpha)\eta\varepsilon b\psi}{mAS[2mkG_9 - ikC_1]} \times [\frac{(e^{z_2(t_T - t_c)} - 1)e^{t z_1} z_1}{e^{t_T z_1} - e^{z_1 t_c + z_2(t_T - t_c)}}$$

$$-z_2 e^{z_2(t - t_c)} - \frac{(e^{z_2(t_T - t_c)} - 1)e^{z_2(t - t_c)} z_2}{e^{t_T z_1} - e^{t_c z_1 + z_2(t_T - t_c)}} + \frac{1}{m}]. \quad (131)$$

We observe that $e^{z_2(t_T - t_c)} - 1 < 0$ since $e^{z_2(t_T - t_c)} \in (0,1)$ because$z_2 < 0$ and $t_T > t_c$. In addition, $e^{z_1 t} > 1$ since $t > 0$ and $z_1 > 0$. In addition, $e^{z_1 t_T} > 1$. Therefore, $(e^{z_2(t_T - t_c)} - 1)e^{z_1 t} z_1 < 0$, and $e^{z_1 t_T} - e^{z_1 t_c + z_2(t_T - t_c)} > 0$ because $e^{z_1 t_T} > e^{z_1 t_c + z_2(t_T - t_c)}$ implies $e^{z_1} > e^{z_2}$ always which is true since $e^{z_1} > 0$ and $e^{z_2} \in (0,1)$. Therefore, $\frac{(e^{z_2(t_T - t_c)} - 1)e^{t z_1} z_1}{e^{t_T z_1} - e^{z_1 t_c + z_2(t_T - t_c)}} < 0$. the term $\frac{1}{m} < 0$ since $m < 0$. Furthermore, $z_2 e^{z_2(t - t_c)} < 0$ since $z_2 < 0$, and $e^{z_2(t - t_c)} \in (0,1)$ because $z_2 < 0$ and $t > t_c$. In addition, the final term in the bracket is $\frac{(e^{z_2(t_T - t_c)} - 1)e^{z_2(t - t_c)} z_2}{e^{t_T z_1} - e^{t_c z_1 + z_2(t_T - t_c)}} < 0$. The terms $2m^2 ASkG_9 < 0$, $mASikC_1 < 0$, and $mAS[2mkG_9 - ikC_1] < 0$ since $2m^2 kG_9 AS > mASikC_1$ implies $\frac{2mG_9}{C_1} > i$ where $i \in (0,1)$ and $G_9 > 0$ implies $\frac{2mG_9}{C_1} > 0$. The whole derivative is negative because

$$\frac{(e^{z_2(t_T - t_c)} - 1)e^{t z_1} z_1}{e^{t_T z_1} - e^{z_1 t_c + z_2(t_T - t_c)}} > z_2 e^{z_2(t - t_c)} + \frac{(e^{z_2(t_T - t_c)} - 1)e^{z_2(t - t_c)} z_2}{e^{t_T z_1} - e^{t_c z_1 + z_2(t_T - t_c)}} + \frac{1}{m} \quad (132)$$

The Left Hand Side (LHS) is less than zero and the Right Hand Side (RHS) is also less than zero, but the RHS is more negative than the other because

$$\frac{z_2 e^{z_2(t-t_c)}}{e^{z_1 t} z_1} > \frac{(e^{z_2(t_T-t_c)}-1)e^{z_2(t-t_c)} z_2}{e^{t_T z_1}} + \frac{1}{m}. \tag{133}$$

Therefore, a higher Pigouvian tax reduces the optimal level of groundwater extraction and raises the optimal water table level.

Appendix 7. Proof of Proposition 4.

To determine the impact of the tax per unit of land sinking on ecosystem health, we differentiate the functional GDEsHS with respect to β.

$$\frac{\partial GDEsHS(H^*)}{\partial \beta} = 2(H^* - H_T)(1+\eta\varepsilon b\psi)^2 \frac{\rho-\gamma}{(d_c)^2} \frac{ik(1-\alpha)\eta\varepsilon b\psi}{mAS[2mkG_9 - ikC_1]}$$

$$\times \left[\frac{(e^{z_2(t_T-t_c)}-1)e^{tz_1} z_1}{e^{t_T z_1} - e^{z_1 t_c + z_2(t_T-t_c)}} - z_2 e^{z_2(t-t_c)} - \frac{(e^{z_2(t_T-t_c)}-1)e^{z_2(t-t_c)} z_2}{e^{t_T z_1} - e^{t_c z_1 + z_2(t_T-t_c)}} + \frac{1}{m}\right]. \tag{134}$$

We observe that $H^* - H_T > 0$ since $H^* > H_T$. If $H^* = H_T$, the ecosystem health has reached the critical thtreshold beyond which it change sto the critical unhealthy phase. In addition, $(1+\eta\varepsilon b\psi)^2 > 0$ and $\frac{\rho-\gamma}{(d_c)^2} > 0$ since $\rho > \gamma$. We further observe that $e^{z_2(t_T-t_c)} - 1 < 0$ since $e^{z_2(t_T-t_c)} \in (0,1)$ because$z_2 < 0$ and $t_T > t_c$. In addition, $e^{z_1 t} > 1$ since $t > 0$ and $z_1 > 0$. In addition, $e^{z_1 t_T} > 1$. Therefore, $(e^{z_2(t_T-t_c)} - 1)e^{z_1 t} z_1 < 0$, and $e^{z_1 t_T} - e^{z_1 t_c + z_2(t_T-t_c)} > 0$ because $e^{z_1 t_T} > e^{z_1 t_c + z_2(t_T-t_c)}$ implies $e^{z_1} > e^{z_2}$ always which is true since $e^{z_1} > 0$ and $e^{z_2} \in (0,1)$. Therefore, $\frac{(e^{z_2(t_T-t_c)}-1)e^{tz_1} z_1}{e^{t_T z_1} - e^{z_1 t_c + z_2(t_T-t_c)}} < 0$. the term $\frac{1}{m} < 0$ since $m < 0$. Furthermore, $z_2 e^{z_2(t-t_c)} < 0$ since $z_2 < 0$, and $e^{z_2(t-t_c)} \in (0,1)$ because $z_2 < 0$ and $t > t_c$. In addition, the final term in the bracket is $\frac{(e^{z_2(t_T-t_c)}-1)e^{z_2(t-t_c)} z_2}{e^{t_T z_1} - e^{t_c z_1 + z_2(t_T-t_c)}} < 0$. The terms $2m^2ASkG_9 < 0$, $mASikC_1 < 0$, and $mAS[2mkG_9 - ikC_1] < 0$ since $2m^2kG_9AS > mASikC_1$ implies $\frac{2mG_9}{C_1} > i$ where $i \in (0,1)$ and $G_9 > 0$ implies $\frac{2mG_9}{C_1} > 0$. The whole derivative is negative because

$$\frac{(e^{z_2(t_T-t_c)}-1)e^{tz_1} z_1}{e^{t_T z_1} - e^{z_1 t_c + z_2(t_T-t_c)}} > z_2 e^{z_2(t-t_c)} + \frac{(e^{z_2(t_T-t_c)}-1)e^{z_2(t-t_c)} z_2}{e^{t_T z_1} - e^{t_c z_1 + z_2(t_T-t_c)}} + \frac{1}{m} \tag{135}$$

The Left Hand Side (LHS) is less than zero and the Right Hand Side (RHS) is also less than zero, but the RHS is more negative than the other because

$$\frac{z_2 e^{z_2(t-t_c)}}{e^{z_1 t} z_1} > \frac{(e^{z_2(t_T-t_c)}-1)e^{z_2(t-t_c)} z_2}{e^{t_T z_1}} + \frac{1}{m}. \tag{136}$$

Therefore, the higher the Pigouvian tax the higher the optimal level of the GDEs' health.

Appendix 8. Detailed solution of the second sub-problem on taxes

We can now solve for the second sub-problem since we have the solution (SP_3^*) to the third sub-problem. The hamiltonian function of the system (25), (26), (27) is given as follows

$$\mathcal{H}_2(t, W_2, H_2, \lambda_2) = -\mathrm{e}^{-it}[\frac{W_2^2}{2k} - \frac{gW_2}{k} - (C_0 + C_1 H_2)W_2 + \theta[\frac{(\delta-\rho)}{(H_u-H_c)^2} \cdot (H_2 - H_c)^2 + \rho]] + \lambda_2 \cdot \frac{[R+(\alpha-1)W_2]}{AS} \tag{137}$$

Equation (137) can be rewritten as follows.

$$\mathcal{H}_2(t, W_2, H_2, \lambda_2) = -\mathrm{e}^{-it}[\frac{W_2^2}{2k} - \frac{gW_2}{k} - (C_0 + C_1 H_2)W_2 + G_{10}(H_2 - H_c)^2 + \theta\rho] + \lambda_2 \cdot \frac{[R+(\alpha-1)W_2]}{AS} \tag{138}$$

Where

$$G_{10} = \frac{\theta(\delta-\rho)}{[H_u-H_c]^2}. \tag{139}$$

Hence, the first order conditions are as follows

$$\frac{\partial \mathcal{H}_2}{\partial W_2} = -\mathrm{e}^{-it}[\frac{W_2}{k} - \frac{g}{k} - C_0 - C_1 H_2] + \lambda_2[\frac{(\alpha-1)}{AS}] = 0. \tag{140}$$

$$\dot{\lambda}_2 = -\frac{\partial \mathcal{H}_2}{\partial H_2}. \tag{141}$$

$$\lambda_2^*(t_c, W_2^*(t_c), H_2^*(t_c)) = \lambda_3^*(t_c, W_3^*(t_c), H_3^*(t_c)) \tag{142}$$

$$\mathcal{H}_2^*(t_c) = \frac{\partial SP_3^*(t_c, W_3^*(t_c), H_3^*(t_c))}{\partial t_c}, \tag{143}$$

$$\dot{H}_2 = \frac{1}{AS}[R + (\alpha - 1)W_2]. \tag{144}$$

The transversality condition is given by $\lim_{t\to\infty}\lambda_2(t) = 0$. From Equation (140), we obtain the value for the costate variable λ_2 as follows.

$$\lambda_2 = \frac{1}{m}\mathrm{e}^{-it}[\frac{W_2}{k} - \frac{g}{k} - C_0 - C_1H_2], \tag{145}$$

where $m = \frac{(\alpha-1)}{AS}$. The derivative of λ_2 with respect to t is given by

$$\dot{\lambda}_2 = \frac{1}{m}\mathrm{e}^{-it}[-\frac{iW_2}{k} + \frac{ig}{k} + iC_0 + iC_1H_2 \ \ -\frac{C_1R}{AS} - C_1mW_2 + \frac{\dot{W}_2}{k}]. \tag{146}$$

The derivative of $\mathcal{H}_2$ with respect to the water table height H_3 is given by

$$-\frac{\partial\mathcal{H}_2}{\partial H_2} = -\mathrm{e}^{-it}[C_1W_2 - 2G_{10}H_2 + 2G_{10}H_c]. \tag{147}$$

From Equation (141) and (146), we obtain the following equation.

$$-C_1W_2 + 2G_{10}H_2 - 2G_{10}H_c = \frac{1}{m}[-\frac{iW_2}{k} + \frac{ig}{k} + iC_0 + iC_1H_2$$
$$-\frac{C_1R}{AS} - C_1mW_2 + \frac{\dot{W}_2}{k}]. \tag{148}$$

Solving for $\dot{W}_2$ in the above equation we get the following equations.

$$\frac{\dot{W}_2}{mk} = \frac{iW_2}{mk} - \frac{ig}{mk} - \frac{iC_0}{m} - \frac{iC_1H_2}{m} + \frac{C_1R}{ASm} + 2G_{10}H_2 - 2G_{10}H_c \tag{149}$$

$$\frac{\dot{W}_2}{k} = \frac{iW_2}{k} - \frac{ig}{k} - iC_0 - iC_1H_2 + \frac{C_1R}{AS} + 2mG_{10}H_2 - 2mG_{10}H_c \tag{150}$$

$$\dot{W}_2 = iW_2 - ig - ikC_0 - ikC_1H_2 + \frac{C_1Rk}{AS} + 2mkG_{10}H_2 - 2mkG_{10}H_c \tag{151}$$

$$\dot{W}_2 = iW_2 + [2mkG_{10} - ikC_1]H_2 + [-ig - ikC_0 + \frac{C_1Rk}{AS} - 2mkG_{10}H_c] \tag{152}$$

Likewise, the value for $\dot{H}_2$ can be rewritten as

$$\dot{H}_2 = \frac{(\alpha-1)W_2}{AS} + \frac{R}{AS}. \tag{153}$$

Consequently, we now have to solve the two simultaneous differential equations ((152) and (153)). Thus, by letting $m = \frac{(\alpha-1)}{AS}$, $ddd = 2mkG_{10} - ikC_1$, $PPP = -ig - ikC_0 + \frac{C_1Rk}{AS} - 2mkG_{10}H_c$ and $M = \frac{R}{AS}$, we get the following system of differential equations.

$$\dot{W}_2 = iW_2 + ddd \cdot H_2 + PPP. \tag{154}$$
$$\dot{H}_2 = m \cdot W_2 + M. \tag{155}$$

Putting the above system of differential equations in a D operator format (where $D = \frac{d}{dt}$), and solving for W_2 yields the following second order linear non-homogeneous differential equation.

$$[(D^2 - Di) - ddd \cdot m]W_2 = ddd \cdot M. \qquad (156)$$

The particular solution of the above differential equation is given by: $-\frac{M}{m}$ and the characteristic roots by $q_{1,2} = \frac{i \pm \sqrt{i^2 + 4 \cdot ddd \cdot m}}{2}$. Furthermore, the steady state level water table is given by

$$H_2^* = [\frac{i\frac{M}{m} - PPP}{ddd}] \qquad (157)$$

Hence, the solution for $W_2^*(t)$ and $H_2^*(t)$ are given as follows, respectively.

$$W_2^*(t) = \overline{EA}\mathrm{e}^{tq_1} + \overline{EB}\mathrm{e}^{tq_2} - \frac{M}{m}, \qquad (158)$$

$$H_2^*(t) = \frac{m \cdot \overline{EA}}{q_1}\mathrm{e}^{tq_1} + \frac{m \cdot \overline{EB}}{q_2}\mathrm{e}^{tq_2} + \frac{i\frac{M}{m} - PPP}{ddd}. \qquad (159)$$

Where $\overline{EA}$ and $\overline{EB}$ are obtained by imposing the initial conditions.

$$\overline{EB} = \frac{q_2}{m}\mathrm{e}^{-q_2 t_u}[H_u - \frac{\frac{iM}{m} - PPP}{ddd} - \frac{[H_c - \frac{\frac{iM}{m} - PPP}{ddd}] - [H_u - \frac{\frac{iM}{m} - PPP}{ddd}]\mathrm{e}^{q_2(t_c - t_u)}}{\mathrm{e}^{q_1(t_c - t_u)} - \mathrm{e}^{q_2(t_c - t_u)}}]. \qquad (160)$$

$$\overline{EA} = \frac{q_1}{m}[\frac{[H_c - \frac{\frac{iM}{m} - PPP}{ddd}] - [H_u - \frac{\frac{iM}{m} - PPP}{ddd}]\mathrm{e}^{q_2(t_c - t_u)}}{\mathrm{e}^{q_1 t_c} - \mathrm{e}^{q_1 t_u + q_2(t_c - t_u)}}]. \qquad (161)$$

Therefore, the functional defined in (25) is verified to be a convergent integral.

Appendix 9. Detailed solution of the first sub-problem on taxes

We can now solve for the first sub-problem since we have the solution (SP_2^*) to the second sub-problem. The hamiltonian function of the system (34), (35), (36) is given as follows

$$\mathcal{H}_1(t, W_1, H_1, \lambda_1) = -\mathrm{e}^{-it}[\frac{W_1^2}{2k} - \frac{gW_1}{k} - (C_0 + C_1 H_1)W_1 + \theta[\frac{(\delta - 1)}{(S_l - H_u)^2}$$

$$\cdot (S_l - H_1)^2 + 1]] + \lambda_1 \cdot \frac{[R+(\alpha-1)W_1]}{AS} \tag{162}$$

Equation (162) can be rewritten as follows.

$$\mathcal{H}_1(t, W_1, H_1, \lambda_1) = -\mathrm{e}^{-it}[\frac{W_1^2}{2k} - \frac{gW_1}{k} - (C_0 + C_1H_1)W_1 + G_{11}(S_l - H_1)^2 + \theta]$$

$$+\lambda_1 \cdot \frac{[R+(\alpha-1)W_1]}{AS} \tag{163}$$

Where

$$G_{11} = \frac{\theta(\delta-1)}{[S_l - H_u]^2}. \tag{164}$$

Hence, the first order conditions are as follows

$$\frac{\partial \mathcal{H}_1}{\partial W_1} = -\mathrm{e}^{-it}[\frac{W_1}{k} - \frac{g}{k} - C_0 - C_1H_1] + \lambda_1[\frac{(\alpha-1)}{AS}] = 0. \tag{165}$$

$$\dot{\lambda}_1 = -\frac{\partial \mathcal{H}_1}{\partial H_1}. \tag{166}$$

$$\lambda_1^*(t_u, W_1^*(t_u), H_1^*(t_u)) = \lambda_2^*(t_u, W_2^*(t_u), H_2^*(t_u)) \tag{167}$$

$$\mathcal{H}_1^*(t_u) = \frac{\partial SP_2^*(t_u, W_2^*(t_u), H_2^*(t_u))}{\partial t_u}, \tag{168}$$

$$\dot{H}_1 = \frac{1}{AS}[R + (\alpha - 1)W_1]. \tag{169}$$

The transversality condition is given by $\lim_{t\to\infty}\lambda_1(t) = 0$. From Equation (165), we obtain the value for the costate variable λ_1 as follows.

$$\lambda_1 = \frac{1}{m}\mathrm{e}^{-it}[\frac{W_1}{k} - \frac{g}{k} - C_0 - C_1H_1], \tag{170}$$

where $m = \frac{(\alpha-1)}{AS}$. The derivative of λ_1 with respect to t is given by

$$\dot{\lambda}_1 = \frac{1}{m}\mathrm{e}^{-it}[-\frac{iW_1}{k} + \frac{ig}{k} + iC_0 + iC_1H_1 \quad - \frac{C_1R}{AS} - C_1mW_1 + \frac{\dot{W}_1}{k}]. \tag{171}$$

The derivative of $\mathcal{H}_1$ with respect to the water table height H_1 is given by

$$-\frac{\partial \mathcal{H}_1}{\partial H_1} = -\mathrm{e}^{-it}[C_1W_1 + 2G_{11}S_l - 2G_{11}H_1]. \tag{172}$$

From Equation (166) and (171), we obtain the following equation.

$$-C_1W_1 - 2G_{11}S_l + 2G_{11}H_1 = \frac{1}{m}[-\frac{iW_1}{k} + \frac{ig}{k} + iC_0 + iC_1H_1$$
$$-\frac{C_1R}{AS} - C_1mW_1 + \frac{\dot{W}_1}{k}]. \quad (173)$$

Solving for $\dot{W}_1$ in the above equation we get the following equations.

$$\frac{\dot{W}_1}{mk} = \frac{iW_1}{mk} - \frac{ig}{mk} - \frac{iC_0}{m} - \frac{iC_1H_1}{m} + \frac{C_1R}{ASm} + 2G_{11}H_1 - 2G_{11}S_l \quad (174)$$

$$\frac{\dot{W}_1}{k} = \frac{iW_1}{k} - \frac{ig}{k} - iC_0 - iC_1H_1 + \frac{C_1R}{AS} + 2mG_{11}H_1 - 2mG_{11}S_l \quad (175)$$

$$\dot{W}_1 = iW_1 - ig - ikC_0 - ikC_1H_1 + \frac{C_1Rk}{AS} + 2mkG_{11}H_1 - 2mkG_{11}S_l \quad (176)$$

$$\dot{W}_1 = iW_1 + [2mkG_{11} - ikC_1]H_1 + [-ig - ikC_0 + \frac{C_1Rk}{AS} - 2mkG_{11}S_l] \quad (177)$$

Likewise, the value for $\dot{H}_1$ can be rewritten as

$$\dot{H}_1 = \frac{(\alpha-1)W_1}{AS} + \frac{R}{AS}. \quad (178)$$

Consequently, we now have to solve the two simultaneous differential equations ((177) and (178)). Thus, by letting $m = \frac{(\alpha-1)}{AS}$, $u = 2mkG_{11} - ikC_1$, $N = -ig - ikC_0 + \frac{C_1Rk}{AS} - 2mkG_{11}S_l$ and $M = \frac{R}{AS}$, we get the following system of differential equations.

$$\dot{W}_1 = iW_1 + u \cdot H_1 + N. \quad (179)$$
$$\dot{H}_1 = m \cdot W_1 + M. \quad (180)$$

Putting the above system of differential equations in a D operator format (where $D = \frac{d}{dt}$), and solving for W_1 yields the following second order linear non-homogeneous differential equation.

$$[(D^2 - Di) - u \cdot m]W_1 = u \cdot M. \quad (181)$$

The particular solution of the above differential equation is given by: $-\frac{M}{m}$ and the characteristic roots by $y_{1,2} = \frac{i \pm \sqrt{i^2 + 4u \cdot m}}{2}$. Furthermore, the steady state level water table is given by

$$H_1^* = [\frac{i\frac{M}{m}-N}{u}] \quad (182)$$

Hence, the solution for $W_1^*(t)$ and $H_1^*(t)$ are given as follows, respectively.

$$W_1^*(t) = \overline{A}\mathrm{e}^{ty_1} + \overline{B}\mathrm{e}^{ty_2} - \frac{M}{m}, \quad (183)$$

$$H_1^*(t) = \frac{m\cdot\overline{A}}{y_1}\mathrm{e}^{ty_1} + \frac{m\cdot\overline{B}}{y_2}\mathrm{e}^{ty_2} + \frac{i\frac{M}{m}-N}{u}. \quad (184)$$

Where $\overline{A}$ and $\overline{B}$ are obtained by imposing the initial conditions.

$$\overline{B} = \frac{y_2}{m}[H_0 - \frac{\frac{iM}{m}-N}{u}$$
$$-\frac{[H_u-\frac{\frac{iM}{m}-N}{u}]-[H_0-\frac{\frac{iM}{m}-N}{u}]\mathrm{e}^{y_2 t_u}}{\mathrm{e}^{y_1 t_u}-\mathrm{e}^{y_2 t_u}}]. \quad (185)$$

$$\overline{A} = \frac{y_1}{m}[\frac{[H_u-\frac{\frac{iM}{m}-N}{u}]-[H_0-\frac{\frac{iM}{m}-N}{u}]\mathrm{e}^{y_2 t_u}}{\mathrm{e}^{y_1 t_u}-\mathrm{e}^{y_2 t_u}}]. \quad (186)$$

Therefore, the functional defined in (34) is verified to be a convergent integral.

Appendix 10. Detailed solution of the Quotas system resolution

The hamiltonian function of the system (41), (42), (43), and (44) is given as follows

$$\mathcal{H}(t,W,H,\lambda) = -\mathrm{e}^{-it}[\frac{W^2}{2k} - \frac{gW}{k} - (C_0 + C_1H)W + \theta[\frac{(\delta-1)}{(S_l-H_u)^2}$$
$$\cdot (S_l - H)^2 + 1]] + \lambda \cdot \frac{[R+(\alpha-1)W]}{AS} \quad (187)$$

Equation (187) can be rewritten as follows.

$$\mathcal{H}(t,W,H,\lambda) = -\mathrm{e}^{-it}[\frac{W^2}{2k} - \frac{gW}{k} - (C_0 + C_1H)W + G_{11}(S_l - H)^2 + \theta]$$
$$+\lambda \cdot \frac{[R+(\alpha-1)W]}{AS} \quad (188)$$

Where

$$G_{11} = \frac{\theta(\delta-1)}{[S_l-H_u]^2}. \quad (189)$$

Hence, the first order conditions are as follows

$$\frac{\partial \mathcal{H}}{\partial W} = -\mathrm{e}^{-it}[\frac{W}{k} - \frac{g}{k} - C_0 - C_1 H] + \lambda[\frac{(\alpha-1)}{AS}] = 0. \tag{190}$$

$$\dot{\lambda} = -\frac{\partial \mathcal{H}}{\partial H}. \tag{191}$$

$$\dot{H} = \frac{1}{AS}[R + (\alpha - 1)W]. \tag{192}$$

The transversality condition is given by $\lim_{t\to\infty}\lambda(t) = 0$. From Equation (190), we obtain the value for the costate variable λ as follows.

$$\lambda = \frac{1}{m}\mathrm{e}^{-it}[\frac{W}{k} - \frac{g}{k} - C_0 - C_1 H], \tag{193}$$

where $m = \frac{(\alpha-1)}{AS}$. The derivative of λ with respect to t is given by

$$\dot{\lambda} = \frac{1}{m}\mathrm{e}^{-it}[-\frac{iW}{k} + \frac{ig}{k} + iC_0 + iC_1 H$$
$$-\frac{C_1 R}{AS} - C_1 mW + \frac{\dot{W}}{k}]. \tag{194}$$

The derivative of $\mathcal{H}$ with respect to the water table height H is given by

$$-\frac{\partial \mathcal{H}}{\partial H} = -\mathrm{e}^{-it}[C_1 W + 2G_{11}S_l - 2G_{11}H]. \tag{195}$$

From Equation (191) and (194), we obtain the following equation.

$$-C_1 W - 2G_{11}S_l + 2G_{11}H = \frac{1}{m}[-\frac{iW}{k} + \frac{ig}{k} + iC_0 + iC_1 H$$
$$-\frac{C_1 R}{AS} - C_1 mW + \frac{\dot{W}}{k}]. \tag{196}$$

Solving for $\dot{W}$ in the above equation we get the following equations.

$$\frac{\dot{W}}{mk} = \frac{iW}{mk} - \frac{ig}{mk} - \frac{iC_0}{m} - \frac{iC_1 H}{m} + \frac{C_1 R}{ASm} + 2G_{11}H - 2G_{11}S_l \tag{197}$$

$$\frac{\dot{W}}{k} = \frac{iW}{k} - \frac{ig}{k} - iC_0 - iC_1 H + \frac{C_1 R}{AS} + 2mG_{11}H - 2mG_{11}S_l \tag{198}$$

$$\dot{W} = iW - ig - ikC_0 - ikC_1 H + \frac{C_1 Rk}{AS} + 2mkG_{11}H - 2mkG_{11}S_l \tag{199}$$

$$\dot{W} = iW + [2mkG_{11} - ikC_1]H + [-ig - ikC_0 + \frac{C_1Rk}{AS} - 2mkG_{11}S_l] \quad (200)$$

Likewise, the value for $\dot{H}$ can be rewritten as

$$\dot{H} = \frac{(\alpha-1)W}{AS} + \frac{R}{AS}. \quad (201)$$

Consequently, we now have to solve the two simultaneous differential equations ((200) and (201)). Thus, by letting $m = \frac{(\alpha-1)}{AS}$, $\overline{u} = -2mkG_{11} + ikC_1$, $N = -ig - ikC_0 + \frac{C_1Rk}{AS} - 2mkG_{11}S_l$ and $M = \frac{R}{AS}$, we get the following system of differential equations.

$$\dot{W} = iW - \overline{u} \cdot H + N. \quad (202)$$

$$\dot{H} = m \cdot W + M. \quad (203)$$

Putting the above system of differential equations in a D operator format (where $D = \frac{d}{dt}$), and solving for W yields the following second order linear non-homogeneous differential equation.

$$[(D^2 - Di) + \overline{u} \cdot m]W = -\overline{u} \cdot M. \quad (204)$$

The particular solution of the above differential equation is given by: $-\frac{M}{m}$ and the solution to the homogeneous differential equation ($[(D^2 - Di) + \overline{u} \cdot m]W = 0$) by

$$W(t) = A_0 e^{tr_1} + B_0 e^{tr_2}, \quad (205)$$

where $r_{1,2} = \frac{i \pm \sqrt{i^2 - 4\overline{u}m}}{2}$ are the characteristic roots. The parameters A_0 and B_0 are constants to be determined by imposing the initial conditions. Substituting the right hand side (RHS) of (205) for $W(t)$ in the homogenous DE ($\dot{H} = m \cdot W$) and integrating gives the solution for the water table level $H(t)$ as follows.

$$H(t) = \frac{m \cdot A_0}{r_1} e^{tr_1} + \frac{m \cdot B_0}{r_2} e^{tr_2}. \quad (206)$$

Furthermore, the steady state level water table is given by

$$H^* = [\frac{-i\frac{M}{m} + N}{\overline{u}}] \quad (207)$$

Hence, the solution for $W^*(t)$ and $H^*(t)$ are given as follows, respectively.

$$W^*(t) = A_0 e^{tr_1} + B_0 e^{tr_2} - \frac{M}{m}, \quad (208)$$

$$H^*(t) = \frac{m \cdot A_0}{r_1} \mathrm{e}^{tr_1} + \frac{m \cdot B_0}{x_2} \mathrm{e}^{tr_2} + \frac{N - i\frac{M}{m}}{\overline{u}}. \quad (209)$$

Similarly to Gisser and Sanchez (1980) results, it is worth mentioning that $-4\overline{u}m > 0$ since $k < 0, C_1 < 0, i > 0, A > 0, S > 0, S_l > 0, H_u > 0, \delta > 0, G_{11} < 0, H_0 > 0, \theta > 0$, and $\alpha < 1 \Longrightarrow (\alpha - 1) < 0$. This implies that $r_1 > i$ and $r_2 < 0$. Therefore, r_2 is the stable characteristic root. Likewise, similarly to Gisser and Sanchez (1980), we obtained that the transversality condition is only satisfied when $A_0 = 0$. By imposing the initial conditions of the sub problem ($H(t_0) = H_0$), we obtain the constant B_0 as follows below.

$$B_0 = \frac{r_2}{m}[H_0 - \frac{N - i\frac{M}{m}}{\overline{u}}]. \quad (210)$$

Therefore, the optimal solutions for $W^*(t)$ and $H^*(t)$ are given as follows below, respectively.

$$W^*(t) = \frac{r_2}{m}[H_0 - \frac{N - i\frac{M}{m}}{\overline{u}}]\mathrm{e}^{r_2 t} - \frac{M}{m}. \quad (211)$$

$$H^*(t) = [H_0 - \frac{N - i\frac{M}{m}}{\overline{u}}]\mathrm{e}^{r_2 t} + \frac{N - i\frac{M}{m}}{\overline{u}}. \quad (212)$$

Let N be equal to N_0, then

$$W^*(t) = \frac{r_2 AS}{\alpha - 1}[H_0 - \frac{N_0 - i\frac{R}{\alpha - 1}}{\overline{u}}]\mathrm{e}^{r_2 t} - \frac{R}{\alpha - 1}, \quad (213)$$

Where $N_0 = -ig - ikC_0 + \frac{C_1 Rk}{AS} - 2mkG_{11}S_l$. Using equation (213), we determine the value of N_0 that satisfies the condition $W^\star(t) \leq \widehat{W}(t)$.

$$\frac{r_2 AS}{\alpha - 1}[H_0 - \frac{N_0 - i\frac{R}{\alpha - 1}}{\overline{u}}]\mathrm{e}^{r_2 t} - \frac{R}{\alpha - 1} \leq \widehat{W} \quad (214)$$

$$\frac{r_2 AS}{\alpha - 1}[H_0 - \frac{N_0 - i\frac{R}{\alpha - 1}}{\overline{u}}]\mathrm{e}^{r_2 t} \leq \frac{\widehat{W}(\alpha - 1) + R}{\alpha - 1} \quad (215)$$

$$[H_0 - \frac{N_0 - i\frac{R}{\alpha - 1}}{\overline{u}}]\mathrm{e}^{r_2 t} \leq \frac{\widehat{W}(\alpha - 1) + R}{r_2 AS} \quad (216)$$

$$[H_0 - \frac{N_0 - i\frac{R}{\alpha-1}}{\overline{u}}] \leq \frac{\widehat{W}(\alpha-1)+R}{r_2 AS} \mathrm{e}^{-r_2 t} \tag{217}$$

$$H_0\overline{u} - \frac{\widehat{W}(\alpha-1)+R}{r_2 AS} \mathrm{e}^{-r_2 t} \cdot \overline{u} \leq N_0 - \frac{iR}{\alpha-1} \tag{218}$$

$$H_0\overline{u} - \frac{\widehat{W}(\alpha-1)+R}{r_2 AS} \mathrm{e}^{-r_2 t} \cdot \overline{u} + \frac{iR}{\alpha-1} \leq N_0 \tag{219}$$

If we let the Left Hand Side of (219) to be equal to $N_A(t)$, we then obtain

$$W^{\star}(t) = \begin{cases} \frac{r_2 AS}{\alpha-1}[H_0 - \frac{N_0 - i\frac{R}{\alpha-1}}{\overline{u}}]\mathrm{e}^{r_2 t} - \frac{R}{\alpha-1} & N_0 \geq N_A(t) \\ \widehat{W} & N_0 < N_A(t) \end{cases} \tag{220}$$

$$H^{\star}(t) = \begin{cases} [H_0 - \frac{N_0 - i\frac{R}{\alpha-1}}{\overline{u}}]\mathrm{e}^{r_2 t} + \frac{N_0 - i\frac{R}{\alpha-1}}{\overline{u}} & N_0 \geq N_A(t) \\ [H_0 - \frac{N_A(t) - i\frac{R}{\alpha-1}}{\overline{u}}]\mathrm{e}^{r_2 t} + \frac{N_A(t) - i\frac{R}{\alpha-1}}{\overline{u}} & N_0 < N_A(t) \end{cases} \tag{221}$$

Where $r_2 = \frac{i - \sqrt{i^2 - 4\overline{u}\frac{\alpha-1}{AS}}}{2}$, $\overline{u} = -2mkG_{11} + ikC_1$, $G_{11} = \frac{\theta(\delta-1)}{[S_l - H_u]^2}$, $N_0 = -ig - ikC_0 + \frac{C_1 Rk}{AS} - 2mkG_{11}S_l$, and $N_A(t) = H_0\overline{u} - \frac{\widehat{W}(\alpha-1)+R}{r_2 AS}\mathrm{e}^{-r_2 t} \cdot \overline{u} + \frac{iR}{\alpha-1}$.

The conditions to ensure that a maximum has been achieved have been verified.

Appendix 11. Proof of Proposition 5.

Take note that N_0 is just a composite constant and $N_A(t)$ is the switching index or decision variable that decides whether the quota binds ($N_0 < N_A(t)$) or not ($N_0 \geq N_A(t)$). The quota binds (binding quota) when farmers want to extract more than the imposed quota level but their unconstrained groundwater extraction optimum level is forced down to the quota level ($\widehat{W}$), which occurs when the policy constraint is active ($N_0 < N_A(t)$). A non-binding quota refers to the case when farmers unconstrained groundwater extraction optimum level is already less than or equal to $\widehat{W}$, which occurs when the policy constraint is inactive ($N_0 \geq N_A(t)$).Therefore, binding means the policy constraint is active while non-bing implies it is inactive. In addition, the comparison between $N_A(t)$ and N_0 tells us whether farmers are constrained by the quota level at that point in time.

At the beginning of the planning horizon ($t = 0$), if $N_A(0) < N_0$, the quota level does not bind initially (although it could bind later if the dynamics push the system across the threshold). Hence, we solve for $N_A(0) = N_0$, this gives us the critical quota level ($\widehat{W}_c$) where the system is exactly on the boundary between binding and non binding at $t = 0$. Thus, if you choose $\widehat{W}$ above (or below) $\widehat{W}_c$, then you start on the non-binding side (or on the binding side). The quotas optimal solutions are as follows.

$$W^{\star}(t) = \begin{cases} \frac{r_2 AS}{\alpha-1}[H_0 - \frac{N_0 - i\frac{R}{\alpha-1}}{\bar{u}}]\mathrm{e}^{r_2 t} - \frac{R}{\alpha-1} & N_0 \geq N_A(t) \\ \widehat{W} & N_0 < N_A(t) \end{cases} \quad (222)$$

$$H^{\star}(t) = \begin{cases} [H_0 - \frac{N_0 - i\frac{R}{\alpha-1}}{\bar{u}}]\mathrm{e}^{r_2 t} + \frac{N_0 - i\frac{R}{\alpha-1}}{\bar{u}} & N_0 \geq N_A(t) \\ [H_0 - \frac{N_A(t) - i\frac{R}{\alpha-1}}{\bar{u}}]\mathrm{e}^{r_2 t} + \frac{N_A(t) - i\frac{R}{\alpha-1}}{\bar{u}} & N_0 < N_A(t) \end{cases} \quad (223)$$

Where $r_2 = \frac{i - \sqrt{i^2 - 4\bar{u}\frac{\alpha-1}{AS}}}{2}$, $\bar{u} = -2mkG_{11} + ikC_1$, $G_{11} = \frac{\theta(\delta-1)}{[S_l - H_u]^2}$, $N_0 = -ig - ikC_0 + \frac{C_1 Rk}{AS} - 2mkG_{11}S_l$, and $N_A(t) = H_0\bar{u} - \frac{\widehat{W}(\alpha-1)+R}{r_2 AS}\mathrm{e}^{-r_2 t} \cdot \bar{u} + \frac{iR}{\alpha-1}$. From the optimal solutions, we get that at $t = 0$,

$$N_A(0) = H_0\bar{u} - \frac{\widehat{W}(\alpha-1)+R}{r_2 AS}\bar{u} + \frac{iR}{\alpha-1} \quad (224)$$

Setting $N_A(0) = N_0$ and solving for $\widehat{W}$, we obtain the following expression.

$$\widehat{W}_c = \frac{r_2 AS}{\alpha-1}\left(\frac{H_0\bar{u} + \frac{iR}{\alpha-1} - N_0}{\bar{u}}\right) - \frac{iR}{\alpha-1} \quad (225)$$

The derivative of $N_A(t)$ with respect to t is given by the following expression.

$$\frac{\partial N_A(t)}{\partial t} = \frac{\bar{u}}{AS}(\widehat{W}(\alpha-1) + R)\mathrm{e}^{-r_2 t} \quad (226)$$

The derivative above is positive since $\frac{\bar{u}}{AS} > 0$, $\bar{u} > 0$ because $-2mkG_{11} + ikC_1 > 0 \Longrightarrow i > \frac{2mG_{11}}{C_1}$ since $\frac{2mG_{11}}{C_1} < 0$ and $i > 0$ ($m < 0,\ C_1 < 0,\ k < 0,\ G_{11} < 0$). The term $(\widehat{W}(\alpha-1) + R) > 0$ since $(\widehat{W}(\alpha-1) + R) > 0 \Longrightarrow \frac{R}{\widehat{W}} > \alpha - 1$ which is true because $\frac{R}{\widehat{W}} > 0$ and $\alpha - 1 < 0$. Finally, the term $\mathrm{e}^{-r_2 t} \geq 1$ since $r_2 < 0$ and $t \geq 0$. The above analysis implies that $N_A(t)$ is strictly increasing. This implies that if $N_A(t)$ is strictly increasing, then for any later time $t >$

0, $N_A(t) \geq N_A(0)$, which means that the gap between N_0 and $N_A(t)$ can only widen (or stay the same if the derivative was zero). This gap can never shrink. Therefore, if N_0 starts at time $t = 0$ below $N_A(0)$, it must remain below $N_A(t)$ for all $t \geq 0$.

If the quota is binding, then $W^*(t) = \widehat{W}$ ($N_0 < N_A(t)$). If the quota is not binding, then $W^*(t) < \widehat{W}$. Therefore, if the system changes from binding to non binding at $t = 0$ when $\widehat{W} = \widehat{W}_c$, any $\widehat{W} < \widehat{W}_c$ implies the quota is binding, and any $\widehat{W} \geq \widehat{W}_c$ implies the quota is non binding at time $t = 0$. Thus, if the quota is low enough ($\widehat{W} < \widehat{W}_c$), then once $N_0 < N_A(0)$ hold, it continues to hold forever. Thus, the system stays quota binding for the rest of the planning period. If $\widehat{W} \geq \widehat{W}_c$, we have that $N_0 \geq N_A(0)$ and $N_A(t)$ might grow bigger than N_0 at a later time $t > 0$ since $N_A(t)$ is strictly increasing. This means that the quota can bind at a later time $t > 0$.

Appendix 12. Proof of Proposition 6.

Assume the quota is binding at $t = 0$, that is $N_0 < N_A(0)$. The derivative of $N_A(t)$ with respect to θ is given by the following expression.

$$\frac{\partial N_A(t)}{\partial \theta} = -\frac{2H_0 mk(\delta-1)}{(S_l-H_u)^2} + \frac{\widehat{W}(\alpha-1)+R}{AS}\frac{\mathrm{e}^{-r_2 t}}{r_2}\frac{mk(\delta-1)}{(S_l-H_u)^2}$$
$$\times \left(2 + \frac{\bar{u}t}{2\sqrt{i^2-4\frac{(\alpha-1)}{AS}\bar{u}}} + \frac{\bar{u}}{2r_2\sqrt{i^2-4\frac{(\alpha-1)}{AS}\bar{u}}}\right) \quad (227)$$

The derivative above is positive. The parameter $\bar{u} > 0$ because $-2mkG_{11} + ikC_1 > 0 \Rightarrow i > \frac{2mG_{11}}{C_1}$ since $\frac{2mG_{11}}{C_1} < 0$ and $i > 0$ ($m < 0,\ C_1 < 0,\ k < 0,\ G_{11} < 0$). The first term above is negative since $m < 0$, $k < 0$, $\delta - 1 < 0$, and $H_0 > 0$. We also observe that $\frac{\widehat{W}(\alpha-1)+R}{AS} > 0$ since term $(\widehat{W}(\alpha-1)+R) > 0$ since $(\widehat{W}(\alpha-1)+R) > 0 \Rightarrow \frac{R}{\widehat{W}} > \alpha - 1$ which is true because $\frac{R}{\widehat{W}} > 0$ and $\alpha - 1 < 0$. Therefore, the factor outside the brackets of the second term is negative since $\mathrm{e}^{-r_2 t} \geq 1$ and $r_2 < 0$. The second term inside the brackets is greater than or equal to zero since $\bar{u} > 0$, $t \geq 0$, and $\sqrt{i^2 - 4\frac{(\alpha-1)}{AS}\bar{u}} \geq 0$. The last term inside the brackets is less than or equal to zero since $\bar{u} > 0$, $r_2 < 0$, and $\sqrt{i^2 - 4\frac{(\alpha-1)}{AS}\bar{u}} \geq 0$. For the overall derivative to be positive, the following inequality should be true.

$$-\frac{2H_0 mk(\alpha-1)}{(S_l-H_u)^2}+\frac{\widehat{W}(\alpha-1)+R}{AS}\frac{\mathrm{e}^{-r_2 t}}{r_2}\frac{mk(\alpha-1)}{(S_l-H_u)^2}\times\left(2+\frac{\bar{u}t}{2\sqrt{i^2-4\frac{(\alpha-1)}{AS}\bar{u}}}+\frac{\bar{u}}{2r_2\sqrt{i^2-4\frac{(\alpha-1)}{AS}\bar{u}}}\right)>0$$

(228)

$$\Longrightarrow \frac{\bar{u}(\widehat{W}(\alpha-1)+R)\mathrm{e}^{-r_2 t}}{2ASr_2^2\sqrt{i^2-4\frac{(\alpha-1)}{AS}\bar{u}}}>H_0-\frac{(\widehat{W}(\alpha-1)+R)\mathrm{e}^{-r_2 t}}{r_2}\left(2+\frac{\bar{u}t}{2\sqrt{i^2-4\frac{(\alpha-1)}{AS}\bar{u}}}\right) \quad (229)$$

$$\Longrightarrow \mathrm{e}^{-r_2 t}>H_0^{-1}\left(\frac{\bar{u}(\widehat{W}(\alpha-1)+R)}{2ASr_2^2\sqrt{i^2-4\frac{(\alpha-1)}{AS}\bar{u}}}+\frac{2(\widehat{W}(\alpha-1)+R)}{ASr_2}+\frac{\bar{u}t(\widehat{W}(\alpha-1)+R)}{2ASr_2\sqrt{i^2-4\frac{(\alpha-1)}{AS}\bar{u}}}\right) \quad (230)$$

The Left hand Side of the above inequality is negative if the following condition is true.

$$H_0^{-1}\left(\frac{\bar{u}(\widehat{W}(\alpha-1)+R)}{2ASr_2^2\sqrt{i^2-4\frac{(\alpha-1)}{AS}\bar{u}}}+\frac{2(\widehat{W}(\alpha-1)+R)}{ASr_2}+\frac{\bar{u}t(\widehat{W}(\alpha-1)+R)}{2ASr_2\sqrt{i^2-4\frac{(\alpha-1)}{AS}\bar{u}}}\right)<0 \quad (231)$$

$$\Longrightarrow \frac{\bar{u}}{2r_2\sqrt{i^2-4\frac{(\alpha-1)}{AS}\bar{u}}}<-2-\frac{\bar{u}t}{2\sqrt{i^2-4\frac{(\alpha-1)}{AS}\bar{u}}} \quad (232)$$

$$\Longrightarrow \bar{u}<-4r_2\sqrt{i^2-4\frac{(\alpha-1)}{AS}\bar{u}}-\bar{u}tr_2 \quad (233)$$

$$\Longrightarrow r_2>\frac{\bar{u}}{-4\sqrt{i^2-4\frac{(\alpha-1)}{AS}\bar{u}}-\bar{u}t} \quad (234)$$

Intuitively, r_2 should be smaller in terms of magnitude compared to $\frac{\bar{u}}{-4\sqrt{i^2-4\frac{(\alpha-1)}{AS}\bar{u}}-\bar{u}t}$ because it is equal to $\frac{i-\sqrt{i^2-4\frac{(\alpha-1)}{AS}\bar{u}}}{2}$ where $i\in(0,1)$ and smaller negative values are bigger than large negative values for all t. If $t=0$, the Right Hand Side reduces in terms of magnitude. Hence the derivative is proved to be positive.

This means that for every t, a larger θ pushes $N_A(t)$ upward. Next, we explain how the quota binding phase is lengthened. Recall that $N_A(t)$ is an increasing function of time (as we derived in the proof of Proposition 5) and N_0 is fixed. Quota binding phase ends at time t^* where the equality $N_0 = N_A(t^*)$. If θ rises, the whole curve $N_A(t)$ shifts upward. That is, at $t = 0$, the inequality $N_0 < N_A(0)$ still holds, but now the gap is bigger. Since the curve is above N_0 by a bigger margin, it takes longer for $N_A(t)$ to be equal to N_0 if it ever does. Mathematically, the solution t^* to $N_0 = N_A(t^*)$ shifts to the right. Hence, our results is proved.

Appendix 13. Proof of Proposition 7.

When the quota is binding ($N_0 < N_A(t)$) for $t > 0$, the derivative of the water table level with respect to the quota level is given by the following equation.

$$\frac{\partial H^*(t)}{\partial \widehat{W}} = \frac{\alpha - 1}{r_2 AS}(1 - \mathrm{e}^{-r_2 t}) < 0, \ t > 0, \tag{235}$$

because $\mathrm{e}^{-r_2 t} > 1$, $(\alpha - 1) < 0$, $r_2 < 0$, and $AS > 0$. This means that every marginal increase in $\widehat{W}$ lowers the water table by a predictable amount for $t > 0$. Economically, this makes sense, if the quota level ($\widehat{W}$) is relaxed upward, farmers extract more, so the water table ($H^*(t)$) falls (negative derivative). This yields a closed form condition, that to keep $H^*(t) \geq \widetilde{H}_j, \ t > 0, \ j = 1,2,3$ ($\widetilde{H}_j$ represents the critical thresholds for the water table height), it suffices to impose the following condition.

$$\widehat{W} = \widehat{W}_0 + \ \min_{t\in(0,\infty)}\left\{\frac{r_2 AS}{1-\alpha} \cdot \frac{H^*(t,\widehat{W}_0) - \widetilde{H}^*}{1 - \mathrm{e}^{-r_2 t}}\right\} = \widehat{W}_b. \tag{236}$$

Where $\widehat{W}_0$ and $\widetilde{H}^*$ represent the quota level at $t = 0$, and the the maximum of all critical thresholds for the water table height, respectively. Thus, regulators can quantitatively determine the maximum allowable quota consistent with keeping the water table height above any ecological threshold, i.e., $H_u, \ H_c, \ H_T$. Take note that due to the complexity of the minimisation expression in terms of our optimal solution for the water table height, we could not solve for the explicit $\widehat{W}_b$ value. We just propose that maybe with numerical solvers, this may be solved.

Appendix 14. Detailed solution of the Packaging and sequencing resolution

The optimal solution for the third sub-problem on taxes (SP_3^*) is given by

$$W^*(t) = \overline{DA}\mathrm{e}^{tz_1} + \overline{DB}\mathrm{e}^{tz_2} - \frac{R}{\alpha-1}, \quad (237)$$

$$H^*(t) = \frac{(\alpha-1)\overline{DA}}{ASz_1}\mathrm{e}^{tz_1} + \frac{(\alpha-1)\overline{DB}}{ASz_2}\mathrm{e}^{tz_2} + \frac{\frac{iR}{\alpha-1}-NNN}{uuu}. \quad (238)$$

where $z_{1,2} = \frac{i\pm\sqrt{i^2+4\cdot uuu\cdot\frac{\alpha-1}{AS}}}{2}$, $G_2 = \frac{\beta\eta\varepsilon b\psi}{AS}$, $G_9 = \frac{\theta(\rho-\gamma)}{[H_T-H_c]^2}$, $uuu = 2mkG_9 - ikC_1$, $NNN = -ig - ikC_0 - ikG_2(1-\alpha) + \frac{C_1Rk}{AS} - 2mkG_9H_T$, and

$$\overline{DB} = \frac{z_2AS}{\alpha-1}\mathrm{e}^{-z_2t_c}[H_c - \frac{\frac{iR}{\alpha-1}-NNN}{uuu} - \frac{[H_T-\frac{\frac{iR}{\alpha-1}-NNN}{uuu}]-[H_c-\frac{\frac{iR}{\alpha-1}-NNN}{uuu}]\mathrm{e}^{z_2(t_T-t_c)}}{\mathrm{e}^{z_1(t_T-t_c)}-\mathrm{e}^{z_2(t_T-t_c)}}]. \quad (239)$$

$$\overline{DA} = \frac{z_1AS}{\alpha-1}[\frac{[H_T-\frac{\frac{iR}{\alpha-1}-NNN}{uuu}]-[H_c-\frac{\frac{iR}{\alpha-1}-NNN}{uuu}]\mathrm{e}^{z_2(t_T-t_c)}}{\mathrm{e}^{z_1t_T}-\mathrm{e}^{z_1t_c+z_2(t_T-t_c)}}]. \quad (240)$$

If we let $\beta = 0$, it implies making $G_2 = 0$ in SP_3^*. The resulting solution below gives us the optimal solution for the severe unhealthy phase under a quota restriction. Take note that the whole proof on SP_3^* under taxes (Appendix 8) was analysed to ensure that letting $G_2 = 0$ in SP_3^* is mathematically correct.

$$W^*(t) = \overline{DA2}\mathrm{e}^{tz_1} + \overline{DB2}\mathrm{e}^{tz_2} - \frac{R}{\alpha-1}, \quad (241)$$

$$H^*(t) = \frac{(\alpha-1)\overline{DA2}}{ASz_1}\mathrm{e}^{tz_1} + \frac{(\alpha-1)\overline{DB2}}{ASz_2}\mathrm{e}^{tz_2} + \frac{\frac{iR}{\alpha-1}-PP}{uuu}. \quad (242)$$

where $z_{1,2} = \frac{i\pm\sqrt{i^2+4\cdot uuu\cdot\frac{\alpha-1}{AS}}}{2}$, $G_9 = \frac{\theta(\rho-\gamma)}{[H_T-H_c]^2}$, $uuu = 2mkG_9 - ikC_1$, $PP = -ig - ikC_0 + \frac{C_1Rk}{AS} - 2mkG_9H_T$, and

$$\overline{DB2} = \frac{z_2AS}{\alpha-1}\mathrm{e}^{-z_2t_c}[H_c - \frac{\frac{iR}{\alpha-1}-PP}{uuu} - \frac{[H_T-\frac{\frac{iR}{\alpha-1}-PP}{uuu}]-[H_c-\frac{\frac{iR}{\alpha-1}-PP}{uuu}]\mathrm{e}^{z_2(t_T-t_c)}}{\mathrm{e}^{z_1(t_T-t_c)}-\mathrm{e}^{z_2(t_T-t_c)}}]. \quad (243)$$

$$\overline{DA2} = \frac{z_1AS}{\alpha-1}[\frac{[H_T-\frac{\frac{iR}{\alpha-1}-PP}{uuu}]-[H_c-\frac{\frac{iR}{\alpha-1}-PP}{uuu}]\mathrm{e}^{z_2(t_T-t_c)}}{\mathrm{e}^{z_1t_T}-\mathrm{e}^{z_1t_c+z_2(t_T-t_c)}}]. \quad (244)$$

Using equation (244), we determine the value of $\overline{DA2}$ that satisfies the condition $W^*(t) \leq$

$\widehat{W}$.

$$\overline{DA2}\mathrm{e}^{tz_1} + \overline{DB2}\mathrm{e}^{tz_2} - \frac{R}{\alpha-1} \leq \widehat{W} \tag{245}$$

$$\overline{DA2} \leq \frac{\mathrm{e}^{-tz_1}[\widehat{W}(\alpha-1)+R]}{\alpha-1} - \overline{DB2}\mathrm{e}^{t(z_2-z_1)}. \tag{246}$$

If we let the Right Hand Side of (246) to be equal to $N_K(t)$, and taking into considerations that extraction levels above $\widehat{W}$ are subject to taxation, we then obtain

$$W^{\star}(t) = \begin{cases} \overline{DA2}\mathrm{e}^{tz_1} + \overline{DB2}\mathrm{e}^{tz_2} - \frac{R}{\alpha-1} & \overline{DA2} \leq N_K(t) \\ \overline{DA}\mathrm{e}^{tz_1} + \overline{DB}\mathrm{e}^{tz_2} - \frac{R}{\alpha-1} & \overline{DA2} > N_K(t) \end{cases} \tag{247}$$

$$H^{\star}(t) = \begin{cases} \frac{(\alpha-1)\overline{DA2}}{ASz_1}\mathrm{e}^{tz_1} + \frac{(\alpha-1)\overline{DB2}}{ASz_2}\mathrm{e}^{tz_2} + \frac{\frac{iR}{\alpha-1}-PP}{uuu} & \overline{DA2} \leq N_K(t) \\ \frac{(\alpha-1)\overline{DA}}{ASz_1}\mathrm{e}^{tz_1} + \frac{(\alpha-1)\overline{DB}}{ASz_2}\mathrm{e}^{tz_2} + \frac{\frac{iR}{\alpha-1}-NNN}{uuu} & \overline{DA2} > N_K(t) \end{cases} \tag{248}$$

Where $z_{1,2} = \frac{i\pm\sqrt{i^2+4\cdot uuu\cdot\frac{\alpha-1}{AS}}}{2}$, $G_2 = \frac{\beta\eta\varepsilon b\psi}{AS}$, $G_9 = \frac{\theta(\rho-\gamma)}{[H_T-H_c]^2}$, $uuu = 2mkG_9 - ikC_1$, $NNN = -ig - ikC_0 - ikG_2(1-\alpha) + \frac{C_1Rk}{AS} - 2mkG_9H_T$, $PP = -ig - ikC_0 + \frac{C_1Rk}{AS} - 2mkG_9H_T$, $N_K(t) = \frac{\mathrm{e}^{-tz_1}[\widehat{W}(\alpha-1)+R]}{\alpha-1} - \overline{DB2}\mathrm{e}^{t(z_2-z_1)}$, and

$$\overline{DB} = \frac{z_2AS}{\alpha-1}\mathrm{e}^{-z_2t_c}\left[H_c - \frac{\frac{iR}{\alpha-1}-NNN}{uuu} - \frac{[H_T-\frac{\frac{iR}{\alpha-1}-NNN}{uuu}]-[H_c-\frac{\frac{iR}{\alpha-1}-NNN}{uuu}]\mathrm{e}^{z_2(t_T-t_c)}}{\mathrm{e}^{z_1(t_T-t_c)}-\mathrm{e}^{z_2(t_T-t_c)}}\right]. \tag{249}$$

$$\overline{DA} = \frac{z_1AS}{\alpha-1}\left[\frac{[H_T-\frac{\frac{iR}{\alpha-1}-NNN}{uuu}]-[H_c-\frac{\frac{iR}{\alpha-1}-NNN}{uuu}]\mathrm{e}^{z_2(t_T-t_c)}}{\mathrm{e}^{z_1t_T}-\mathrm{e}^{z_1t_c+z_2(t_T-t_c)}}\right]. \tag{250}$$

$$\overline{DB2} = \frac{z_2AS}{\alpha-1}\mathrm{e}^{-z_2t_c}\left[H_c - \frac{\frac{iR}{\alpha-1}-PP}{uuu} - \frac{[H_T-\frac{\frac{iR}{\alpha-1}-PP}{uuu}]-[H_c-\frac{\frac{iR}{\alpha-1}-PP}{uuu}]\mathrm{e}^{z_2(t_T-t_c)}}{\mathrm{e}^{z_1(t_T-t_c)}-\mathrm{e}^{z_2(t_T-t_c)}}\right]. \tag{251}$$

$$\overline{DA2} = \frac{z_1 AS}{\alpha-1}\left[\frac{[H_T - \frac{\frac{iR}{\alpha-1}-PP}{uuu}] - [H_c - \frac{\frac{iR}{\alpha-1}-PP}{uuu}]\mathrm{e}^{z_2(t_T-t_c)}}{\mathrm{e}^{z_1 t_T} - \mathrm{e}^{z_1 t_c + z_2(t_T-t_c)}}\right]. \tag{252}$$

Applying the same principle on SP_4^* (Appendix 2) that we used on SP_3^*, we let $G_5 = G_3 = G_4 = G_2 = 0$, $G_7 = -1$, and $G_8 = 1$ to obtain the following optimal solutions for the critical unhealthy phase under quota restrictions alone.

$$W^*(t) = \frac{a_2 AS\Omega}{\alpha-1}[H_T - \frac{\frac{iR}{\alpha-1}-N_1}{\overline{u1}}]\mathrm{e}^{a_2(t-t_T)} - \frac{R}{\alpha-1}, \tag{253}$$

$$H^*(t) = [H_T - \frac{\frac{iR}{\alpha-1}-N_1}{\overline{u1}}]\mathrm{e}^{a_2(t-t_T)} + \frac{\frac{iR}{\alpha-1}-N_1}{\overline{u1}}, \tag{254}$$

where, $a_2 = \frac{i-\sqrt{i^2+4\overline{u1}\frac{\alpha-1}{\Omega AS}}}{2}$ <0, $G_6 = \frac{\theta\gamma}{[H_T-H_B]^2}$, $\overline{u1} = -ikC_1 + \frac{2mkG_6}{\Omega}$, and $N_1 = -ig - ikC_0 + \frac{kC_1 R}{\Omega AS} - 2mkG_6 H_B$.

Using equation (254), we determine the value of N_1 that satisfies the condition $W^*(t) \leq \widehat{W}$.

$$\frac{a_2 AS\Omega}{\alpha-1}[H_T - \frac{\frac{iR}{\alpha-1}-N_1}{\overline{u1}}]\mathrm{e}^{a_2(t-t_T)} - \frac{R}{\alpha-1} \leq \widehat{W} \tag{255}$$

$$N_1 \leq \frac{\overline{u1}[\widehat{W}(\alpha-1)+R]}{a_2 AS\Omega}\mathrm{e}^{-a_2(t-t_T)} - H_T\overline{u1} + \frac{iR}{\alpha-1} \tag{256}$$

If we let the Right Hand Side of (256) to be equal to $N_B(t)$, then we obtain

$$W^\star(t) = \begin{cases} \frac{a_2 AS\Omega}{\alpha-1}[H_T - \frac{\frac{iR}{\alpha-1}-N_1}{\overline{u1}}]\mathrm{e}^{a_2(t-t_T)} - \frac{R}{\alpha-1} & N_1 \leq N_B(t) \\ \widehat{W} & N_1 > N_B(t) \end{cases} \tag{257}$$

$$H^\star(t) = \begin{cases} [H_T - \frac{\frac{iR}{\alpha-1}-N_1}{\overline{u1}}]\mathrm{e}^{a_2(t-t_T)} + \frac{\frac{iR}{\alpha-1}-N_1}{\overline{u1}} & N_1 \leq N_B(t) \\ [H_T - \frac{\frac{iR}{\alpha-1}-N_B(t)}{\overline{u1}}]\mathrm{e}^{a_2(t-t_T)} + \frac{\frac{iR}{\alpha-1}-N_B(t)}{\overline{u1}} & N_1 > N_B(t) \end{cases} \tag{258}$$

where, $a_2 = \frac{i-\sqrt{i^2+4\overline{u1}\frac{\alpha-1}{\Omega AS}}}{2}$ <0, $G_6 = \frac{\theta\gamma}{[H_T-H_B]^2}$, $\overline{u1} = -ikC_1 + \frac{2mkG_6}{\Omega}$, $N_1 = -ig - ikC_0 + \frac{kC_1 R}{\Omega AS} - 2mkG_6 H_B$, and $N_B(t) = \frac{\overline{u1}[\widehat{W}(\alpha-1)+R]}{a_2 AS\Omega}\mathrm{e}^{-a_2(t-t_T)} - H_T\overline{u1} + \frac{iR}{\alpha-1}$

Therefore, the final solution is given by

$$W^*(t)=\begin{cases}\overline{A}e^{ty_1}+\overline{B}e^{ty_2}-\frac{R}{\alpha-1}, & \text{if } t\le t_u,\\ \overline{EA}e^{tq_1}+\overline{EB}e^{tq_2}-\frac{R}{\alpha-1}, & \text{if } t_u<t\le t_c,\\ \overline{DA2}e^{tz_1}+\overline{DB2}e^{tz_2}-\frac{R}{\alpha-1}, & \text{if} t_c<t\le t_T\ \&\ \overline{DA2}\le N_K(t),\\ \overline{DA}e^{tz_1}+\overline{DB}e^{tz_2}-\frac{R}{\alpha-1}, & \text{if } t_c<t\le t_T\ \&\ \overline{DA2}>N_K(t),\\ \frac{a_2AS\Omega}{\alpha-1}[H_T-\frac{\frac{iR}{\alpha-1}-N_1}{\overline{u1}}]e^{a_2(t-t_T)}-\frac{R}{\alpha-1}, & \text{if } t>t_T\ \&\ N_1\le N_B(t),\\ \widehat{W}, & \text{if } t>t_T\ \&\ N_1>N_B(t).\end{cases}$$

(259)

$$H^*(t)=\begin{cases}\frac{(\alpha-1)\overline{A}}{ASy_1}e^{ty_1}+\frac{(\alpha-1)\overline{B}}{ASy_2}e^{ty_2}+\frac{\frac{iR}{\alpha-1}-N}{u}, & \text{if } t\le t_u,\\ \frac{(\alpha-1)\overline{EA}}{ASq_1}e^{tq_1}+\frac{(\alpha-1)\overline{EB}}{ASq_2}e^{tq_2}+\frac{\frac{iR}{\alpha-1}-PPP}{ddd}, & \text{if } t_u<t\le t_c,\\ \frac{(\alpha-1)\overline{DA2}}{ASz_1}e^{tz_1}+\frac{(\alpha-1)\overline{DB2}}{ASz_2}e^{tz_2}+\frac{\frac{iR}{\alpha-1}-PP}{uuu}, & \text{if } t_c<t\le t_T\ \&\ \overline{DA2}\le N_K(t),\\ \frac{(\alpha-1)\overline{DA}}{ASz_1}e^{tz_1}+\frac{(\alpha-1)\overline{DB}}{ASz_2}e^{tz_2}+\frac{\frac{iR}{\alpha-1}-NNN}{uuu}, & \text{if } t_c<t\le t_T\ \&\ \overline{DA2}>N_K(t),\\ [H_T-\frac{\frac{iR}{\alpha-1}-N_1}{\overline{u1}}]e^{a_2(t-t_T)}+\frac{\frac{iR}{\alpha-1}-N_1}{\overline{u1}}, & \text{if } t>t_T\ \&\ N_1\le N_B(t),\\ [H_T-\frac{\frac{iR}{\alpha-1}-N_B(t)}{\overline{u1}}]e^{a_2(t-t_T)}+\frac{\frac{iR}{\alpha-1}-N_B(t)}{\overline{u1}}, & \text{if } t>t_T\ \&\ N_1>N_B(t).\end{cases}$$

(260)

Where $y_{1,2}=\frac{i\pm\sqrt{i^2+4u\frac{\alpha-1}{AS}}}{2}, u=2mkG_{11}-ikC_1, N=-ig-ikC_0+\frac{C_1Rk}{AS}-2mkG_{11}S_l, G_{11}=\frac{\theta(\delta-1)}{[S_l-H_u]^2}$, and

$$\overline{B}=\frac{y_2AS}{\alpha-1}[H_0-\frac{\frac{iR}{\alpha-1}-N}{u}-\frac{[H_u-\frac{\frac{iR}{\alpha-1}-N}{u}]-[H_0-\frac{\frac{iR}{\alpha-1}-N}{u}]e^{y_2t_u}}{e^{y_1t_u}-e^{y_2t_u}}], \tag{261}$$

$$\overline{A}=\frac{y_1AS}{\alpha-1}[\frac{[H_u-\frac{\frac{iR}{\alpha-1}-N}{u}]-[H_0-\frac{\frac{iR}{\alpha-1}-N}{u}]e^{y_2t_u}}{e^{y_1t_u}-e^{y_2t_u}}]. \tag{262}$$

$q_{1,2}=\frac{i\pm\sqrt{i^2+4\cdot ddd\cdot\frac{\alpha-1}{AS}}}{2}, G_{10}=\frac{\theta(\delta-\rho)}{[H_u-H_c]^2}, ddd=2mkG_{10}-ikC_1, PPP=-ig-ikC_0+\frac{C_1Rk}{AS}-$

$2mkG_{10}H_c$, and

$$\overline{EB} = \frac{q_2}{m}\,\mathrm{e}^{-q_2 t_u}\Big[H_u - \frac{\frac{iM}{m}-PPP}{ddd} - \frac{[H_c-\frac{\frac{iM}{m}-PPP}{ddd}]-[H_u-\frac{\frac{iM}{m}-PPP}{ddd}]\mathrm{e}^{q_2(t_c-t_u)}}{\mathrm{e}^{q_1(t_c-t_u)}-\mathrm{e}^{q_2(t_c-t_u)}}\Big]. \quad (263)$$

$$\overline{EA} = \frac{q_1}{m}\Big[\frac{[H_c-\frac{\frac{iM}{m}-PPP}{ddd}]-[H_u-\frac{\frac{iM}{m}-PPP}{ddd}]\mathrm{e}^{q_2(t_c-t_u)}}{\mathrm{e}^{q_1 t_c}-\mathrm{e}^{q_1 t_u+q_2(t_c-t_u)}}\Big]. \quad (264)$$

$z_{1,2} = \frac{i\pm\sqrt{i^2+4\cdot uuu\cdot\frac{\alpha-1}{AS}}}{2}$, $G_2 = \frac{\beta\eta\varepsilon b\psi}{AS}$, $G_9 = \frac{\theta(\rho-\gamma)}{[H_T-H_c]^2}$, $uuu = 2mkG_9 - ikC_1$, $NNN = -ig - ikC_0 - ikG_2(1-\alpha) + \frac{C_1Rk}{AS} - 2mkG_9H_T$, $PP = -ig - ikC_0 + \frac{C_1Rk}{AS} - 2mkG_9H_T$, $N_K(t) = \frac{\mathrm{e}^{-tz_1}[\widehat{W}(\alpha-1)+R]}{\alpha-1} - \overline{DB2}\mathrm{e}^{t(z_2-z_1)}$, and

$$\overline{DB} = \frac{z_2AS}{\alpha-1}\,\mathrm{e}^{-z_2 t_c}\Big[H_c - \frac{\frac{iR}{\alpha-1}-NNN}{uuu} - \frac{[H_T-\frac{\frac{iR}{\alpha-1}-NNN}{uuu}]-[H_c-\frac{\frac{iR}{\alpha-1}-NNN}{uuu}]\mathrm{e}^{z_2(t_T-t_c)}}{\mathrm{e}^{z_1(t_T-t_c)}-\mathrm{e}^{z_2(t_T-t_c)}}\Big]. \quad (265)$$

$$\overline{DA} = \frac{z_1AS}{\alpha-1}\Big[\frac{[H_T-\frac{\frac{iR}{\alpha-1}-NNN}{uuu}]-[H_c-\frac{\frac{iR}{\alpha-1}-NNN}{uuu}]\mathrm{e}^{z_2(t_T-t_c)}}{\mathrm{e}^{z_1 t_T}-\mathrm{e}^{z_1 t_c+z_2(t_T-t_c)}}\Big]. \quad (266)$$

$$\overline{DB2} = \frac{z_2AS}{\alpha-1}\,\mathrm{e}^{-z_2 t_c}\Big[H_c - \frac{\frac{iR}{\alpha-1}-PP}{uuu} - \frac{[H_T-\frac{\frac{iR}{\alpha-1}-PP}{uuu}]-[H_c-\frac{\frac{iR}{\alpha-1}-PP}{uuu}]\mathrm{e}^{z_2(t_T-t_c)}}{\mathrm{e}^{z_1(t_T-t_c)}-\mathrm{e}^{z_2(t_T-t_c)}}\Big]. \quad (267)$$

$$\overline{DA2} = \frac{z_1AS}{\alpha-1}\Big[\frac{[H_T-\frac{\frac{iR}{\alpha-1}-PP}{uuu}]-[H_c-\frac{\frac{iR}{\alpha-1}-PP}{uuu}]\mathrm{e}^{z_2(t_T-t_c)}}{\mathrm{e}^{z_1 t_T}-\mathrm{e}^{z_1 t_c+z_2(t_T-t_c)}}\Big]. \quad (268)$$

$a_2 = \frac{i-\sqrt{i^2+4\overline{u1}\frac{\alpha-1}{\Omega AS}}}{2}$ <0, $G_6 = \frac{\theta\gamma}{[H_T-H_B]^2}$, $\overline{u1} = -ikC_1 + \frac{2mkG_6}{\Omega}$, $N_1 = -ig - ikC_0 + \frac{kC_1R}{\Omega AS} - 2mkG_6H_B$, and $N_B(t) = \frac{\overline{u1}[\widehat{W}(\alpha-1)+R]}{a_2AS\Omega}\mathrm{e}^{-a_2(t-t_T)} - H_T\overline{u1} + \frac{iR}{\alpha-1}$. Therefore, the optimal solutions are proved.

Appendix 15. Proof of Proposition 8.

Take note that N_1 is just a composite constant and $N_B(t)$ is the decision variable that decides whether the quota binds ($N_1 > N_B(t)$) or not ($N_1 \leq N_B(t)$). The quota binds (binding quota) when farmers want to extract more than the imposed quota level but their unconstrained groundwater extraction optimum level is forced down to the quota level ($\widehat{W}$), which occurs when the policy constraint is active ($N_1 > N_B(t)$). A non-binding quota refers to the case when farmers unconstrained groundwater extraction optimum level is already less than or equal to $\widehat{W}$, which occurs when the policy constraint is inactive ($N_1 \leq N_B(t)$).Therefore, binding means the policy constraint is active while non-bing implies it is inactive. In addition, the comparison between $N_B(t)$ and N_1 tells us whether farmers are constrained by the quota level at that point in time.

At the beginning of the critically unhealthy phase ($t = T$), if $N_B(T) \geq N_1$, the quota level does not bind initially (although it could bind later if the dynamics push the system across the threshold). Hence, we solve for $N_B(T) = N_1$, this gives us the critical quota level ($\widehat{W}_c$) where the system is exactly on the boundary between binding and non binding at $t = T$. Thus, if you choose $\widehat{W}$ above (or below) $\widehat{W}_c$, then you start on the non-binding side (or on the binding side). The optimal solutions for the critically unhealthy phase under packaging and sequencing of taxes and quotas are as follows.

$$W^{\star}(t) = \begin{cases} \frac{a_2 AS\Omega}{\alpha-1}[H_T - \frac{\frac{iR}{\alpha-1}-N_1}{\overline{u1}}]\mathrm{e}^{a_2(t-t_T)} - \frac{R}{\alpha-1}, & \text{if } t > t_T \ \& \ N_1 \leq N_B(t), \\ \widehat{W}, & \text{if } t > t_T \ \& \ N_1 > N_B(t). \end{cases} \quad (269)$$

$$H^{\star}(t) = \begin{cases} [H_T - \frac{\frac{iR}{\alpha-1}-N_1}{\overline{u1}}]\mathrm{e}^{a_2(t-t_T)} + \frac{\frac{iR}{\alpha-1}-N_1}{\overline{u1}}, & \text{if } t > t_T \ \& \ N_1 \leq N_B(t), \\ [H_T - \frac{\frac{iR}{\alpha-1}-N_B(t)}{\overline{u1}}]\mathrm{e}^{a_2(t-t_T)} + \frac{\frac{iR}{\alpha-1}-N_B(t)}{\overline{u1}}, & \text{if } t > t_T \ \& \ N_1 > N_B(t). \end{cases} \quad (270)$$

where, $a_2 = \frac{i-\sqrt{i^2+4\overline{u1}\frac{\alpha-1}{\Omega AS}}}{2}$ <0, $G_6 = \frac{\theta\gamma}{[H_T-H_B]^2}$, $\overline{u1} = -ikC_1 + \frac{2mkG_6}{\Omega}$, $N_1 = -ig - ikC_0 + \frac{kC_1 R}{\Omega AS} - 2mkG_6 H_B$, and $N_B(t) = \frac{\overline{u1}[\widehat{W}(\alpha-1)+R]}{a_2 AS\Omega}\mathrm{e}^{-a_2(t-t_T)} - H_T\overline{u1} + \frac{iR}{\alpha-1}$. From the optimal solutions, we get that at $t = T$,

$$N_B(T) = -H_T\overline{u1} + \frac{\widehat{W}(\alpha-1)+R}{a_2 AS\Omega}\overline{u1} + \frac{iR}{\alpha-1} \quad (271)$$

Setting $N_B(T) = N_1$ and solving for $\widehat{W}$, we obtain the following expression.

$$\widehat{W}_c = \frac{a_2 AS\Omega}{(\alpha-1)\overline{u1}}\left(N_1 + H_T\overline{u1} - \frac{iR}{\alpha-1}\right) - \frac{R}{\alpha-1} \quad (272)$$

The derivative of $N_B(t)$ with respect to t is given by the following expression.

$$\frac{\partial N_B(t)}{\partial t} = \frac{\overline{u1}}{AS\Omega}(\widehat{W}(\alpha-1)+R)\mathrm{e}^{-a_2(t-t_T)} \quad (273)$$

The derivative above is positive since $\frac{\overline{u1}}{AS\Omega} > 0$, $\overline{u1} > 0$ and $AS\Omega > 0$. The term $(\widehat{W}(\alpha-1) + R) > 0$ since $(\widehat{W}(\alpha-1)+R) > 0 \Longrightarrow \frac{R}{\widehat{W}} > \alpha - 1$ which is true because $\frac{R}{\widehat{W}} > 0$ and $\alpha - 1 < 0$. Finally, the term $\mathrm{e}^{-a_2(t-t_T)} \geq 1$ since $a_2 < 0$ and $(t - t_T) \geq 0$. The above analysis implies that $N_B(t)$ is strictly increasing. This implies that if $N_B(t)$ is strictly increasing, then for any later time $t > T$, $N_B(t) \geq N_B(T)$, which means that the gap between N_1 and $N_B(t)$ can only lessen/reduce (or stay the same if the derivative was zero). This gap can never widen. Therefore, if N_1 starts at time $t = T$ above $N_B(T)$, $N_B(t)$ will surpass N_1 at some finite time $t > T$, and the system will exit into the non-binding quota phase until the end of the planning period.

If the quota is binding, then $W^*(t) = \widehat{W}$ $(N_1 > N_B(t))$. If the quota is not binding, then $W^*(t) < \widehat{W}$. Therefore, if the system changes from binding to non binding at $t = T$ when $\widehat{W} = \widehat{W}_c$, any $\widehat{W} < \widehat{W}_c$ implies the quota is binding, and any $\widehat{W} \geq \widehat{W}_c$ implies the quota is non binding at time $t = T$. Thus, if the quota is low enough ($\widehat{W} < \widehat{W}_c$), then once $N_1 > N_B(T)$ hold, it only holds for a limited duration. Thus, the system transitions into the non-binding quota phase until the end of the planning period. If $\widehat{W} \geq \widehat{W}_c$, we have that $N_1 \leq N_B(T)$ and $N_B(t)$ will continue growing higher than N_1 until $t = \infty$ because $N_B(t)$ is strictly increasing. This means that the quota stays non-binding until the end of the planning period.

Appendix 16. Proof of Proposition 9.

When the quota is binding ($N_1 > N_B(t)$) for $t > T$, the derivative of the water table level with respect to the quota level is given by the following equation.

$$\frac{\partial H^*(t)}{\partial \widehat{W}} = \frac{\alpha-1}{a_2 AS\Omega}(1 - \mathrm{e}^{-a_2(t-t_T)}) < 0,\ t > T, \quad (274)$$

because $\mathrm{e}^{-a_2(t-t_T)} > 1$, $(\alpha - 1) < 0$, $a_2 < 0$, and $AS\Omega > 0$. This means that every marginal increase in $\widehat{W}$ lowers the water table by a predictable amount for $t > T$. Economically, this makes sense, if the quota level ($\widehat{W}$) is relaxed upward, farmers extract more, so the water table ($H^*(t)$) falls (negative derivative). This yields a closed form condition, that to keep $H^*(t) > H_B$ (H_B represents the aquifer system bottom), it suffices to impose the following condition.

$$\widehat{W} = \widehat{W}_T + \ \min_{t\in(T,\infty)}\{\frac{a_2 AS\Omega}{1-\alpha} \cdot \frac{H^*(t,\widehat{W}_T)-H_B}{1-\mathrm{e}^{-a_2(t-t_T)}}\} = \widehat{W}_k. \qquad (275)$$

Where $\widehat{W}_T$ represents the quota level at $t = t_T$. Thus, regulators can quantitatively determine the maximum allowable quota consistent with keeping the water table height above the aquifer bottom and prevent GDEs from disappearing. The GDEs collapse when $H^*(t) = H_B$, as assumed in the derivation of our GDEs health status functional. Likewise, take note that due to the complexity of the minimisation expression in terms of our optimal solution for the water table height, we could also not solve for the explicit $\widehat{W}_k$ value. We just propose that maybe with numerical solvers, this may be solved.

Appendix 17. Proof of Proposition 10.

Assume the quota is binding at $t = T$, that is $N_1 > N_B(T)$. The derivative of $N_B(t)$ with respect to θ is given by the following expression.

$$\frac{\partial N_A(t)}{\partial\theta} = \frac{2H_T mk\gamma}{(H_T-H_B)^2} - \frac{\widehat{W}(\alpha-1)+R}{AS\Omega}\frac{\mathrm{e}^{-a_2(t-t_T)}}{a_2}\frac{mk\gamma}{(H_T-H_B)^2}$$

$$\times\left(-2 - \frac{\overline{u1}t}{2\sqrt{i^2+4\frac{(\alpha-1)}{AS\Omega}\overline{u1}}} - \frac{\overline{u1}}{2a_2\sqrt{i^2+4\frac{(\alpha-1)}{AS\Omega}\overline{u1}}}\right) \qquad (276)$$

The derivative above is positive. The parameter $\overline{u1} > 0$ because $\frac{2mkG_6}{\Omega} - ikC_1 > 0 \Longrightarrow i < \frac{2mG_6}{C_1\Omega}$ and $i \in (0,1)$, $\frac{2mG_6}{\Omega C_1} > 0$ since $m < 0,\ C_1 < 0,\ k < 0,\ G_6 > 0,\ \gamma > 0$). The first term above is positive since $m < 0$, $k < 0$, $\gamma > 0$, and $H_T > 0$. We also observe that $\frac{\widehat{W}(\alpha-1)+R}{AS\Omega} > 0$ since term $(\widehat{W}(\alpha-1)+R) > 0$ since $(\widehat{W}(\alpha-1)+R) > 0 \Longrightarrow \frac{R}{\widehat{W}} > \alpha - 1$ which is true because $\frac{R}{\widehat{W}} > 0$ and $\alpha - 1 < 0$. Therefore, the factor outside the brackets of the second term is positive since $\mathrm{e}^{-a_2(t-t_T)} \geq 1$ and $a_2 < 0$. The second term inside the brackets is negative since $\overline{u1} > 0$, $t \geq T$, and $\sqrt{i^2 + 4\frac{(\alpha-1)}{AS\Omega}\overline{u1}} \geq 0$. The last term inside the brackets is positive since $\overline{u1} > 0$, $a_2 < 0$, and $\sqrt{i^2 + 4\frac{(\alpha-1)}{AS\Omega}\overline{u1}} \geq 0$. For the overall derivative to be positive, the following inequality should be true.

$$-2 - \frac{\overline{u1}t}{2\sqrt{i^2+4\frac{(\alpha-1)}{AS\Omega}\overline{u1}}} - \frac{\overline{u1}}{2a_2\sqrt{i^2+4\frac{(\alpha-1)}{AS\Omega}\overline{u1}}} > 0 \quad (277)$$

$$\Rightarrow -\frac{\overline{u1}}{2a_2\sqrt{i^2+4\frac{(\alpha-1)}{AS\Omega}\overline{u1}}} > 2 + \frac{\overline{u1}t}{2\sqrt{i^2+4\frac{(\alpha-1)}{AS\Omega}\overline{u1}}} \quad (278)$$

$$\Rightarrow a_2 < -\frac{\overline{u1}}{4\sqrt{i^2+4\frac{(\alpha-1)}{AS\Omega}\overline{u1}}+\overline{u1}t} \quad (279)$$

Intuitively, a_2 should be bigger in terms of magnitude compared to $\frac{\overline{u1}}{4\sqrt{i^2+4\frac{(\alpha-1)}{AS\Omega}\overline{u1}}+\overline{u1}t}$ because it is equal to $\frac{i-\sqrt{i^2+4\frac{(\alpha-1)}{AS\Omega}\overline{u1}}}{2}$ where $i \in (0,1)$ and bigger negative values are smaller than small negative values for all t. If $t = T$, the Right Hand Side reduces in terms of magnitude. Hence the derivative is proved to be positive.

This means that for every t, a larger θ pushes $N_B(t)$ upward. Next, we explain how the quota binding phase is shortened. Recall that $N_B(t)$ is an increasing function of time (as we derived in the proof of Proposition 8) and N_1 is fixed. Quota binding phase ends at time t^* where the equality $N_1 = N_B(t^*)$. If θ rises, the whole curve $N_B(t)$ shifts upward. That is, at $t = T$, the inequality $N_1 > N_B(T)$ still holds, but now the gap is smaller. Since the curve is below N_1 by a smaller margin, it takes a short time for $N_B(t)$ to be equal to N_1. Mathematically, the solution t^* to $N_1 = N_B(t^*)$ shifts to the left. Hence, our results is proved.

Appendix 18. Detailed solution when there is LS but no policy interventions

The hamiltonian function for phase four of the system (55), (56), (57) is given as follows

$$\mathcal{H}_4(t, W_4, H_4, \lambda_4) = -\mathrm{e}^{-it}[\frac{W_4^2}{2k} - \frac{gW_4}{k} - (C_0 + C_1 H_4)W_4 +$$
$$\theta[\frac{\gamma}{((1+\eta\varepsilon b\psi)(H_T - H_B))^2}$$
$$\cdot (H_4 + \eta\varepsilon b\psi(H_4 - H_c) - H_B - \eta\varepsilon b\psi(H_B - H_c))^2]]$$
$$+\lambda_4 \cdot \frac{[R + (\alpha - 1)W_4]}{\Omega \cdot AS} \quad (280)$$

Equation (280) can be rewritten as follows.

$$\mathcal{H}_4(t, W_4, H_4, \lambda_4) = -\mathrm{e}^{-it}[\frac{W_4^2}{2k} - \frac{gW_4}{k} - (C_0 + C_1 H_4)W_4 + G_6(H_4 - H_B)^2]$$
$$+\lambda_4 \cdot \frac{[R + (\alpha - 1)W_4]}{\Omega \cdot AS} \quad (281)$$

Where

$$G_6 = \frac{\theta\gamma}{[H_T - H_B]^2}. \quad (282)$$

Hence, the first order conditions are as follows

$$\frac{\partial \mathcal{H}_4}{\partial W_4} = -\mathrm{e}^{-it}[\frac{W_4}{k} - \frac{g}{k} - C_0 - C_1 H_4] + \lambda_4[\frac{(\alpha - 1)}{\Omega \cdot AS}] = 0. \quad (283)$$

$$\dot{\lambda}_4 = -\frac{\partial \mathcal{H}_4}{\partial H_4}. \quad (284)$$

$$\dot{H}_4 = \frac{1}{\Omega \cdot AS}[R + (\alpha - 1)W_4]. \quad (285)$$

The transversality condition is given by $\lim_{t\to\infty}\lambda_4(t) = 0$. From Equation (283), we obtain the value for the costate variable λ_4 as follows.

$$\lambda_4 = \frac{\Omega}{m}\mathrm{e}^{-it}[\frac{W_4}{k} - \frac{g}{k} - C_0 - C_1 H_4], \quad (286)$$

where $m = \frac{(\alpha-1)}{AS}$. The derivative of λ_4 with respect to t is given by

$$\dot{\lambda}_4 = \frac{\Omega}{m}\mathrm{e}^{-it}[-\frac{iW_4}{k} + \frac{ig}{k} + iC_0 + iC_1 H_4 - \frac{C_1 R}{\Omega \cdot AS} - \frac{C_1 m}{\Omega}W_4 + \frac{\dot{W}_4}{k}]. \quad (287)$$

The derivative of $\mathcal{H}_4$ with respect to the water table height H_4 is given by

$$-\frac{\partial \mathcal{H}_4}{\partial H_4} = -\mathrm{e}^{-it}[C_1 W_4 + 2G_6 H_B - 2G_6 H_4]. \quad (288)$$

From Equation (288) and (287), we obtain the following equation.

$$-C_1W_4 - 2G_6H_B + 2G_6H_4 = \frac{\Omega}{m}[-\frac{iW_4}{k} + \frac{ig}{k} + iC_0 + iC_1H_4$$
$$-\frac{C_1R}{\Omega\cdot AS} - \frac{C_1m}{\Omega}W_4 + \frac{\dot{W}_4}{k}]. \quad (289)$$

Solving for $\dot{W}_4$ in the above equation we get the following equations.

$$\frac{\Omega\dot{W}_4}{mk} = \frac{\Omega iW_4}{mk} - \frac{\Omega C_1 iH_4}{m} + 2G_6H_4 - \frac{\Omega ig}{mk} - \frac{\Omega iC_0}{m}$$
$$+\frac{C_1R}{ASm\Omega} - 2G_6H_B \quad (290)$$

$$\frac{\dot{W}_4}{k} = \frac{iW_4}{k} - C_1iH_4 + \frac{2mG_6H_4}{\Omega} - \frac{ig}{k} - iC_0$$
$$+\frac{C_1R}{AS\Omega} - \frac{2mG_6H_B}{\Omega} \quad (291)$$

$$\dot{W}_4 = iW_4 - ikC_1H_4 + \frac{2mkG_6H_4}{\Omega} - ig - ikC_0 + \frac{kC_1R}{\Omega AS}$$
$$-2mkG_6H_B \quad (292)$$

$$\dot{W}_4 = iW_4 + [-ikC_1 + \frac{2mkG_6}{\Omega}]H_4 + [-ig - ikC_0 + \frac{kC_1R}{\Omega AS}$$
$$-2mkG_6H_B] \quad (293)$$

Likewise, the value for $\dot{H}_4$ can be rewritten as

$$\dot{H}_4 = \frac{(\alpha-1)W_4}{\Omega\cdot AS} + \frac{R}{\Omega\cdot AS}. \quad (294)$$

Consequently, we now have to solve the two simultaneous differential equations ((293) and (294)). Thus, by letting $mm = \frac{(\alpha-1)}{\Omega AS}$, $\overline{a} = -ikC_1 + \frac{2mkG_6}{\Omega}$, $\overline{N} = -ig - ikC_0 + \frac{kC_1R}{\Omega AS} - 2mkG_6H_B$ and $MM = \frac{R}{\Omega AS}$, we get the following system of differential equations.

$$\dot{W}_4 = iW_4 + \overline{a}\cdot H_4 + \overline{N}. \quad (295)$$
$$\dot{H}_4 = mm\cdot W_4 + MM. \quad (296)$$

Putting the above system of differential equations in a D operator format (where $D = \frac{d}{dt}$), and solving for W_4 yields the following second order linear non-homogeneous differential equation.

$$[(D^2 - Di) - \overline{a} \cdot mm]W_4 = \overline{a} \cdot MM. \quad (297)$$

The particular solution of the above differential equation is given by: $-\frac{MM}{mm}$ and the solution to the homogeneous differential equation ($[(D^2 - Di) - \overline{a} \cdot mm]W_4 = 0$) by

$$W_3(t) = \overline{KA}e^{tv_1} + \overline{KB}e^{tv_2}, \quad (298)$$

where $v_{1,2} = \frac{i \pm \sqrt{i^2 + 4\overline{a} \cdot mm}}{2}$ are the characteristic roots. The parameters $\overline{KA}$ and $\overline{KB}$ are constants to be determined by imposing the initial conditions. Substituting the right hand side (RHS) of (298) for $W_4(t)$ in the homogenous DE ($\dot{H}_4 = mm \cdot W_4$) and integrating gives the solution for the water table level $H_4(t)$ as follows.

$$H_4(t) = \frac{mm \cdot \overline{KA}}{v_1}e^{tv_1} + \frac{mm \cdot \overline{KB}}{v_2}e^{tv_2}. \quad (299)$$

Furthermore, the steady state level water table is given by

$$H_4^* = [\frac{i\frac{MM}{mm} - \overline{N}}{\overline{a}}] \quad (300)$$

Hence, the solution for $W_4^*(t)$ and $H_4^*(t)$ are given as follows, respectively.

$$W_4^*(t) = \overline{KA}e^{tv_1} + \overline{KB}e^{tv_2} - \frac{MM}{mm}, \quad (301)$$

$$H_4^*(t) = \frac{mm \cdot \overline{KA}}{v_1}e^{tv_1} + \frac{mm \cdot \overline{KB}}{v_2}e^{tv_2} + \frac{i\frac{MM}{mm} - \overline{N}}{\overline{a}}. \quad (302)$$

Similarly to Gisser and Sanchez (1980) results, it is worth mentioning that $+4uumm > 0$ since $k < 0, C_1 < 0, i > 0, A > 0, S > 0, \Omega > 0, H_B > 0, H_T > 0, \psi > 0, \theta > 0, \gamma > 0, \eta > 0, \varepsilon > 0$, $b > 0$, $G_6 > 0$, $\alpha < 1 \Longrightarrow (\alpha - 1) < 0$ or $(1 - \alpha) > 0$, and $m < 0$. Furthermore, we observe that $-\frac{ikC_1(\alpha-1)}{\Omega AS} > 0$ and $\frac{2mkG_6(\alpha-1)}{\Omega^2 AS} < 0$. It can also be proved that $-\frac{ikC_1(\alpha-1)}{\Omega AS} > \frac{2mkG_6(\alpha-1)}{\Omega^2 AS}$. Hence, $+4\overline{a} \cdot mm = 4[-\frac{ikC_1(\alpha-1)}{\Omega AS} + \frac{2mkG_6(\alpha-1)}{\Omega^2 AS}] > 0$. This implies that $v_1 > i$ and $v_2 < 0$. Therefore, v_2 is the stable characteristic root. Likewise, similarly to Gisser and Sanchez (1980), we obtained that the transversality condition is only satisfied when $\overline{KA} = 0$. By imposing the initial conditions of the sub problem ($H_4(t_T) = H_T$), we obtain the constant $\overline{KB}$ as follows below.

$$\overline{KB} = \frac{v_2}{mm}[H_T - \frac{i\frac{MM}{mm} - \overline{N}}{\overline{a}}]e^{-v_2 t_T}. \quad (303)$$

Therefore, the optimal solutions for $W_4^*(t)$ and $H_4^*(t)$ are given as follows below, respectively.

$$W_4^*(t) = \frac{v_2}{mm}[H_T - \frac{i\frac{MM}{mm} - \overline{N}}{\overline{a}}]e^{v_2(t - t_T)} - \frac{MM}{mm}. \quad (304)$$

$$H_4^*(t) = [H_T - \frac{i\frac{MM}{mm} - \overline{N}}{\overline{a}}]e^{v_2(t-t_T)} + \frac{i\frac{MM}{mm} - \overline{N}}{\overline{a}}. \quad (305)$$

Because $v_2 < 0$ and $i > 0$, the functional defined in phase four is verified to be a convergent integral.

We can now solve for the third sub-problem since we have the solution (SP_4^*) to the fourth sub-problem. The hamiltonian function of phase 3 is given as follows

$$\mathcal{H}_3(t, W_3, H_3, \lambda_3) = -e^{-it}[\frac{W_3^2}{2k} - \frac{gW_3}{k} - (C_0 + C_1H_3)W_3 +$$
$$\theta[\frac{\gamma}{((1+\eta\varepsilon b\psi)(H_T - H_c))^2}$$
$$\cdot (H_3 + \eta\varepsilon b\psi(H_3 - H_c) - H_T - \eta\varepsilon b\psi(H_T - H_c))^2]]$$
$$+\lambda_3 \cdot \frac{[R + (\alpha - 1)W_3]}{AS} \quad (306)$$

Equation (306) can be rewritten as follows.

$$\mathcal{H}_3(t, W_3, H_3, \lambda_3) = -e^{-it}[\frac{W_3^2}{2k} - \frac{gW_3}{k} - (C_0 + C_1H_3)W_3 + G_9(H_3 - H_T)^2$$
$$+\theta\gamma] + \lambda_3 \cdot \frac{[R + (\alpha - 1)W_3]}{AS} \quad (307)$$

Where,

$$G_9 = \frac{\theta(\rho - \gamma)}{[H_T - H_c]^2}. \quad (308)$$

Hence, the first order conditions are as follows

$$\frac{\partial \mathcal{H}_3}{\partial W_3} = -e^{-it}[\frac{W_3}{k} - \frac{g}{k} - C_0 - C_1H_3] + \lambda_3[\frac{(\alpha - 1)}{AS}] = 0. \quad (309)$$

$$\dot{\lambda}_3 = -\frac{\partial \mathcal{H}_3}{\partial H_3}. \quad (310)$$

$$\lambda_3^*(t_T, W_3^*(t_T), H_3^*(t_T)) = \lambda_4^*(t_T, W_4^*(t_T), H_4^*(t_T)) \quad (311)$$

$$\mathcal{H}_3^*(t_T) = \frac{\partial SP_4^*(t_T, W_4^*(t_T), H_4^*(t_T))}{\partial t_T}, \quad (312)$$

$$\dot{H}_3 = \frac{1}{AS}[R + (\alpha - 1)W_3]. \quad (313)$$

The transversality condition is given by $\lim_{t\to\infty}\lambda_3(t) = 0$. From Equation (309), we obtain the value for the costate variable λ_3 as follows.

$$\lambda_3 = \frac{1}{m}\mathrm{e}^{-it}[\frac{W_3}{k} - \frac{g}{k} - C_0 - C_1H_3], \quad (314)$$

where $m = \frac{(\alpha-1)}{AS}$. The derivative of λ_3 with respect to t is given by

$$\dot{\lambda}_3 = \frac{1}{m}\mathrm{e}^{-it}[-\frac{iW_3}{k} + \frac{ig}{k} + iC_0 + iC_1H_3$$
$$-\frac{C_1R}{AS} - C_1mW_3 + \frac{\dot{W}_3}{k}]. \quad (315)$$

The derivative of $\mathcal{H}_3$ with respect to the water table height H_3 is given by

$$-\frac{\partial \mathcal{H}_3}{\partial H_3} = -\mathrm{e}^{-it}[C_1W_3 - 2G_9H_3 + 2G_9H_T]. \quad (316)$$

From Equation (310) and (315), we obtain the following equation.

$$-C_1W_3 + 2G_9H_3 - 2G_9H_T = \frac{1}{m}[-\frac{iW_3}{k} + \frac{ig}{k} + iC_0 + iC_1H_3$$
$$-\frac{C_1R}{AS} - C_1mW_3 + \frac{\dot{W}_3}{k}]. \quad (317)$$

Solving for $\dot{W}_3$ in the above equation we get the following equations.

$$\frac{\dot{W}_3}{mk} = \frac{iW_3}{mk} - \frac{ig}{mk} - \frac{iC_0}{m} - \frac{iC_1H_3}{m} \quad + \frac{C_1R}{ASm} + 2G_9H_3 - 2G_9H_T \quad (318)$$

$$\frac{\dot{W}_3}{k} = \frac{iW_3}{k} - \frac{ig}{k} - iC_0 - iC_1H_3 \quad + \frac{C_1R}{AS} + 2mG_9H_3 - 2mG_9H_T \quad (319)$$

$$\dot{W}_3 = iW_3 - ig - ikC_0 - ikC_1H_3 \quad + \frac{C_1Rk}{AS} + 2mkG_9H_3 - 2mkG_9H_T \quad (320)$$

$$\dot{W}_3 = iW_3 + [2mkG_9 - ikC_1]H_3 + [-ig - ikC_0 \quad + \frac{C_1Rk}{AS} - 2mkG_9H_T] \quad (321)$$

Likewise, the value for $\dot{H}_3$ can be rewritten as

$$\dot{H}_3 = \frac{(\alpha-1)W_3}{AS} + \frac{R}{AS}. \quad (322)$$

Consequently, we now have to solve the two simultaneous differential equations ((321) and (322)). Thus, by letting $m = \frac{(\alpha-1)}{AS}$, $uuu = 2mkG_9 - ikC_1$, $NNN = -ig - ikC_0 + \frac{C_1Rk}{AS} -$

$2mkG_9H_T$ and $M = \frac{R}{AS}$, we get the following system of differential equations.

$$\dot{W}_3 = iW_3 + uuu \cdot H_3 + NNN1. \tag{323}$$

$$\dot{H}_3 = m \cdot W_3 + M. \tag{324}$$

Putting the above system of differential equations in a D operator format (where $D = \frac{d}{dt}$), and solving for W_3 yields the following second order linear non-homogeneous differential equation.

$$[(D^2 - Di) - uuu \cdot m]W_3 = uuu \cdot M. \tag{325}$$

The particular solution of the above differential equation is given by: $-\frac{M}{m}$ and the characteristic roots by $z_{1,2} = \frac{i \pm \sqrt{i^2 + 4uuu \cdot m}}{2}$. Furthermore, the steady state level water table is given by

$$H_3^* = [\frac{i\frac{M}{m} - NNN1}{uuu}] \tag{326}$$

Hence, the solution for $W_3^*(t)$ and $H_3^*(t)$ are given as follows, respectively.

$$W_3^*(t) = \overline{DA1}\mathrm{e}^{tz_1} + \overline{DB1}\mathrm{e}^{tz_2} - \frac{M}{m}, \tag{327}$$

$$H_3^*(t) = \frac{m \cdot \overline{DA1}}{z_1}\mathrm{e}^{tz_1} + \frac{m \cdot \overline{DB1}}{z_2}\mathrm{e}^{tz_2} + \frac{i\frac{M}{m} - NNN1}{uuu}. \tag{328}$$

Where $\overline{DA1}$ and $\overline{DB1}$ are obtained by imposing the initial conditions.

$$\overline{DB} = \frac{z_2}{m}\mathrm{e}^{-z_2 t_c}[H_c - \frac{\frac{iM}{m} - NNN1}{uuu} - \frac{[H_T - \frac{\frac{iM}{m} - NNN1}{uuu}] - [H_c - \frac{\frac{iM}{m} - NNN1}{uuu}]\mathrm{e}^{z_2(t_T - t_c)}}{\mathrm{e}^{z_1(t_T - t_c)} - \mathrm{e}^{z_2(t_T - t_c)}}]. \tag{329}$$

$$\overline{DA} = \frac{z_1}{m}[\frac{[H_T - \frac{\frac{iM}{m} - NNN1}{uuu}] - [H_c - \frac{\frac{iM}{m} - NNN1}{uuu}]\mathrm{e}^{z_2(t_T - t_c)}}{\mathrm{e}^{z_1 t_T} - \mathrm{e}^{z_1 t_c + z_2(t_T - t_c)}}]. \tag{330}$$

The proves for phase 2 and phase 1 can be found under the proofs of the tax policy (phases 1 and 2). Under the tax policy (phases 1 and 2), we have the same objective functions and constraints as in the case of LS and No policy interventions (phases 1 and 2) because phases 1 and 2 are also not taxed under the tax policy.

Appendix 19. Main results of the sensitivity analysis of the critical thresholds

Table 2. Main results from the scenarios analysed under the LS-GDEs and no policy interventions scenario.

Scenario	Water table height $(m.a.s.l)$	Aquifer depletion after 250 years (Mm^3)	Shifting year	Total aggregate social welfare (Million US dollars)
Baseline (Without GDEs and LS)	1170.87	214	-	0.4032
With GDEs' dynamics (empirical critical thresholds for the water table height and GDEs' health phases): $H_u = 1200.5$, $H_c = 1191.5$, $H_T = 1189.5$; $\delta = 0.5$, $\rho = 0.35$, $\gamma = 0.15$.	1177.53	164.8	$t_u = 157.7$ $t_c = 187.4$ $t_T = 190.1$	0.3415
Sensitivity 1 (lower critical thresholds for the GDEs' health phases): $\delta = 0.4$, $\rho = 0.3$, $\gamma = 0.1$.	1177.65	164	$t_u = 148$ $t_c = 188.3$ $t_T = 191.2$	0.3419
Sensitivity 2 (higher critical thresholds for the GDEs' health phases):	1177.4	165.68	$t_u = 164.3$ $t_c = 187$ $t_T = 188$	0.3414

$\delta = 0.7$, $\rho = 0.4$, $\gamma = 0.2$.				
Sensitivity 3 (lower critical thresholds for the water table height): $H_u = 1195.5$, $H_c = 1190.5$, $H_T = 1184.5$.	1178.5	162.3	$t_u = 158.7$ $t_c = 183.6$ $t_T = 241.8$	0.3482
Sensitivity 4 (higher critical thresholds for the water table height): $H_u = 1205.5$, $H_c = 1196.5$, $H_T = 1192.5$.	1180.98	150.64	$t_u = 173$ $t_c = 189$ $t_T = 195$	0.3349

Table 3. Main results from the scenarios analysed under the tax policy.

Scenario	Water table height $(m.a.s.l)$	Aquifer depletion after 250 years (Mm^3)	Shifting year	Total aggregate social welfare (Million US dollars)
Baseline (Without GDEs and LS)	1170.87	214	-	0.4032
With GDEs' dynamics (empirical critical thresholds for the water table height and GDEs' health phases): $H_u = 1200.5$, $H_c = 1191.5$,	1179.1	158	$t_u = 163.8$ $t_c = 197$ $t_T = 201.4$	0.3414

$H_T = 1189.5$; $\delta = 0.5$, $\rho = 0.35$, $\gamma = 0.15$.				
Sensitivity 1 (lower critical thresholds for the GDEs' health phases): $\delta = 0.4$, $\rho = 0.3$, $\gamma = 0.1$.	1179.04	159	$t_u = 156.8$ $t_c = 198$ $t_T = 201$	0.3415
Sensitivity 2 (higher critical thresholds for the GDEs' health phases): $\delta = 0.7$, $\rho = 0.4$, $\gamma = 0.2$.	1178	160	$t_u = 163$ $t_c = 196$ $t_T = 199$	0.3413
Sensitivity 3 (lower critical thresholds for the water table height): $H_u = 1195.5$, $H_c = 1190.5$, $H_T = 1184.5$.	1179.2	160	$t_u = 168.8$ $t_c = 193.6$ $t_T = 251.9$	0.3477
Sensitivity 4 (higher critical thresholds for the water table height): $H_u = 1205.5$, $H_c = 1196.5$, $H_T = 1192.5$.	1182.01	146	$t_u = 154$ $t_c = 200$ $t_T = 202.8$	0.3347

Table 4. Main results from the scenarios analysed under the quota policy.

Scenario	Water table height ($m.a.s.l$)	Aquifer depletion after 250 years (Mm^3)	Shifting year	Total aggregate social welfare (Million US dollars)
Baseline (Without GDEs and LS)	1170.87	214	-	0.4032
With GDEs' dynamics (empirical critical thresholds for the water table height and GDEs' health phases): $H_u = 1200.5$, $H_c = 1191.5$, $H_T = 1189.5$; $\delta = 0.5$, $\rho = 0.35$, $\gamma = 0.15$.	1186.47	150.8	t_u =126 t_c =155 t_T = 161	0.1395
Sensitivity 1 (lower critical thresholds for the GDEs' health phases): $\delta = 0.4$, $\rho = 0.3$, $\gamma = 0.1$.	1186.47	150.7	t_u =126 t_c =144 t_T =161	0.1395
Sensitivity 2 (higher critical thresholds for the GDEs' health phases): $\delta = 0.7$, $\rho = 0.4$, $\gamma = 0.2$.	1186.47	150.7	t_u =126 t_c =145 t_T =163	0.1395
Sensitivity 3 (lower	1186.47	150.7	t_u =132	0.1395

critical thresholds for the water table height): $H_u = 1195.5$, $H_c = 1190.5$, $H_T = 1184.5$.			t_c =151 $t_T = N/A$	
Sensitivity 4 (higher critical thresholds for the water table height): $H_u = 1205.5$, $H_c = 1196.5$, $H_T = 1192.5$.	1186.5	150.7	t_u =119 t_c =131 t_T =136	0.1395

Table 5. Main results from the scenarios analysed under packaging and sequencing of taxes and quotas.

Scenario	Water table height $(m.a.s.l)$	Aquifer depletion after 250 years (Mm^3)	Shifting year	Total aggregate social welfare (Million US dollars)
Baseline (Without GDEs and LS)	1170.87	214	-	0.4032
With GDEs' dynamics (empirical critical thresholds for the water table height and GDEs' health phases): $H_u = 1200.5$, $H_c = 1191.5$, $H_T = 1189.5$; $\delta = 0.5$,	1184.8	144.6	$t_u = 163.8$ $t_c = 197$ $t_T = 201.4$	0.3414

$\rho = 0.35$, $\gamma = 0.15$.				
Sensitivity 1 (lower critical thresholds for the GDEs' health phases): $\delta = 0.4$, $\rho = 0.3$, $\gamma = 0.1$.	1184.8	144.6	$t_u = 156$ $t_c = 198$ $t_T = 201$	0.3415
Sensitivity 2 (higher critical thresholds for the GDEs' health phases): $\delta = 0.7$, $\rho = 0.4$, $\gamma = 0.2$.	1184.7	145	$t_u = 163.9$ $t_c = 196$ $t_T = 199$	0.3413
Sensitivity 3 (lower critical thresholds for the water table height): $H_u = 1195.5$, $H_c = 1190.5$, $H_T = 1184.5$.	1182.53	160	$t_u = 168.8$ $t_c = 194$ $t_T = 252$	0.3477
Sensitivity 4 (higher critical thresholds for the water table height): $H_u = 1205.5$, $H_c = 1196.5$, $H_T = 1192.5$.	1187.8	132	$t_u = 154$ $t_c = 200$ $t_T = 202.8$	0.3347

Appendix 20. Monte Carlo simulations

We assume that the natural recharge rate (R) is roughly 7.5 Mm^3, but we don't know the exact constant R, it is uncertain. Although the analytic optimal control solution is derived under constant aquifer recharge R, annual rainfall in the Dendron area varies substantially from year to year. Historical rainfall for the past 115 years is used to estimate the distribution of annual rainfall P_t. Effective recharge is assumed to be a fixed fraction ϕ of rainfall, such that $R_t = \phi P_t$. Where $\phi$is an estimated recharge coefficient (area × fraction that percolates). The empirical mean μ_R is equal to (less or more but close) the deterministic recharge value used in the analytic solution (7.35 Mm^3/year), while the empirical variance provides the dispersion for random draws. For each Monte Carlo run k, recharge is drawn as: $R^{(k)} \sim f(\mu_R, \sigma_R^2)$. Where f is the fitted distribution of rainfall values from the Dendron area. The optimal control model is then solved using the closed-form analytic expressions for each phase, with R replaced by the draw $R^{(k)}$. These yields switching times $t_u^{(k)}, t_c^{(k)}, t_T^{(k)}$and optimal paths $H^{(k)}(t)$and $W^{(k)}(t)$ for that simulation. Repeating this process 300 times yields distributions for switching times, water-table trajectories, and extraction paths. This approach preserves the analytic solution structure and Pontryagin optimality while incorporating realistic rainfall variability.

We used gridded daily rainfall data (from 1900 to 2015, 115 years) for the Dendron area, extracted using the area's geographical coordinates. These datasets were then converted into annual rainfall datasets. The gridded daily rainfall data was obtained from the Royal Netherlands Meteorological Institute (KNMI) Climate Explorer, and freely available online (https://climexp.knmi.nl/start.cgi). The KNMI Climate Explorer CPC (Climate Prediction Center) database provides gridded daily rainfall data, including long-term means of both monthly and daily precipitation. These data are produced by the NOAA Climate Prediction Center's global unified gauge-based analysis of daily precipitation, which spans the period 1900–2015. The dataset integrates historical and recent land-surface precipitation observations from multiple sources and merges them into global precipitation estimates using advanced data assimilation and forecasting models. The CPC Global Daily Unified Gauge-Based Analysis of Precipitation is provided at a spatial resolution of 0.5° latitude by 0.5° longitude. From the rainfall datasets, we found the mean in excel to be equal to 415.5 mm, close to the theoretical average annual rainfall of amount $407\ mm$ as documented for the Hout river catchment in which the Dendron area is situated. We also fitted several distributions and found that the data best fit the Gamma distribution.

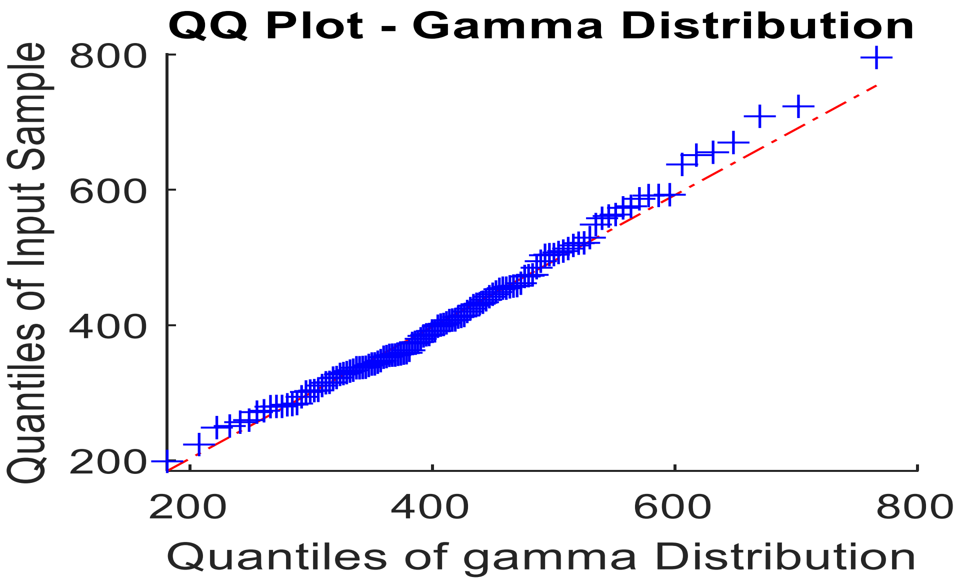

Figure 1. QQ plot for the Gamma distribution generated from the rainfall data.

Figure 2 shows the fitted Gamma distribution of the rainfall datasets. The scale and shape parameters are equal to a = 13.9093 [10.7858, 17.9374] and b = 29.8693 [23.0546, 38.6985], respectively. The mean, variance, and standard deviation is equal to 415.4613, 12409.5447, and 111.3981, respectively.

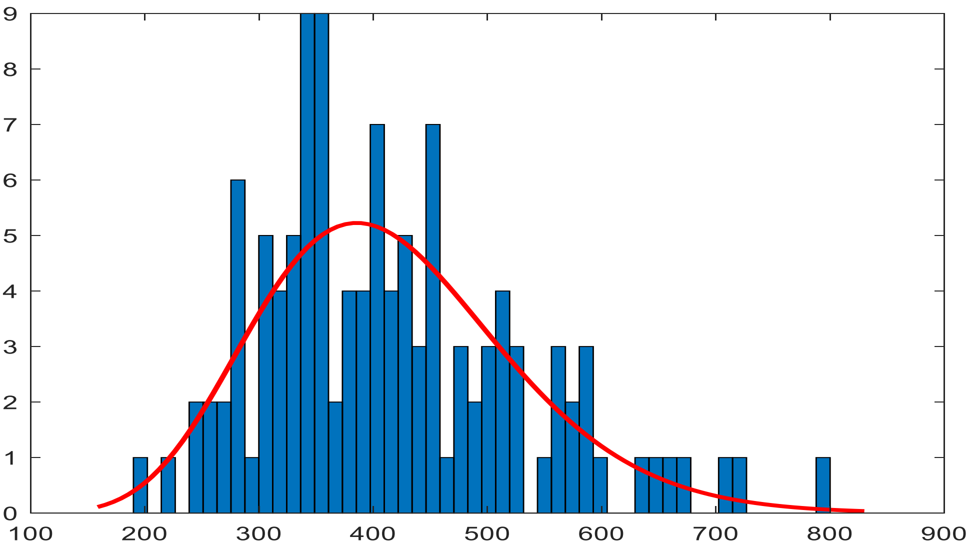

Figure 2. Fitted Gamma distribution of the rainfall data.

We then move onto estimating the annual natural recharge rate using the relation $R_t = \phi P_t$, where ϕ is an estimated recharge coefficient. Since we don't have historical recharge values to run a regression equation, we make use of the relation we stated already. That is, the Mean annual rainfall (MAR) is proportional to Mean annual recharge (MAR_g) through a constant ϕ: $MAR_g = \phi \cdot MAR$. Since we know both means (from long-term rainfall data and long-term groundwater budget studies), we can solve for the constant ϕ: $\phi = \frac{MAR_g}{MAR} = \frac{7.35}{407} = \frac{147}{8140}$. We will also make use of this value for ϕ when running Montecarlo simulation since random recharge rates will be obtained from random rainfall rates that are picked randomly from the Gamma distribution in a Montecarlo simulation. We also went further to make use of the value for ϕ and convert the rainfall data into the recharge rates data to test if this value approximates correctly the natural recharge rates in the aquifer. We obtained a mean of 7.502803 mm in excel, very close to the theoretical annual mean of 7.35 mm. We then carried out the best distribution that fits the data. We again found that the Gamma distribution fits the data best. The scale and shape parameters are equal to a = 13.9093 [10.7858, 17.9374] and b = 0.539409 [0.416342, 0.698854], respectively. The mean, variance, and standard deviation is equal to 7.5028, 4.0471, and 2.0117, respectively. The QQ plot is shown in Figure 3 below.

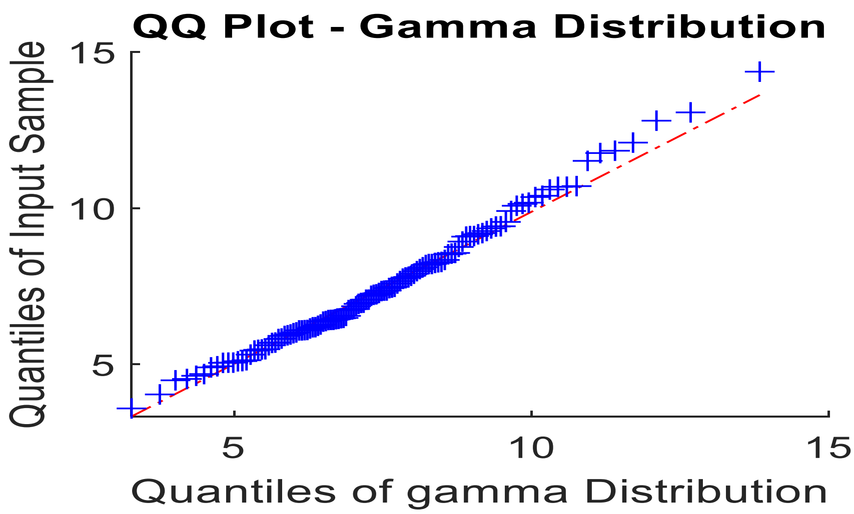

Figure 3. QQ plot for the Gamma distribution using the estimated recharge rates data.

References

Aldous, A. and Bach, L., 2011. Protecting groundwater dependent ecosystems: Gaps and opportunities. *National Wetlands Newsletter*, *33*(3), pp.19-22.

Allen, R. and Gisser, M., 1984. Competition Versus Optimal Control in Groundwater Pumping When Demand is Nonlinear. *Water Resources Research*, 20(7), pp.752-756.

Anderson, S.J., Ankor, B.L. and Sutton, P.C., 2017. Ecosystem service valuations of South Africa using a variety of land cover data sources and resolutions. *Ecosystem Services*, *27*, pp.173-178.

Bagheri-Gavkosh, M., Hosseini, S.M., Ataie-Ashtiani, B., Sohani, Y., Ebrahimian, H., Morovat, F. and Ashrafi, S., 2021. Land subsidence: A global challenge. *Science of The Total Environment*, *778*, p.146193.

Bermudez, V.A.B., Abilgos, A.B.B., Cuaresma, D.C.N. and Rabajante, J.F., 2017. Probability distribution of Philippine daily rainfall data.

Boulton A, Humphreys W, Eberhard S (2003) Imperilled subsurface waters in Australia: biodiversity, threatening processes and conservation. Aquat Ecosyst Health Manage 6(1):41–54.

Brah, W. L. and Jones, L. L. (1978). Institutional Arrangements for Effective Groundwater Management to Halt Land Subsidence. Technical and Special Reports. [online]Texas: Texas Water Resources Institute. Available at: http://hdl.handle.net/1969.1/6285 [Accessed 23 Oct. 2023].

Brander, L.M., De Groot, R., Schägner, J.P., Guisado-Goñi, V., Van't Hoff, V., Solomonides, S., McVittie, A., Eppink, F., Sposato, M., Do, L. and Ghermandi, A., 2024. Economic values for ecosystem services: A global synthesis and way forward. *Ecosystem Services*, *66*, p.101606.

Bredehoeft, J.D. and Young, R.A., 1970. The temporal allocation of ground water—A simulation approach. *Water Resources Research*, *6*(1), pp.3-21.

Brill, T. C. and Burness, H. S. (1994). Planning versus competitive rates of groundwater pumping. *Water Resources Research*, 30(6), pp.1873-1880.

Brown Jr, G. and Deacon, R., 1972. Economic optimization of a single-cell aquifer. *Water Resources Research*, *8*(3), pp.557-564.

Brozovic, N., Sunding, D.L. and Zilberman, D., 2004. Taxes vs. Quotas or Taxes vs. Upper Bounds?. *Working document*.

Chávez, R.O., Clevers, J.G.P.W., Decuyper, M., De Bruin, S. and Herold, M., 2016. 50 years of water extraction in the Pampa del Tamarugal basin: Can Prosopis tamarugo trees survive in the hyper-arid Atacama Desert (Northern Chile)?. *Journal of Arid Environments*, *124*, pp.292-303.

Choi, E.K. and Feinerman, E., 1995. Regulation of nitrogen pollution: taxes versus quotas. *Journal of Agricultural and Resource Economics*, pp.122-134.

Clifton CA, and Evans R (2001). Environmental water requirements to maintain groundwater dependent ecosystems. Environmental flows initiative technical report number 2, Commonwealth of Australia, Canberra.

Cobourn, K.M., 2025. Assessing the Economic Implications of Land Subsidence. *Water Economics & Policy*, *11*(1).

Collen, B., Whitton, F., Dyer, E.E., Baillie, J.E., Cumberlidge, N., Darwall, W.R., Pollock, C., Richman, N.I., Soulsby, A.M. and Böhm, M., 2014. Global patterns of freshwater species diversity, threat and endemism. *Global ecology and Biogeography*, *23*(1), pp.40-51.

Colvin, C., Le Maitre, D., Saayman, I. and Hughes, S., 2007. An introduction to aquifer dependent ecosystems in South Africa. *Pretoria: Natural Resources and the Environment, CSIR*.

Colvin, C., Le Maitre, D.C. and Hughes, S., 2003. *Assessing terrestrial groundwater dependent ecosystems in South Africa* (Vol. 1090). Pretoria: Water Research Commission.

Costanza, R., De Groot, R., Sutton, P., Van der Ploeg, S., Anderson, S.J., Kubiszewski, I., Farber, S. and Turner, R.K., 2014. Changes in the global value of ecosystem services. *Global environmental change*, *26*, pp.152-158.

Costello, C. and Karp, L., 2004. Dynamic taxes and quotas with learning. *Journal of Economic Dynamics and Control*, *28*(8), pp.1661-1680.
Danielopol, D.L., Pospisil, P., 2001. Hidden biodiversity in the groundwater of the Danube Flood Plain National Park (Austria). Biodivers. Conserv. 10, 1711–1721.

Dasgupta P (2021). The Economics of Biodiversity: The Dasgupta Review. HM Treasury, London.

Davis, J., O'Grady, A.P., Dale, A., Arthington, A.H., Gell, P.A., Driver, P.D., Bond, N., Casanova, M., Finlayson, M., Watts, R.J. and Capon, S.J., 2015. When trends intersect: The challenge of protecting freshwater ecosystems under multiple land use and hydrological intensification scenarios. *Science of the Total Environment*, *534*, pp.65-78.

de Frutos Cachorro, J., Erdlenbruch, K. and Tidball, M. (2014). Optimal adaptation strategies to face shocks on groundwater resources. *Journal of Economic Dynamics and Control*, 40, pp.134-153.

Dinar, A., Esteban, E., Calvo, E., Herrera, G., Teatini, P., Tomás, R., Li, Y. and Albiac, J., 2020. Land Subsidence: The Forgotten Enigma of Groundwater (Over)Extraction. In: *ASSA 2020 Annual Meeting*. [online] San Diego, CA: American Economic Association, p.Natural Resources as Assets. Available at: <https://www.aeaweb.org/conference/2020/preliminary/paper/G59BftQy> [Accessed 5 March 2020].

Dinar, A., Esteban, E., Calvo, E., Herrera, G., Teatini, P., Tomás, R., Li, Y., Ezquerro, P. and

Albiac, J., 2021. We lose ground: Global assessment of land subsidence impact extent. *Science of the Total Environment*, *786*, p.147415.

Duke, J.M., Liu, Z., Suter, J.F., Messer, K.D. and Michael, H.A., 2020. Some taxes are better than others: an economic experiment analyzing groundwater management in a spatially explicit aquifer. *Water Resources Research*, *56*(7), p.e2019WR026426.

Eamus D, Froend R, Loomes R, Hose G, Murray B (2006). A functional methodology for determining the groundwater regime needed to maintain the health of groundwater-dependent vegetation. Aust J Bot 54(2):97–114.

Eamus, D., Froend, R., Loomes, R., Hose, G. and Murray, B., 2006. A functional methodology for determining the groundwater regime needed to maintain the health of groundwater-dependent vegetation. *Australian Journal of Botany*, *54*(2), pp.97-114.

Eamus, D., Fu, B., Springer, A.E. and Stevens, L.E., 2016. Groundwater dependent ecosystems: classification, identification techniques and threats. *Integrated groundwater management: concepts, approaches and challenges*, pp.313-346.

Esteban, E. and Albiac, J. (2011). Groundwater and ecosystems damages: Questioning the Gisser-Sanchez effect. *Ecological Economics*, 70(11), pp.2062-2069.

Esteban, E. and Dinar, A. (2013). Modeling Sustainable Groundwater Management: Packaging and sequencing of policy interventions. *Journal of Environmental Management*, 119, pp. 93–102. Available at: https://doi.org/10.1016/j.jenvman.2012.12.047.

Esteban, E. and Dinar, A., 2016. The role of groundwater-dependent ecosystems in groundwater management. *Natural Resource Modeling*, *29*(1), pp.98-129.

Esteban, E., Calvo, E. and Albiac, J., 2021. Ecosystem shifts: Implications for groundwater management. *Environmental and Resource Economics*, *79*(3), pp.483-510.

Esteban, E., Dinar, A., Calvo, E., Albiac, J., Calatrava, J., Herrera, G., Teatini, P., Tomás, R., Ezquerro, P. and Li, Y., 2024. Modeling the optimal management of land subsidence due to aquifers overexploitation. *Journal of Environmental Management*, *349*, p.119333.

Fei, L., Shuwen, Z., Jiuchun, Y., Kun, B., Qing, W., Junmei, T. and Liping, C., 2016. The effects of population density changes on ecosystem services value: A case study in Western Jilin, China. *Ecological indicators*, *61*, pp.328-337.

Feinerman, E. and Knapp, K.C., 1983. Benefits from groundwater management: magnitude, sensitivity, and distribution. *American Journal of Agricultural Economics*, *65*(4), pp.703-710.

Feinerman, E., 1988. Groundwater management: Efficiency and equity considerations. *Agricultural Economics*, *2*(1), pp.1-18.

Froend, R. and Sommer, B., 2010. Phreatophytic vegetation response to climatic and abstraction-induced groundwater drawdown: examples of long-term spatial and temporal variability in community response. *Ecological Engineering*, *36*(9), pp.1191-1200.

Gisser, M. and Sanchez, D. A. (1980). Competition versus optimal control in groundwater pumping. *Water Resources Research*, 16(4), pp.638-642.

Grizzetti, B., Lanzanova, D., Liquete, C., Reynaud, A. and Cardoso, A.C., 2016. Assessing water ecosystem services for water resource management. *Environmental Science & Policy*, *61*, pp.194-203.

Guilfoos, T., Pape, A. D., Khanna, N. and Salvage, K. (2013). Groundwater management: The effect of water flows on welfare gains. *Ecological Economics*, 95, pp.31-40.

Gutrich, J.J., Gigliello, K., Gardner, K.V. and Elmore, A.J., 2016. Economic returns of groundwater management sustaining an ecosystem service of dust suppression by alkali meadow in Owens Valley, California. *Ecological Economics*, *121*, pp.1-11.

Heitmuller FT, and Reece BD (2007). Spatial data for Eurycea salamander habitats associated with three aquifers in south-central Texas. US Geological Survey, Austin, Texas.

Herrera-García, G., Ezquerro, P., Tomás, R., Béjar-Pizarro, M., López-Vinielles, J., Rossi, M., Mateos, R.M., Carreón-Freyre, D., Lambert, J., Teatini, P. and Cabral-Cano, E., 2021. Mapping the global threat of land subsidence. *Science*, *371*(6524), pp.34-36.

Hu, B., Zhou, J., Xu, S., Chen, Z., Wang, J., Wang, D., Wang, L., Guo, J. and Meng, W., 2013. Assessment of hazards and economic losses induced by land subsidence in Tianjin Binhai new area from 2011 to 2020 based on scenario analysis. *Natural Hazards*, *66*(2), pp.873-886.

Husak, G.J., Michaelsen, J. and Funk, C., 2007. Use of the gamma distribution to represent monthly rainfall in Africa for drought monitoring applications. *International Journal of Climatology: A Journal of the Royal Meteorological Society*, *27*(7), pp.935-944.

Josset, L., Lall, U., Prakash, D. and Dinar, A., 2024. Public health, socioeconomic and environmental impacts of urban land subsidence. *Authorea Preprints*.

Kemper, K. E (2007). Instruments and institutions for groundwater management. In: Giordano, M. and Villholth, K. G. (eds.). The agricultural groundwater revolution: opportunities and threats to development. Wallingford, UK: CABI, pp.153-172.

Kim, C.S., Moore, M.R., Hanchar, J.J. and Nieswiadomy, M., 1989. A dynamic model of adaptation to resource depletion: theory and an application to groundwater mining. *Journal of Environmental Economics and Management*, *17*(1), pp.66-82.

Kløve, B., Ala-Aho, P., Bertrand, G., Boukalova, Z., Ertürk, A., Goldscheider, N., Ilmonen, J., Karakaya, N., Kupfersberger, H., Kvœrner, J. and Lundberg, A., 2011. Groundwater dependent ecosystems. Part I: Hydroecological status and trends. *Environmental Science & Policy*, *14*(7), pp.770-781.

Kløve, B., Allan, A., Bertrand, G., Druzynska, E., Ertürk, A., Goldscheider, N., Henry, S., Karakaya, N., Karjalainen, T.P., Koundouri, P. and Kupfersberger, H., 2011. Groundwater dependent ecosystems. Part II. Ecosystem services and management in Europe under risk of climate change and land use intensification. *Environmental Science & Policy*, *14*(7), pp.782-793.

Koundouri, P., 2004. Current issues in the economics of groundwater resource management. *Journal of Economic Surveys*, *18*(5), pp.703-740.

Koundouri, P., 2004. Potential for groundwater management: Gisser-Sanchez effect reconsidered. *Water resources research*, *40*(6).

Kreamer DK, Stevens LE, and Ledbetter, JD (2014). Groundwater dependent ecosystems-science, challenges, and policy. In: Adelana SM (ed) Groundwater. Nova Science Publishers, Hauppauge (NY), pp 205–230. ISBN: 978-1-63321-759-1

Lenouvel, V., Montginoul, M. and Thoyer, S., 2011, June. From a blind truncheon to a one-eyed stick: testing in the lab an optional target-based mechanism adapted to groundwater withdrawals. In *Annual Conference of European Association of Environmental and Resource Economists* (pp. 23-p).

Lenouvel, V., Montginoul, M., Thoyer, S., 2011. From a Blind Truncheon to a Oneeyed Stick: Testing in the Lab an Optional Target-based Mechanism Adapted to Groundwater Withdrawals. European Association of Environmental and Resource Economists, 18th Annual Conference, 29 Junee2 July, Rome.

Loomes RC (2000) Identification of wetland plant hydrotypes on the Swan Coastal Plain Western Australia. PhD Thesis, Edith Cowan University, Perth.

Maddock III, T.H.O.M.A.S. and Haimes, Y.Y., 1975. A tax system for groundwater management. *Water Resources Research*, *11*(1), pp.7-14.
Maddock, T. and Haimes, Y.Y. (1975). Tax system for groundwater management. Water Resources Research 11 (1), 7e14.

Martinez-Villalobos, C. and Neelin, J.D., 2019. Why do precipitation intensities tend to follow gamma distributions?. *Journal of the Atmospheric Sciences*, *76*(11), pp.3611-3631.

MEA, 2005. Millenium ecosystem assessment. In: Ecosystems and Human Well-being: Biodiversity Synthesis, World Resources Institute, Washington, DC.

Mudavanhu, S., Blignaut, J., Stegmann, N., Barnes, G., Prinsloo, W. and Tuckett, A., 2017. The economic value of ecosystem goods and services: The case of Mogale's Gate Biodiversity Centre, South Africa. *Ecosystem Services*, *26*, pp.127-136.

Ndahangwapo, N.N., Thiam, D.R. and Dinar, A., 2024. Land Subsidence Impacts and Optimal Groundwater Management in South Africa. *Environmental and Resource Economics*, *87*(5), pp.1097-1126.

Nusantara, R.W., Hazriani, R. and Suryadi, U.E., 2018, April. Water-table depth and peat subsidence due to land-use change of peatlands. In *IOP Conference Series: Earth and Environmental Science* (Vol. 145, No. 1, p. 012090). IOP Publishing.

Poland, J.F., 1984. Guidebook to studies of land subsidence due to groundwater withdrawal. United Nations Educational, Scientific and Cultural Organization, MI: Chelsea.

Rohde MM, Saito L, Smith R. 2020. Groundwater Thresholds for Ecosystems: A Guide for Practitioners. Global Groundwater Group, The Nature Conservancy.

Rohde, M.M., Froend, R. and Howard, J., 2017. A global synthesis of managing groundwater dependent ecosystems under sustainable groundwater policy. *Groundwater*, *55*(3), pp.293-301.

Rohde, M.M., Sweet, S.B., Ulrich, C. and Howard, J., 2019. A transdisciplinary approach to characterize hydrological controls on groundwater-dependent ecosystem health. *Frontiers in Environmental Science*, *7*, p.175.

Roumasset, J. and Wada, C., 2013. A dynamic approach to PES pricing and finance for interlinked ecosystem services: Watershed conservation and groundwater management. *Ecological Economics*, 87, pp.24-33.

Scheffer, M., Carpenter, S., Foley, J.A., Folke, C. and Walker, B., 2001. Catastrophic shifts in ecosystems. *Nature*, *413*(6856), pp.591-596.

Seidl, C., Page, D. and Wheeler, S.A., 2024. Using managed aquifer recharge to address land subsidence: Insights from a global literature review. *Water Security*, *23*, p.100184.

Şen, Z., 2019. *Groundwater recharge level estimation from rainfall record probability match methodology. Earth Syst Environ 3: 603–612*.

Shafroth PB, Stromberg JC, and Patten DT (2000). Woody riparian vegetation response to different alluvial water table regimes. West N Am Naturalist 60(1):66–76.

Shaheb, M.R., Venkatesh, R. and Shearer, S.A., 2021. A review on the effect of soil compaction and its management for sustainable crop production. *Journal of Biosystems Engineering*, pp.1-23.

Shrestha, P.K., Shakya, N.M., Pandey, V.P., Birkinshaw, S.J. and Shrestha, S., 2017. Model-based estimation of land subsidence in Kathmandu Valley, Nepal. *Geomatics, Natural Hazards and Risk*, *8*(2), pp.974-996.

Smith, R.G. and Majumdar, S., 2020. Groundwater storage loss associated with land subsidence in Western United States mapped using machine learning. *Water Resources Research*, *56*(7), p.e2019WR026621.

Smith, R.G., Knight, R., Chen, J., Reeves, J.A., Zebker, H.A., Farr, T. and Liu, Z., 2017. Estimating the permanent loss of groundwater storage in the southern S an J oaquin V alley, C alifornia. *Water Resources Research*, *53*(3), pp.2133-2148.

Sneed, M., 2001. *Hydraulic and mechanical properties affecting ground-water flow and aquifer-system compaction, San Joaquin Valley, California* (Vol. 1). US Department of the Interior, US Geological Survey.

Soewandita, H., 2008. Studi muka air tanah gambut dan implikasinya terhadap degradasi lahan pada beberapa kubah gambut di Kabupaten Siak. *Jurnal Air Indonesia*, *4*(2).

Sørensen, A. and Herbertsson, T.T., 1998. Policy rules for exploitation of renewable resources: a macroeconomic perspective. *Environmental and Resource Economics*, *12*, pp.53-76.

Stephens, J.C. and Speir, W.H., 1969. Subsidence of organic soils in the USA. *Assn. Intern, of*

Hydro. Soi., Colloque De Tokyo, Pub, 89.

Stephens, J.C. and Stewart, E.H., 1977. Effect of climate on organic soil subsidence.

Stromberg, J.C., Tiller, R. and Richter, B., 1996. Effects of groundwater decline on riparian vegetation of semiarid regions: the San Pedro, Arizona. *Ecological Applications*, *6*(1), pp.113-131.

Tang, S.Y., 1991. Institutional arrangements and the management of common-pool resources. *Public Administration Review*, pp.42-51.

TEEB, 2008. The Economics of Ecosystems and Biodiversity: An interim report.

Tilman, D., Fargione, J., Wolff, B., D'antonio, C., Dobson, A., Howarth, R., Schindler, D., Schlesinger, W.H., Simberloff, D. and Swackhamer, D., 2001. Forecasting agriculturally driven global environmental change. *science*, *292*(5515), pp.281-284.

Tomini, A. (2014). Is the Gisser and Sánchez model too simple to discuss the economic relevance of groundwater management?. *Water Resources and Economics*, 6, pp.18-29.

Turpie, J.K., Forsythe, K.J., Knowles, A., Blignaut, J. and Letley, G., 2017. Mapping and valuation of South Africa's ecosystem services: A local perspective. *Ecosystem services*, *27*, pp.179-192.

Vitousek, P.M., Mooney, H.A., Lubchenco, J. and Melillo, J.M., 1997. Human domination of Earth's ecosystems. *Science*, *277*(5325), pp.494-499.

Wade, C.M., Cobourn, K.M., Amacher, G.S. and Hester, E.T., 2018. Policy targeting to reduce economic damages from land subsidence. *Water Resources Research*, *54*(7), pp.4401-4416.
Weitzman M (1974) Prices vs. quantities. Rev Econ Stud 41(128):477–491.

Weitzman, M.L., 1974. Prices vs. quantities. Review of Economic Studies 41 (128), 477e491.

Winter, T.C., Harvey, J.W., Franke, O.L., Alley, W.M., 1998. Ground water and surface water; a single resource. U.S. Geological Survey Circular 1139. USGS, Denver, Colorado, pp. 7.

Wösten, J.H.M., Clymans, E., Page, S.E., Rieley, J.O. and Limin, S.H., 2008. Peat–water interrelationships in a tropical peatland ecosystem in Southeast Asia. *Catena*, *73*(2), pp.212-224.

Wösten, J.H.M., Ismail, A.B. and Van Wijk, A.L.M., 1997. Peat subsidence and its practical implications: a case study in Malaysia. *Geoderma*, *78*(1-2), pp.25-36.

Ximenes, P.D.S.M.P., Silva, A.S.A.D., Ashkar, F. and Stosic, T., 2021. Best-fit probability distribution models for monthly rainfall of Northeastern Brazil. *Water Science and Technology*, *84*(6), pp.1541-1556.

Zekri, S., 2008. Using economic incentives and regulations to reduce seawater intrusion in the Batinah coastal area of Oman. *Agricultural Water Management*, *95*(3), pp.243-252.

Zektser S, Loa´iciga HA, and Wolf JT (2005). Environmental impacts of groundwater overdraft: selected case studies in the southwestern United States. Environ Geol 47(3):396-404. doi:10.1007/s00254-004-1164-3